Flow stability and Introduction to turbulence

Christophe Bailly & Andréa Maffioli

Centrale Lyon – 2A FLE-1a – 17-12-2023

http://acoustique.ec-lyon.fr

Introduction to turbulence

Textbooks

Batchelor, G.K., 1967, An introduction to fluid dynamics, *Cambridge University Press*, Cambridge.

Bailly C. & **Comte Bellot** G., 2003 Turbulence, *CNRS éditions*, Paris (out of print).
———, 2015, *Turbulence* (in english), Springer, Heidelberg.
(360 pages, 147 illustrations, Foreword by Charles Meneveau, 53 € for ECL students)

Bailly C. & Comte Bellot G., 2003, *Turbulence* (in french), CNRS éditions, Paris.
———, 2015, *Turbulence* (in english), Springer, Heidelberg.

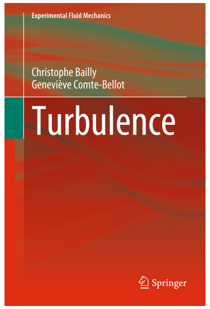

Springer, ISBN 978-3-319-16159-4,
360 pages, 147 illustrations.
(discount for students, 53 €)

Candel S., 1995, Mécanique des fluides, *Dunod Université*, 2nd édition, Paris.

Cousteix, J., 1989, Turbulence et couche limite, Cépaduès, Toulouse.

Davidson P.A., 2004, *Turbulence. An introduction for scientists and engineers*, Oxford University Press, Oxford.

Davidson, P.A., **Kaneda**, Y., **Moffatt**, H.K. & **Sreenivasan**, K.R., Edts, 2011, *A voyage through Turbulence*, Cambridge University Press, Cambridge.

Guyon E., **Hulin** J.P. & **Petit** L., 2001, Physical hydrodynamics, *EDP Sciences / Editions du CNRS*, première édition 1991, Paris - Meudon.

Textbooks (cont.)

Hinze J.O., 1975, Turbulence, *McGraw-Hill International Book Company*, New York, 1ère édition en 1959.

Landau L. & **Lifchitz** E., 1971, Mécanique des fluides, *Editions MIR, Moscou*.
Also *Pergamon Press*, 2nd edition, 1987.

Lesieur M., 2008, Turbulence in fluids : stochastic and numerical modelling, *Kluwer Academic Publishers, 4th revised and enlarged ed.*, Springer.

Pope S.B., 2000, Turbulent flows, *Cambridge University Press*.

Tennekes H. & **Lumley** J.L., 1972, A first course in turbulence, *MIT Press*, Cambridge, Massachussetts.

Van Dyke M., 1982, An album of fluid motion, *The Parabolic Press*, Stanford, California.

White F., 1991, Viscous flow, *McGraw-Hill, Inc.*, New-York, first edition 1974.

Introduction

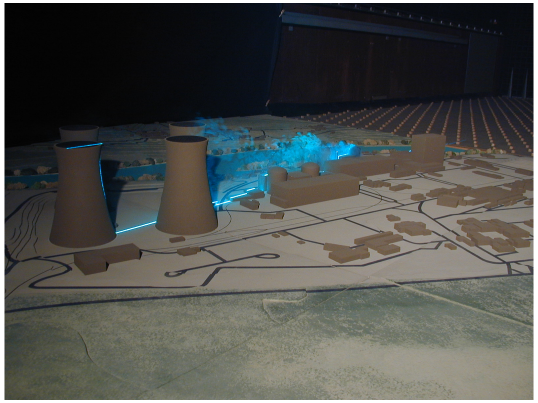


Atmospheric wind tunnel (LMFA)

Turbulent flows are part of everyday life!

- Geophysical flows
  astrophysics, climate, wheather, environment, hydraulics
- Transportation industry : space, aeronautics, marine & submarine
  and also sport applications
- Transport of fluids (energy industry, chemistry), production of energy
- Biology (physiology, biomechanics, medicine)
- Complex flows (two-phase flows, including solid particles, ...)

External aerodynamics • Noise of turbulent flows (aeroacoustics) • Sound propagation (atmosphere, ocean) • Fluid-solid coupling and vibroacoustics • Combustion (reactive flows)

Fluid mechanics is involved in many societal challenges

Turbulent flows

- unsteady aperiodic motion
- unpredictable behaviour
- presence of a wide range of scales (eddies)

Turbulence appears when the source of the kinetic energy which drives the fluid motion is able to overcome viscosity effects

- **Simulation of the growth of cosmic structure (galaxies and voids)** (cosmological hydrodynamics)

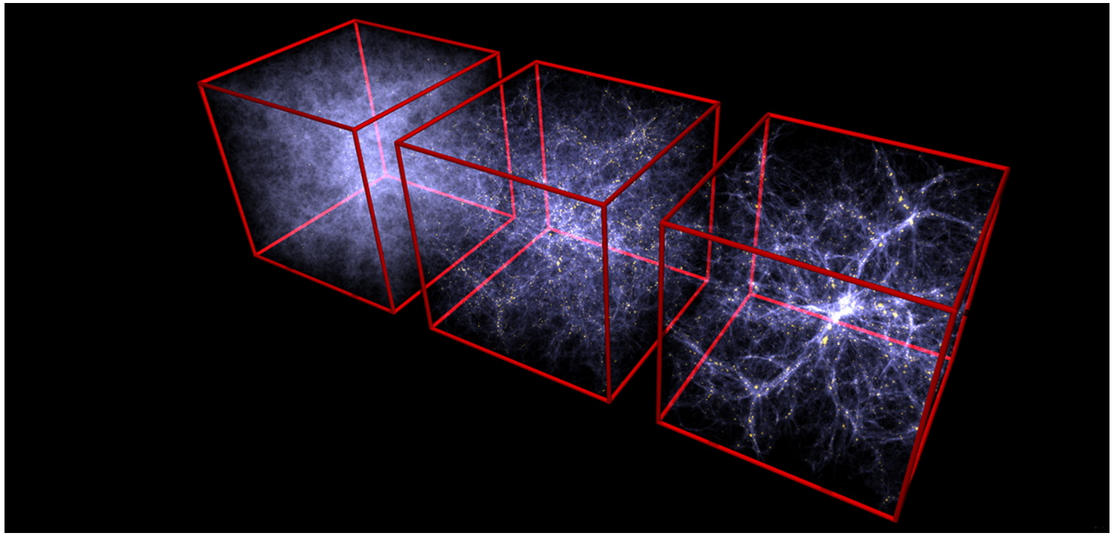

Simulation of the growth of cosmic structure (galaxies and voids) when the Universe was 0.9 billion years old, then 3.2 billion and 13.7 billion years old (today)

Volker Springel / Max Planck Institute for Astrophysics

https://news.cnrs.fr/articles/euclid-on-a-quest-to-understand-dark-energy

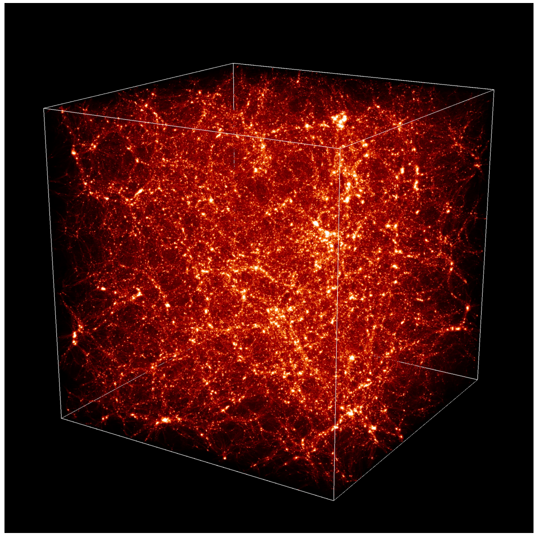

Structure formation in an expanding universe : N-body simulation (red temperature) with 70 billions particles ; 500 million light-years long on each side

Institut d'Astrophysique de Paris (Pichon) & CEA (Teyssier)

- **Weather satellite images**
  www.meteofrance.com • www.meteo-lyon.net
  https://www.meteoblue.com/fr/meteo/semaine/lyon_france_2996944

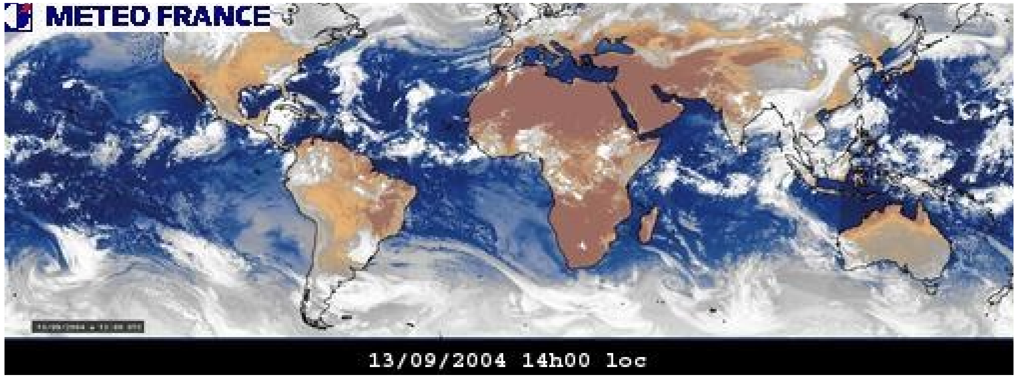

Intertropical convergence zone

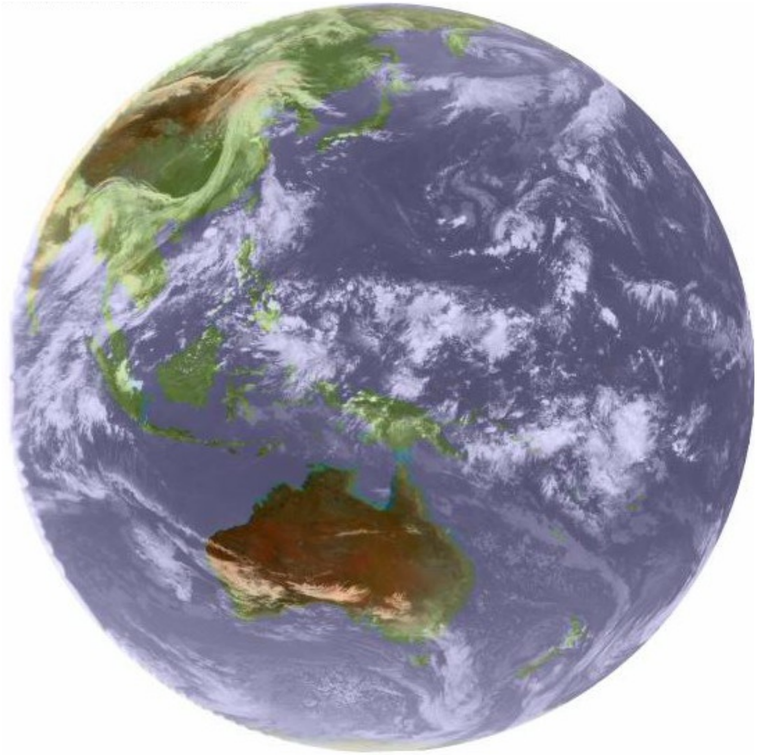

- **Annual mean temperature in Lyon - Bron Airport - from 1921 to 2018**
(from Météo France, Le Monde 08.01.2019)

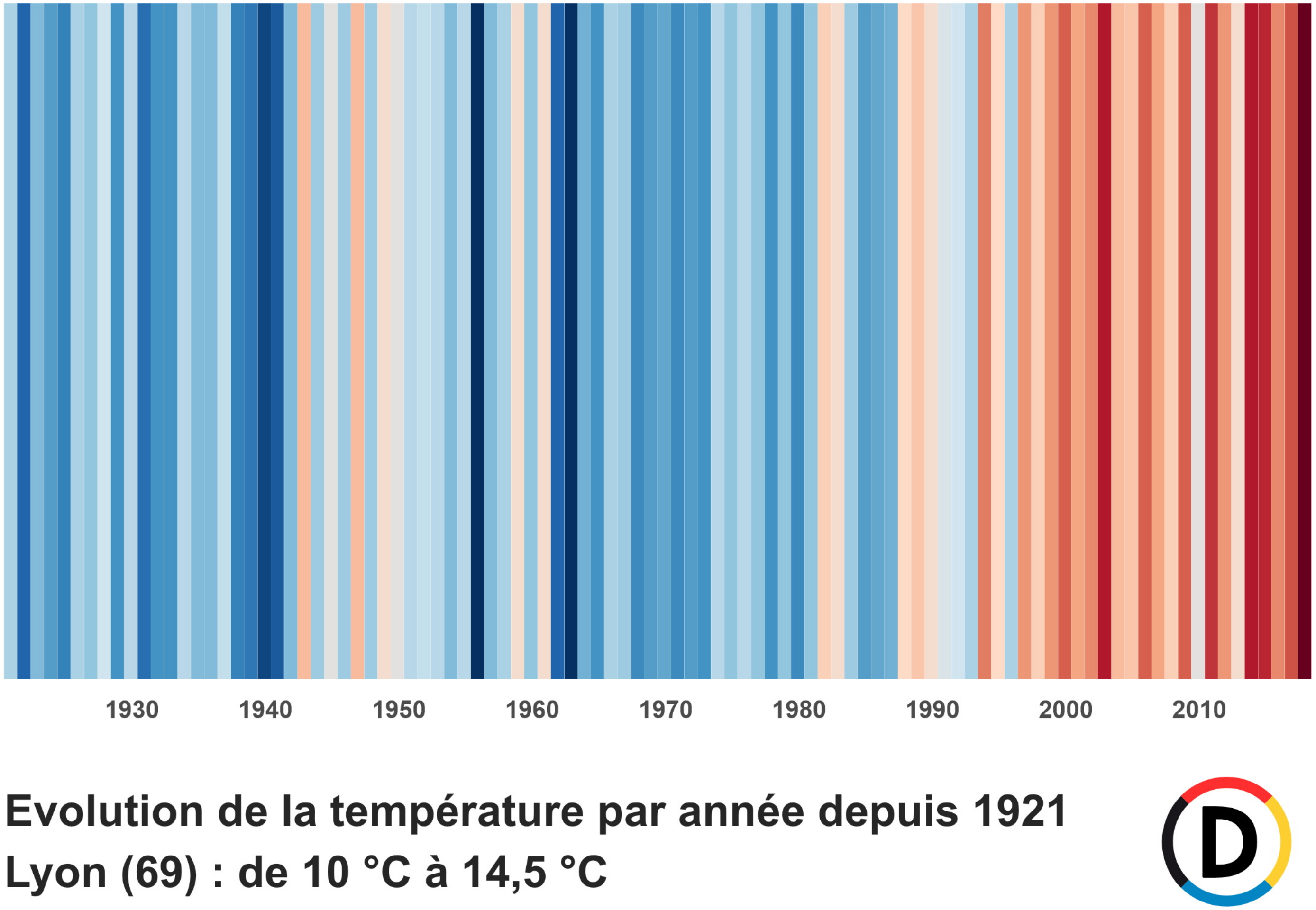

Cyclone Katrina - Sept. 2005 - Category 5

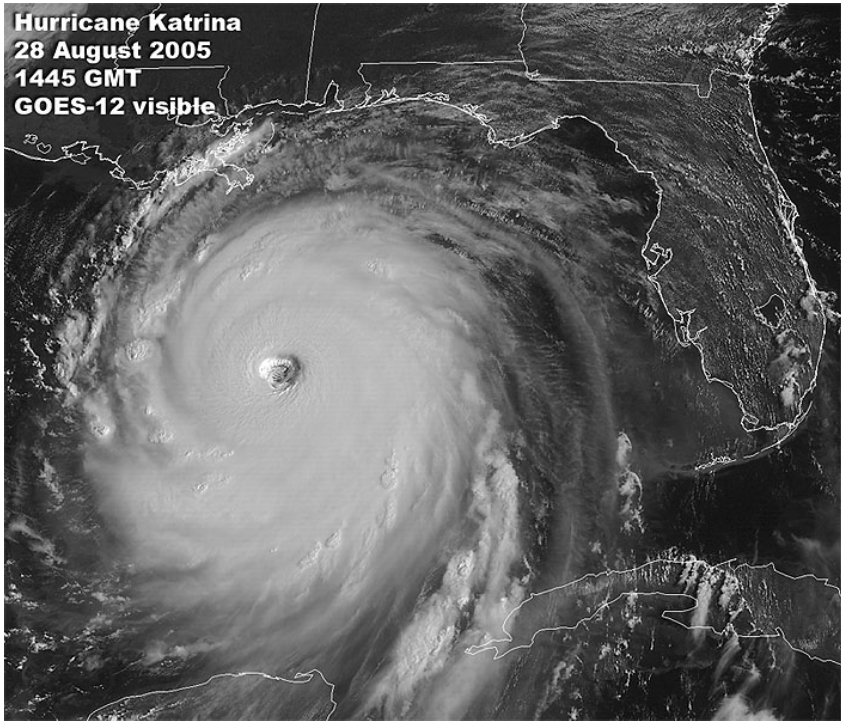

Wind gusts of 280 km/h (average during 1 minute in USA), 80% of New Orleans was flooded, Dixon *et al.*, 2006, *Nature*, **441**, 586-587

(1464 people died in the hurricane and subsequent floods according to the Louisiana Department of Health)

- **Earth's (land and marine) surface temperature from 1850 to 2020**
  expressed as 'anomaly' from 1961-90 in dashed line
  data from www.cru.uea.ac.uk

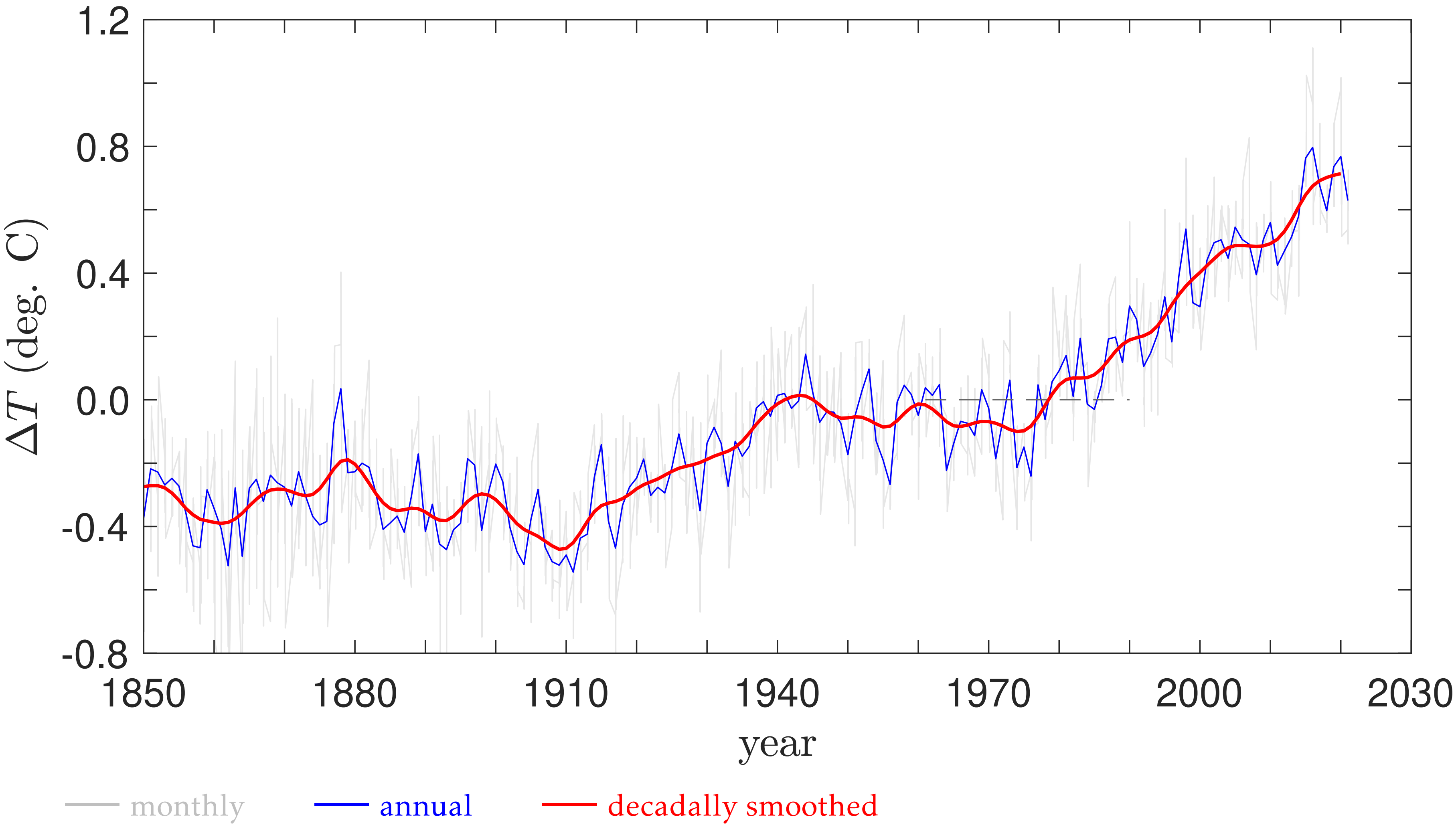

- **Near-surface wind speeds 10 meters above the Atlantic Ocean**
  Data collected by the SeaWinds scatterometer on-board NASA's QuikSCAT satellite (NASA's Jet Propulsion Laboratory)

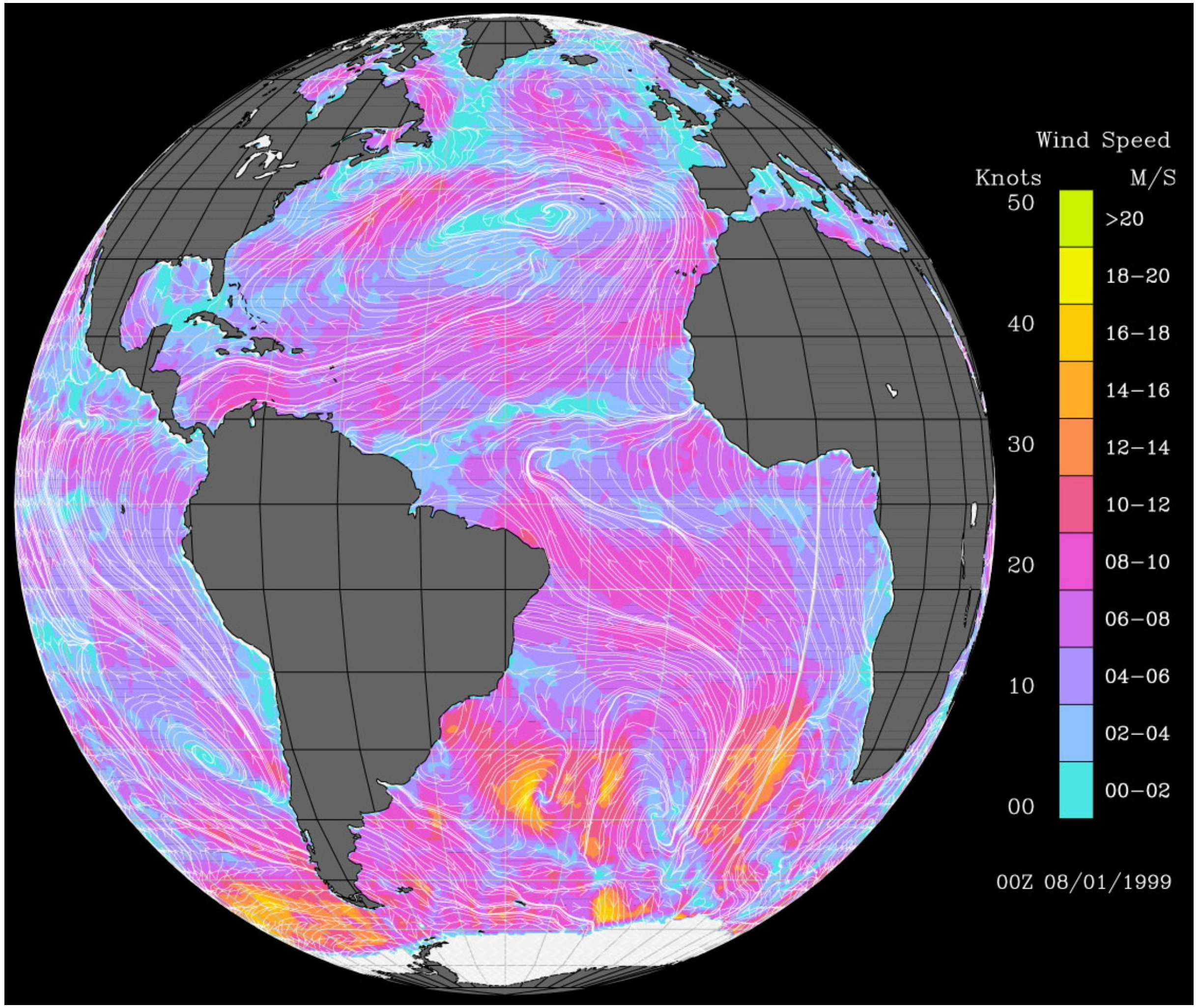

- **Eruption of the subglacial Grimsvötn volcano, Iceland, on 21 May 2011**
  An initial large plume of smoke and ash rose up to about 17 km height.
  Courtesy of Thördïs Högnadóttir, Institute of Earth Sciences, University of Iceland

Propeller hydrodynamics

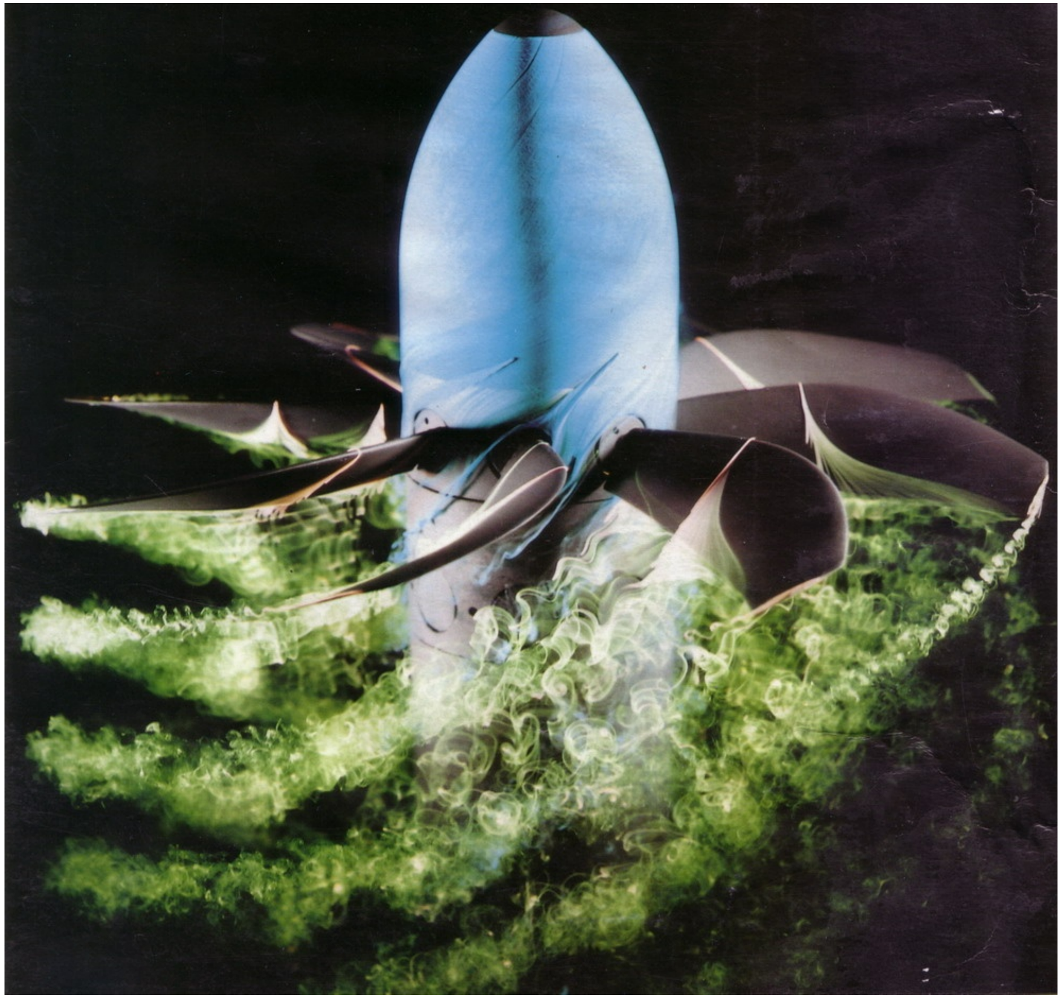

(propeller cavitation)

Hydrodynamics : azimuth thruster

Cruise vessel
Harmony of the Seas
(2016)

Azimuth thruster : configuration of marine propellers placed in pods that can be rotated to any horizontal angle (azimuth), making a rudder unnecessary. It is equipped with a new-generation exhaust gas cleaning system (multi-stream scrubbers) and also features a hull lubrication system allowing the ship to float on air bubbles (created around the hull) thus reducing drag and increasing fuel efficiency.

Aeronautics

Tip vortex behind an airplane

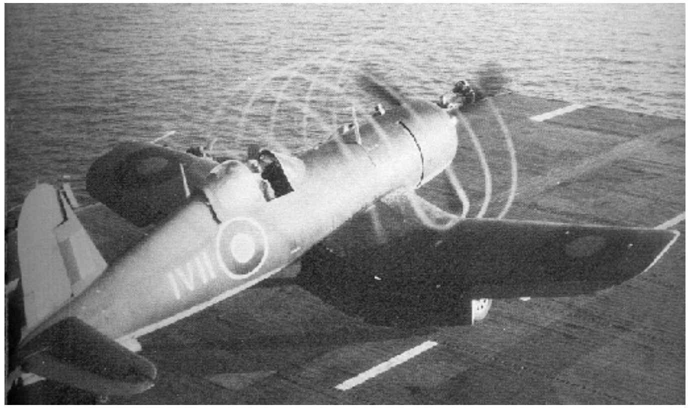

Fleet Air Arm Corsair III in 1944, (unintended) visualization of the propeller wake

Boeing 767-370/ER

- **Emirates A380-800 over Arabian Sea on Jan 7th 2017, wake turbulence sends business jet in uncontrolled descent** www.avherald.com

The CL-604 passed 1000 feet below an Airbus A380-800 while enroute over the Arabian Sea, when a short time later (1-2 minutes) the aircraft encountered wake turbulence sending the aircraft in uncontrolled roll turning the aircraft around at least 3 times, both engines flamed out, the Ram Air Turbine could not deploy possibly as result of G-forces and structural stress, the aircraft lost about 10,000 feet until the crew was able to recover the aircraft exercising raw muscle force, restart the engines and divert to Muscat.

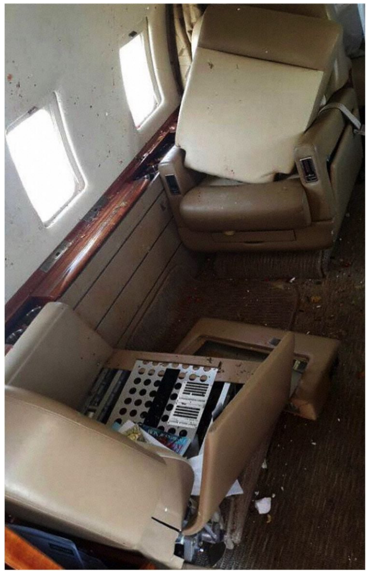

wingspan of 19.6 m (Canadair Challenger 604) versus 79.7 m (A380)

Aerodynamics of cars and trucks

Optifuel Lab 3 - Renault Trucks laboratory vehicule - aims to reduce fuel consumption by 13%

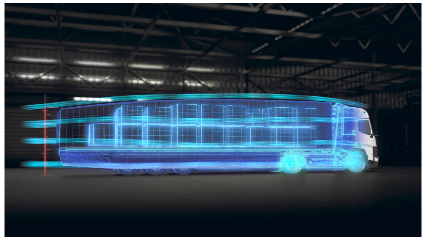

High Reynolds number wake control to improve acoustic and aerodynamic performance

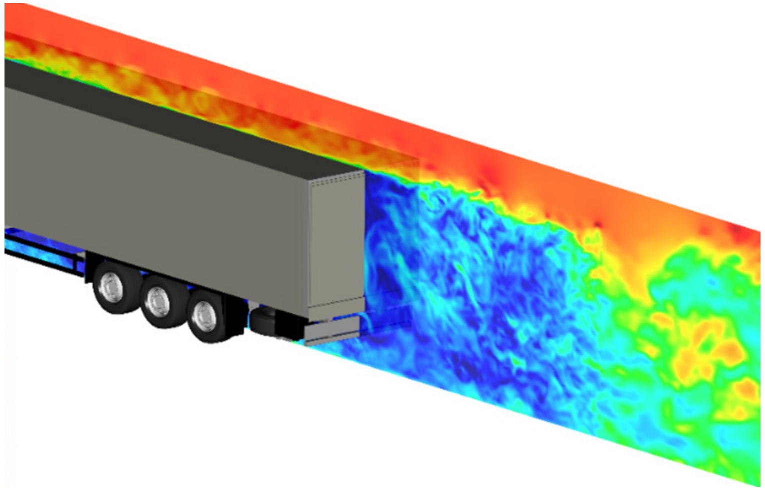

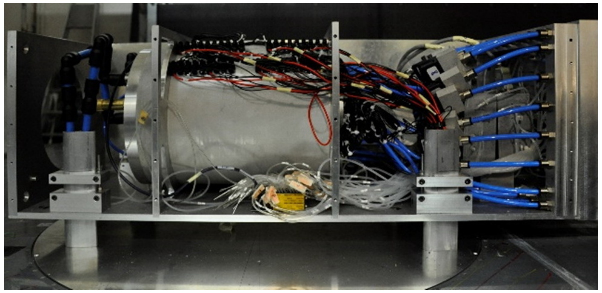

(LMFA - T. Castelain ; Renault Trucks, Pprime, PSA, Ampère)

Aerodynamics of cars and trucks (cont.)

Characterisation of the flow in a water-puddle under a rolling tire with refracted PIV method

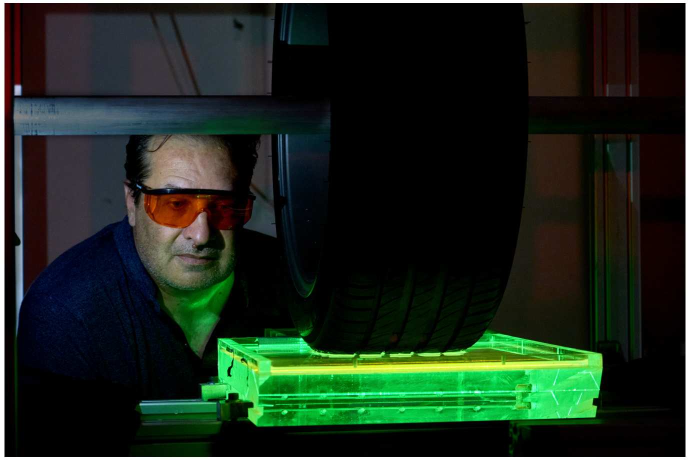

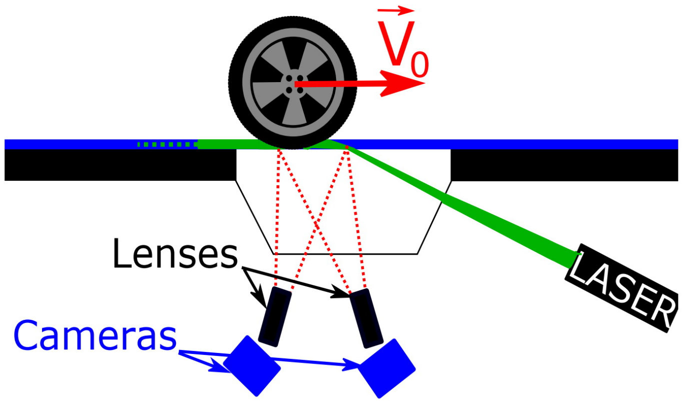

(LMFA, LHEEA, Nextflow Software, Michelin ; S. Simoens & M. Michard)

- **Elite cyclist : reduction of drag ...** (Blocken & Toparlar, *J. Wing. Eng. Ind. Aerodyn.*, 2015)
  ... when a cyclist rides in front of a car

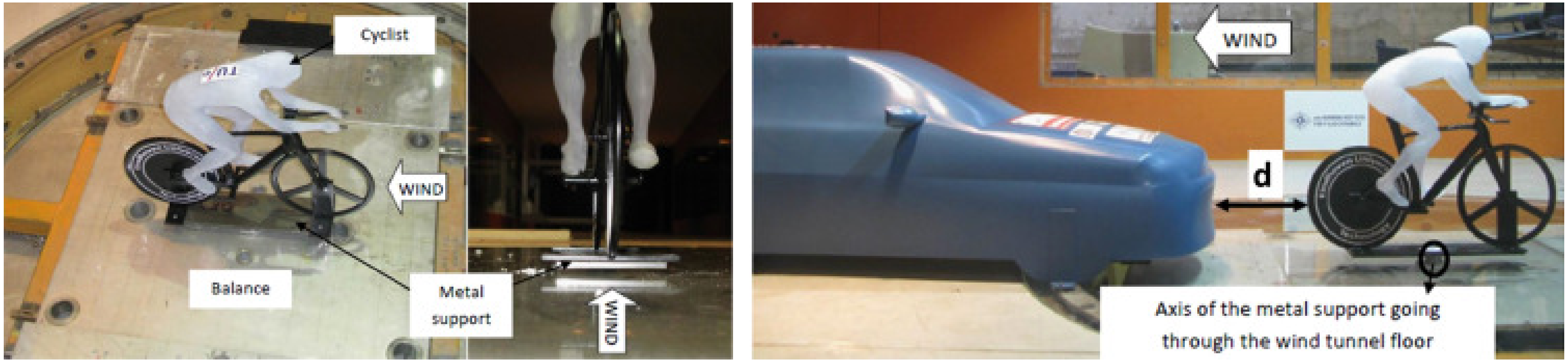

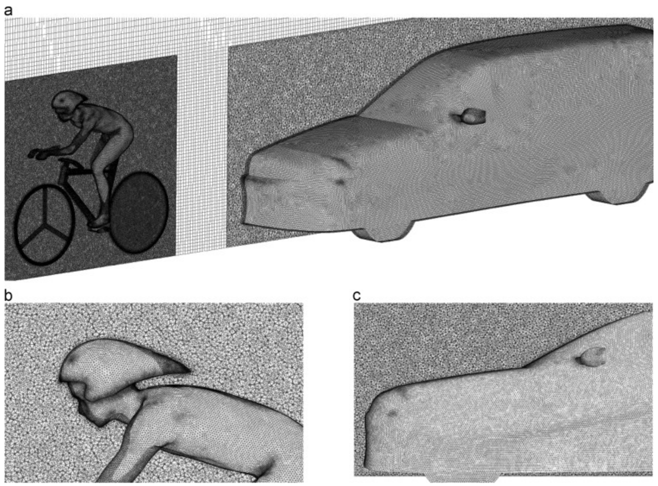

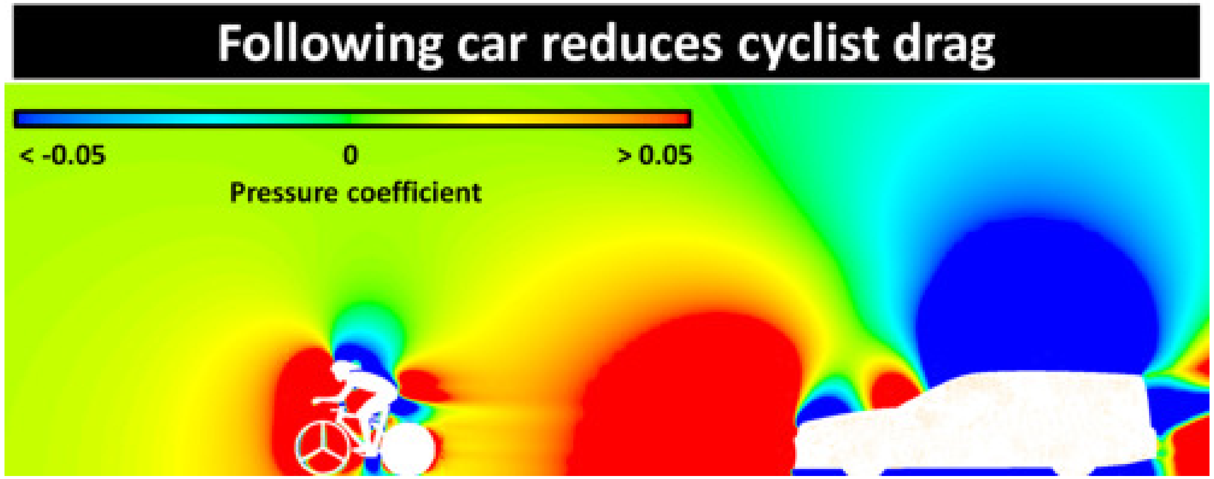

For a 50 km individual time trial : $3 \leq d \leq 10$ m $\Longrightarrow$ 1 mm $\rightarrow$ 4 s time reduction !
Recommendation for UCI, $d \geq 30$ m

Sport Aerodynamics

Influence of crosswind on a cyclist formation (Par 2019)

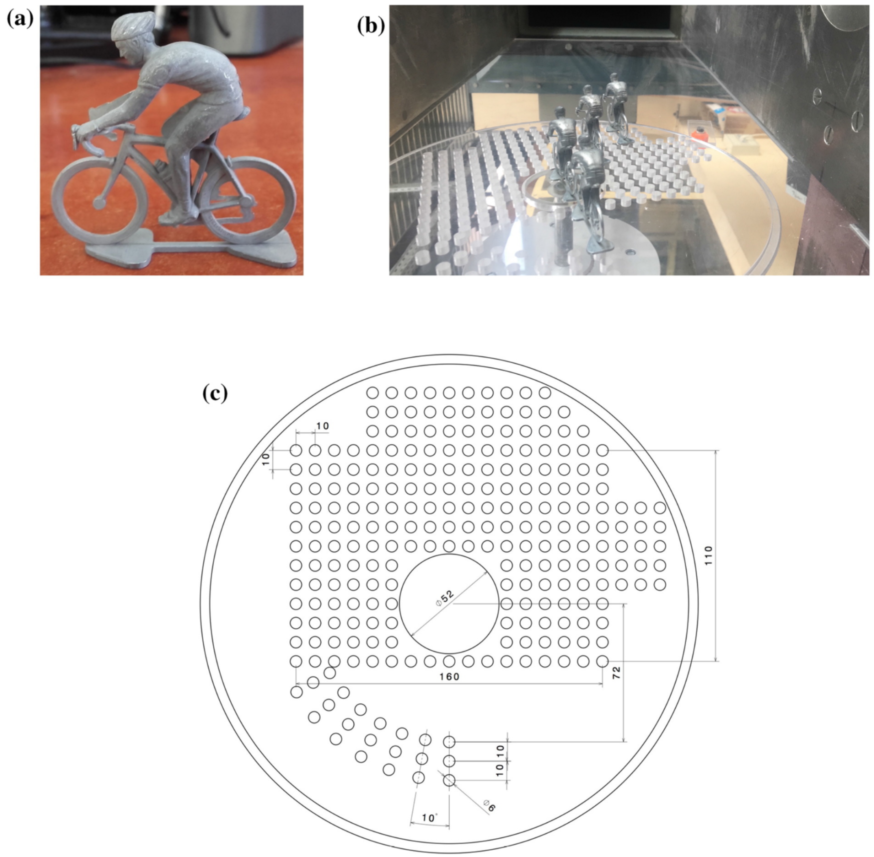

Kraemer *et al.*, 2021, *SN Applied Sciences*

Pacer formations for a top runner (Par 2021)

Massimo Marro, **Jack Leckert**‡, **Ethan Rollier**‡, Pietro Salizzoni and Christophe Bailly
Wind tunnel evaluation of novel drafting formations for an elite marathon runner
Proc. Roy Soc. A, **479**, 2023
‡ undergraduate students at Centrale Lyon

Reynolds' experience (1883) : laminar versus turbulent regime

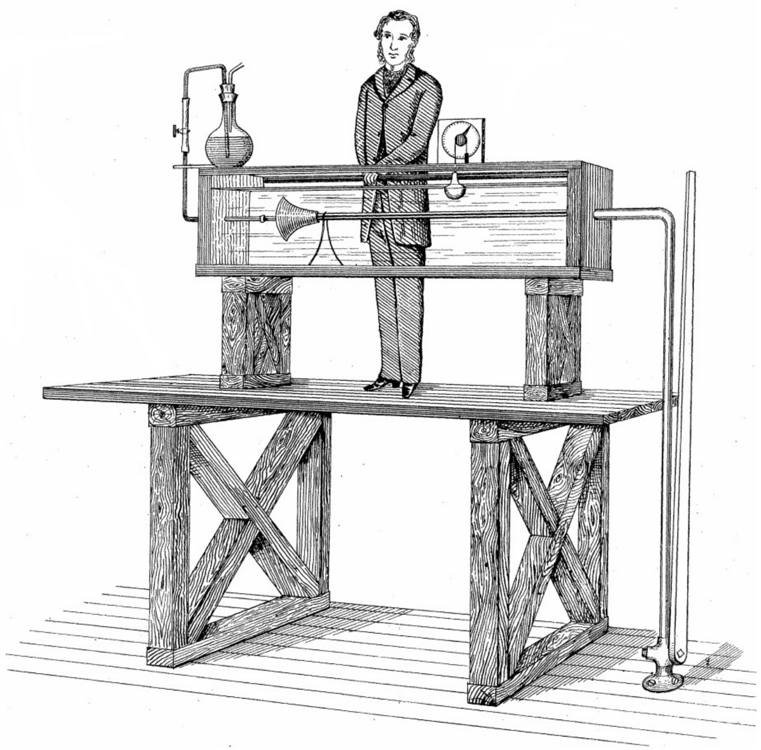

Reynolds, O., 1883, An experimental investigation of the circumstances which determine whether the motion of water shall be direct or sinuous, and of the law of resistance in parallel channels, *Phil. Trans. Roy. Soc.*, **174**, 935-982.

The general results were as follows :—

(1.) When the velocities were sufficiently low, the streak of colour extended in a beautiful straight line through the tube, fig. 3.

Fig. 3.

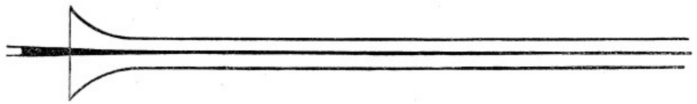

(2.) If the water in the tank had not quite settled to rest, at sufficiently low velocities, the streak would shift about the tube, but there was no appearance of sinuosity.

(3.) As the velocity was increased by small stages, at some point in the tube, always at a considerable distance from the trumpet or intake, the colour band would all at once mix up with the surrounding water, and fill the rest of the tube with a mass of coloured water, as in fig. 4.

Fig. 4.

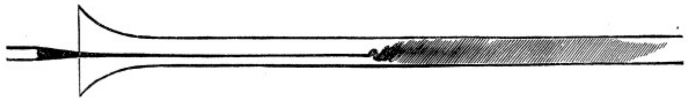

Any increase in the velocity caused the point of break down to approach the trumpet, but with no velocities that were tried did it reach this.

On viewing the tube by the light of an electric spark, the mass of colour resolved itself into a mass of more or less distinct curls, showing eddies, as in fig. 5.

Fig. 5.

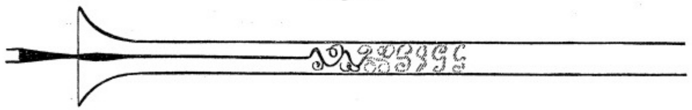

Control parameter : the Reynolds number

$$\mathrm{Re}_D = \frac{\rho U_d D}{\mu} = \frac{U_d D}{\nu} \sim \frac{\text{diffusion time}}{\text{convection time}} \sim \frac{D^2/\nu}{D/U_d}$$

The transition from a laminar to a turbulent state occurs for

$\mathrm{Re}_D \sim 2300$

D characteristic length of the mean shear
U_d bulk velocity

The concept of a turbulent regime (wrt a laminar state) was introduced by Boussinesq (1872, 1877) and Reynolds (1883, 1894)

Osborn Reynolds (1842-1912)

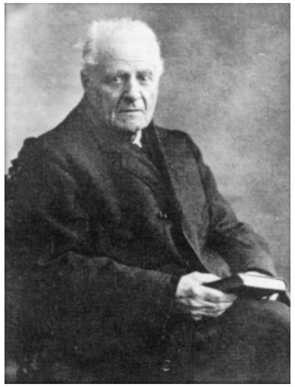

Joseph Boussinesq (1842-1929)

Turbulent subsonic (round) jet

$Re_D = u_j D/\nu$

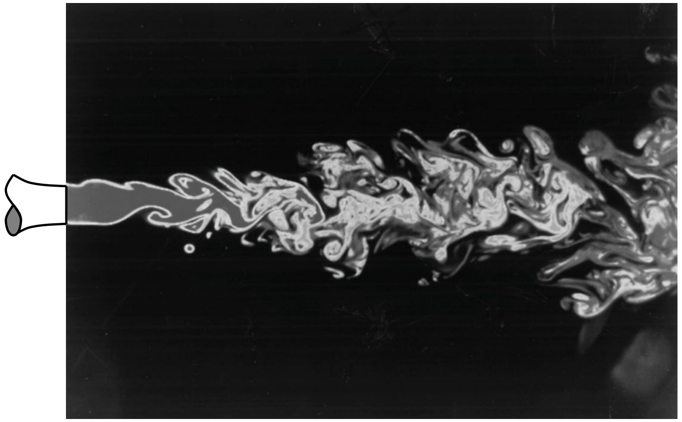

Prasad & Sreenivasan (1989)

$Re_D \simeq 4000$

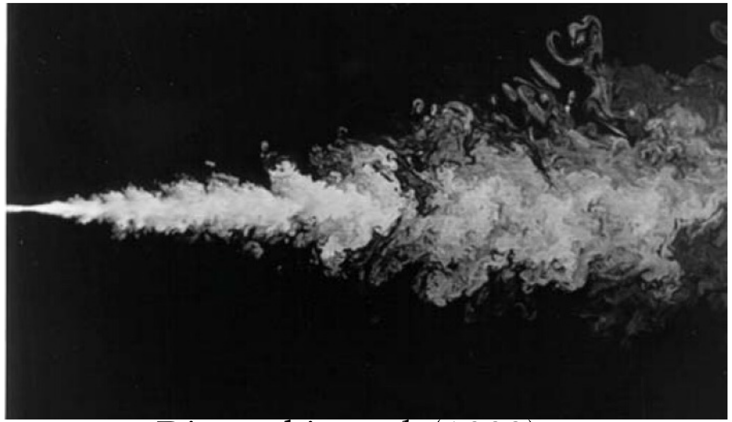

Dimotakis *et al.* (1983)

$Re_D \simeq 10^4$

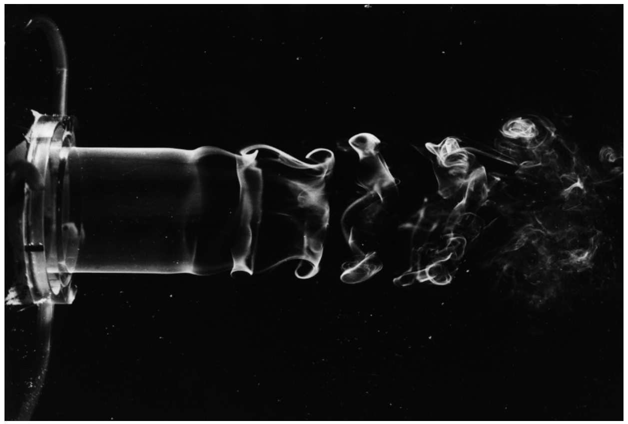

Kurima, Kasagi & Hirata (1983)

$Re_D \simeq 5.6 \times 10^3$

Ayrault, Balint & Schon (1981)

$Re_D \simeq 1.1 \times 10^4$

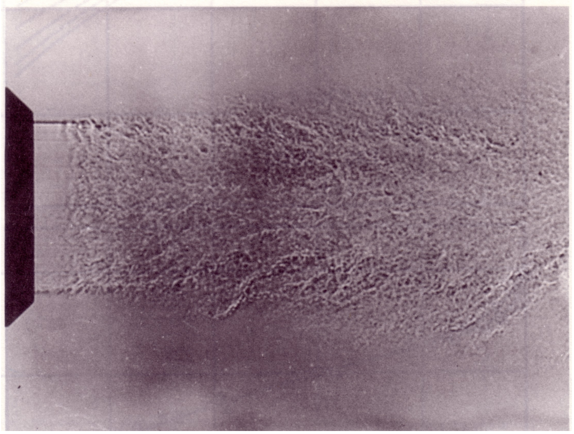

Mollo-Christensen (1963)

$Re_D = 4.6 \times 10^5$

Weak interaction between two wakes

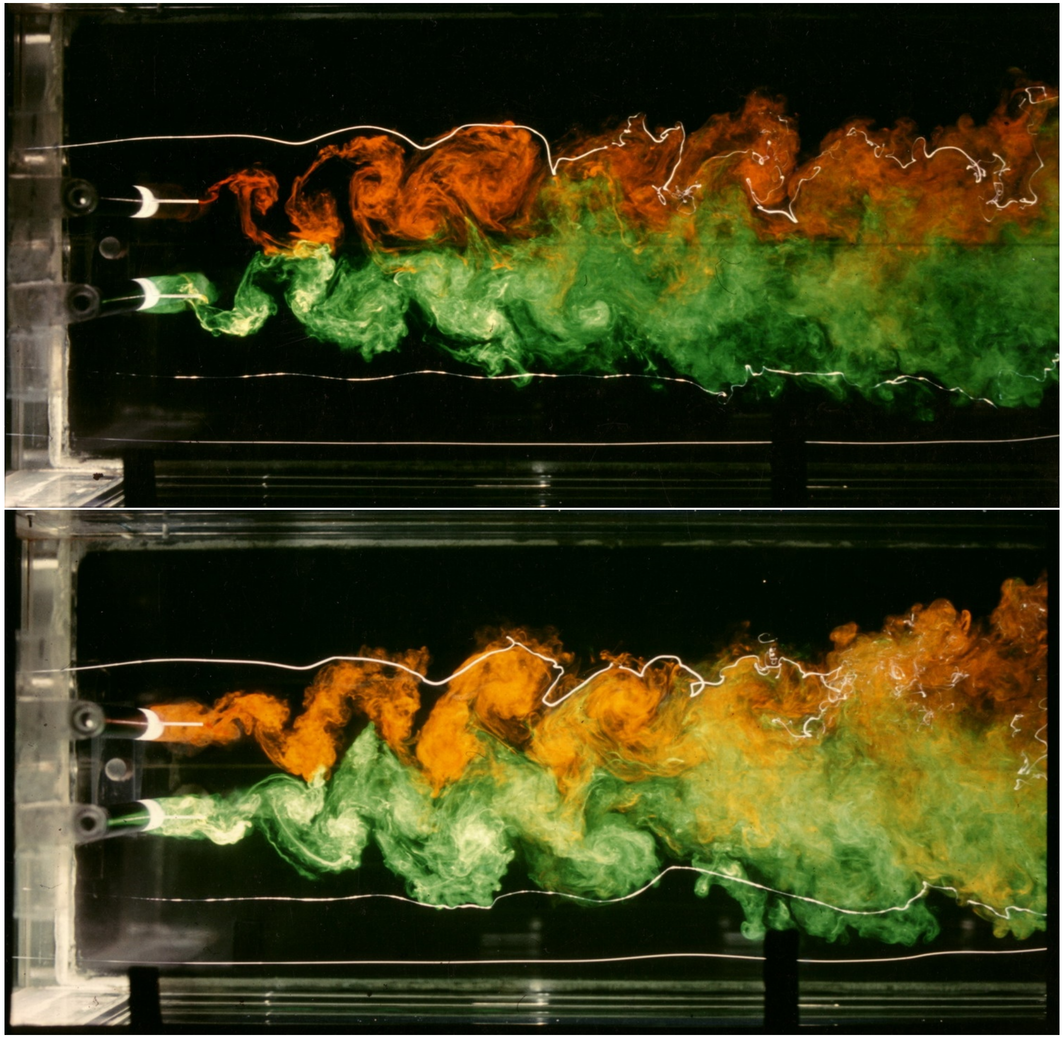

Wakes produced by a couple of cylinders with the same diameter : visualization with fluorescein and congo red dye from the trailing edge cylinders, and laser light-sheet for illumination.

Béguier, C. & Fraunié, F., 1991, Double wake flow with heat transfer, *Int. J. of Heat and Mass Transfert*, **34**(4/5), 973-982

Turbulent signals

- **Fluctuating velocity signal in the shear layer of a subsonic round jet** (measured by crossed-wire probes at $x_1 = 2D$, $x_2 = D/2$, $x_3 = 0$)

  Nozzle diameter $D = 50$ mm, exit velocity $U_j = 30$ m.s^{-1}
  $\rightsquigarrow$ Reynolds number $\mathrm{Re}_D = 10^5$

$u_1'(t)$

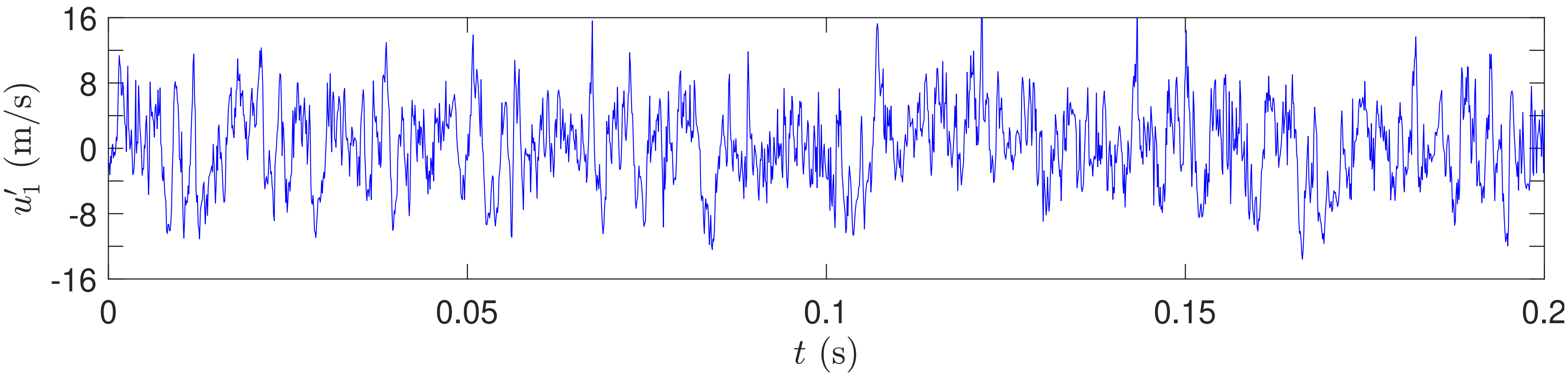

- **Fluctuating velocity signal in the shear layer of a jet (cont.)**
  $u_1'(t)$ and $u_2'(t)$ normalised by their rms value, $\xi = u_\alpha'(t)/u_{\alpha\text{rms}}$

$S_{u_1'} \simeq 0.21 \qquad T_{u_1'} \simeq 2.74$

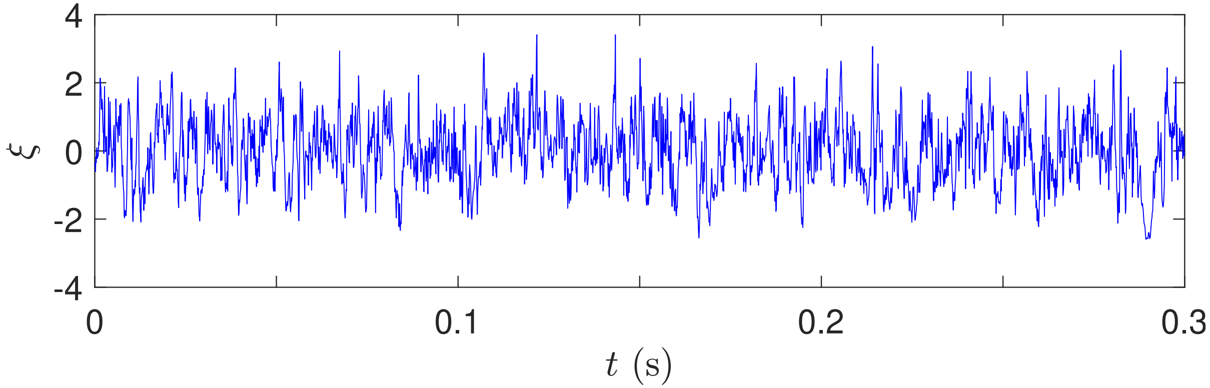

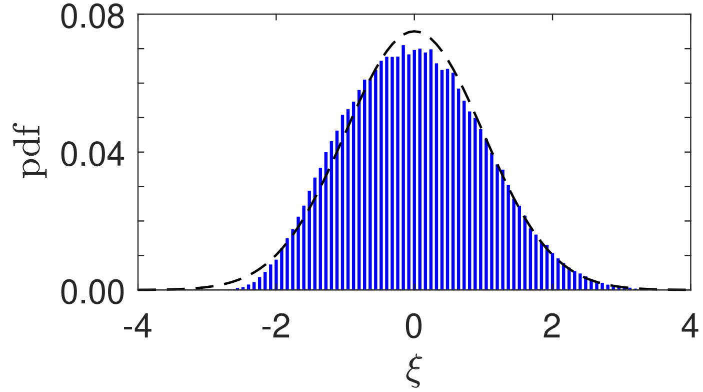

$S_{u_2'} \simeq 0.24 \qquad T_{u_2'} \simeq 2.76$

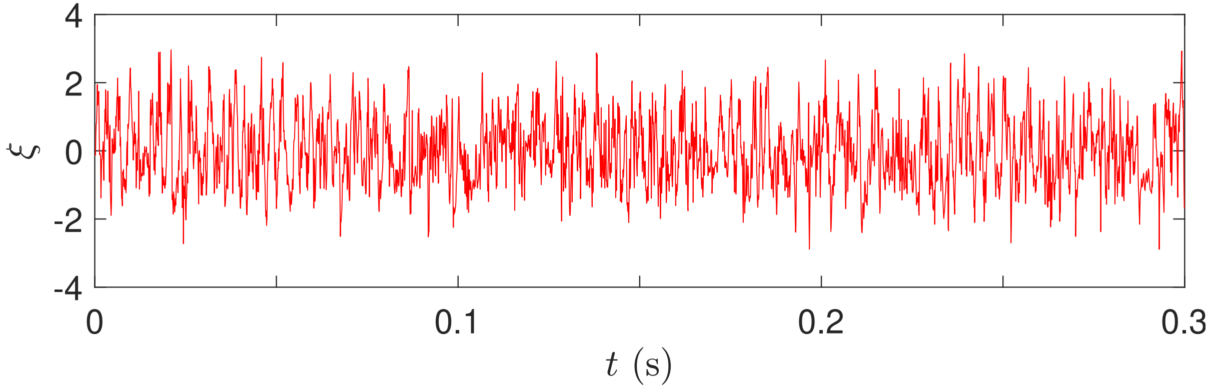

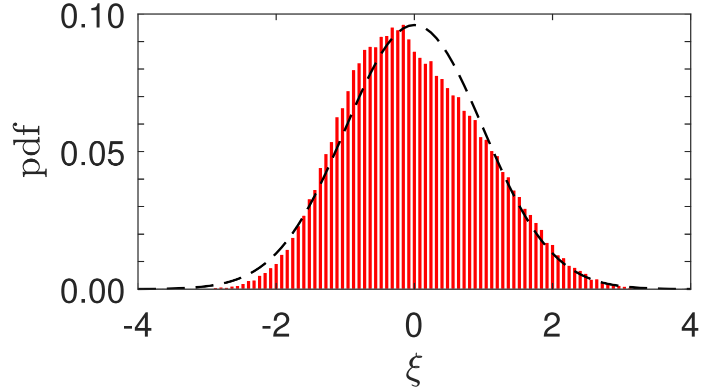

Probability density function of a random variable

Probability density function $p(\zeta)$ of a random variable ζ, for instance $\zeta = u_i'$ (centered variables to simply the writing, $u_i' = u_i - \bar{U}_i$)

$$\int_{-\infty}^{+\infty} p(\zeta) d\zeta = 1 \qquad \overline{\zeta^n} = \int_{-\infty}^{+\infty} \zeta^n p(\zeta) d\zeta$$

Standard deviation (root-mean-square), $\zeta_{\mathrm{rms}} \equiv \left(\overline{\zeta^2}\right)^{1/2} = \sigma_\zeta$

Skewness factor S_ζ, and flatness or kurtosis factor T_ζ,

$$S_\zeta \equiv \frac{\overline{\zeta^3}}{\zeta_{\mathrm{rms}}^3} \qquad T_\zeta \equiv \frac{\overline{\zeta^4}}{\zeta_{\mathrm{rms}}^4}$$

For a Gaussian (normal) distribution : $S_\zeta = 0$ and $T_\zeta = 3$

$$p(\zeta) = \frac{1}{\sqrt{2\pi}\sigma_\zeta} \exp\left(-\frac{\zeta^2}{2\sigma_\zeta^2}\right)$$

Intermittence at the edge of a free shear flow

rotational turbulent flow

$I(t) = 1$ for $t \in T_T$

$T = T_T + T_P$

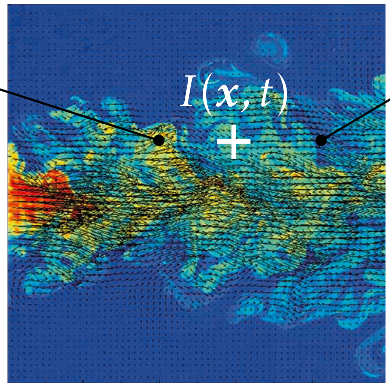

irrotational entrained ambient fluid

$I(t) = 0$ for $t \in T_P$

Intermittency factor $\gamma(\boldsymbol{x})$, the probability that the flow at $(\boldsymbol{x}, t)$ is turbulent

$$\gamma = \bar{I} = \lim_{T\to\infty} \frac{1}{T} \int_0^T I(t)dt = \frac{T_T}{T}$$

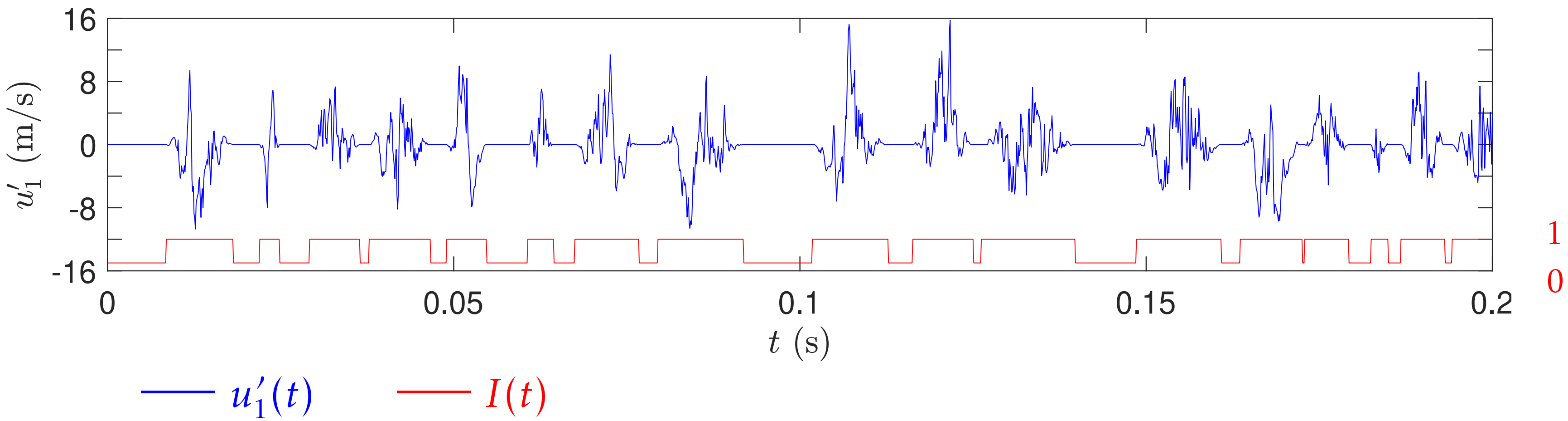

- **Intermittence at the edge of a free shear flow (cont.)**
  Importance of entrainment

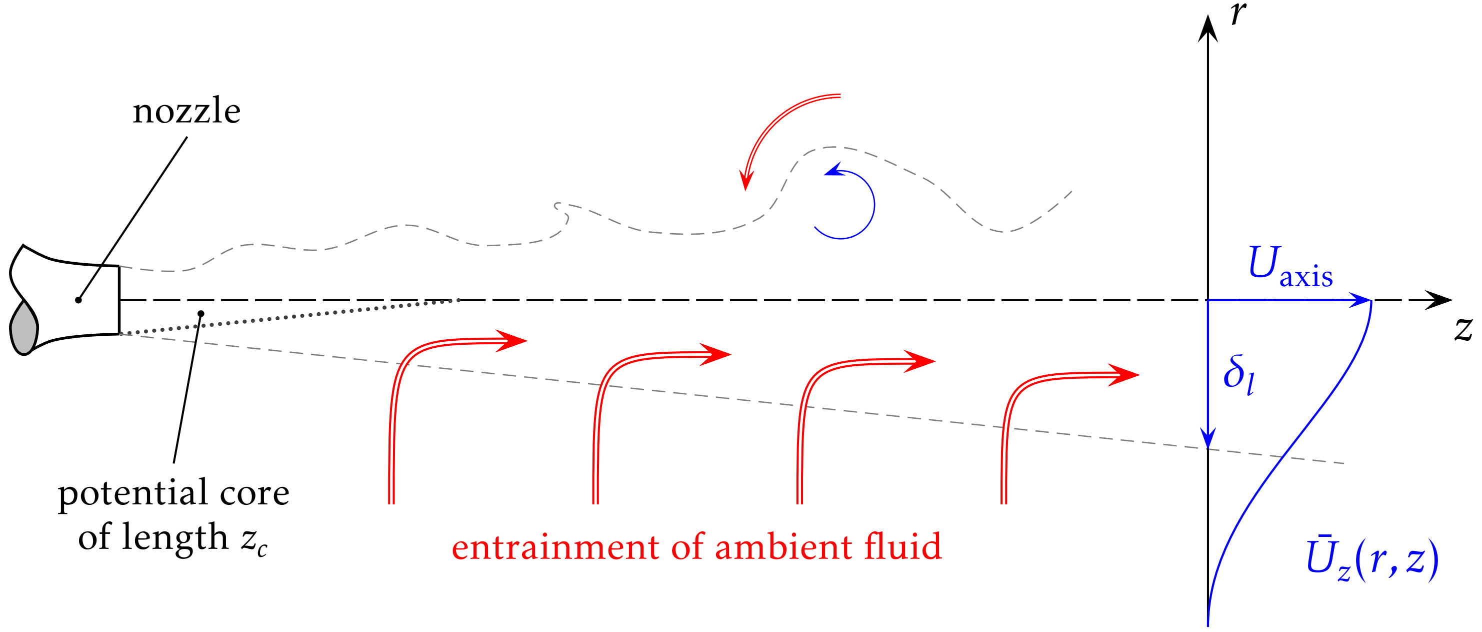

- **Intermittence at the edge of a free shear flow (cont.)**
  Importance of entrainment

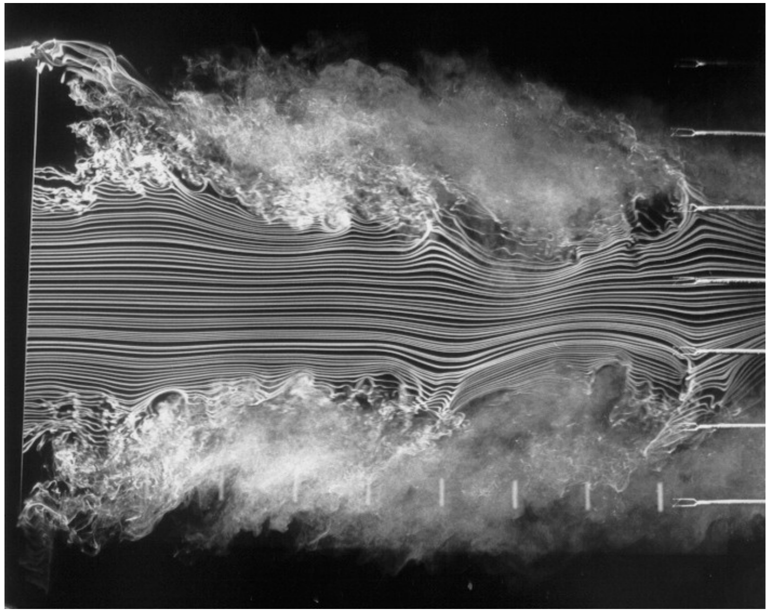

Visualization with smoke wires
$\mathrm{Re}_D \simeq 5.4 \times 10^4$
Courtesy of H. Fiedler (1987)

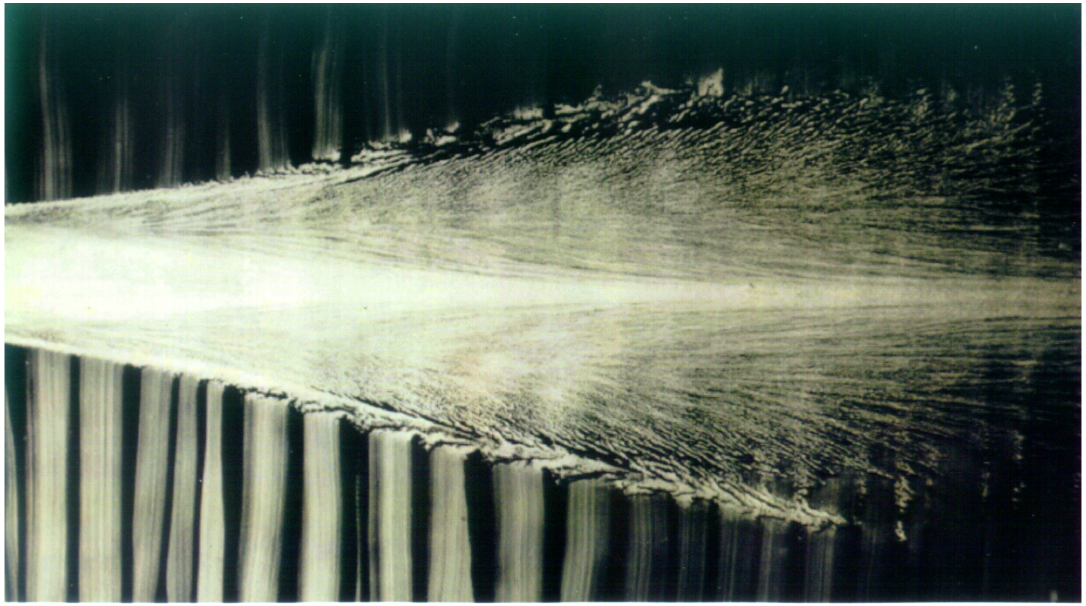

Entrainment by a turbulent round jet from a wall
$\mathrm{Re}_D = 10^6$
Florent, *J. Méc.* (1965)

Intermittence

For a centered fluctuating signal $u_1' = I u_T' + (1-I) u_P'$

where u_T' is the turbulent signal (follows a Gaussian law of variance σ_T^2), and u_P' is the potential entrained fluid ($u_P' = 0$ to simplify here, laminar flow)

$$\overline{u_1'^2} = \lim_{T\to\infty} \frac{1}{T} \int_0^T I^2 u_T'^2 dt = \lim_{T\to\infty} \frac{T_T}{T} \frac{1}{T_T} \int_{T_T} u_T'^2 dt = \gamma\, \overline{u_T'^2}$$

We get the following relations, $\overline{u_1'^2} = \gamma \overline{u_T'^2} = \gamma \sigma_T^2$, and in the same way, $\overline{u_1'^4} = \gamma\, \overline{u_T'^4} = \gamma\, 3\sigma_T^4$ for Gaussian turbulence

Hence, for the complete fluctuating signal,

variance : $\sigma^2 = \gamma \sigma_T^2$ flatness factor : $T = \dfrac{3}{\gamma}$

The flatness (kurtosis) factor is thus larger than for a Gaussian distribution, and the variance is smaller, meaning that very small and very large values of the random variable u_1' are both more probable (wrt a Gaussian pdf) : this is a feature of an intermittent signal

Intermittence (cont.)

A more general approach requires to include the contribution of the mean flow. We now consider both contributions $u_T = I u_1$ and $u_P = (1-I)u_1$. The mean velocity when $I \neq 0$ is given by

$$\overline{I u_1} = \lim_{T\to\infty} \frac{1}{T}\int_0^T I u_1 dt = \lim_{T\to\infty} \frac{1}{T}\int_{T_T} u_1 dt = \frac{T_T}{T}\bar{U}_T = \gamma\,\bar{U}_T$$

and by a similar way, $\overline{(1-I)u_1} = (1-\gamma)\bar{U}_P$.

Hence, the unconditional mean of $u_1 = u_T + u_P$ reads
$\bar{U}_1 = \gamma\bar{U}_T + (1-\gamma)\bar{U}_P$

By considering $u_1' = u_1 - \bar{U}_1$ as usual, the variance is given by (see small classe for a demonstration),

$$\overline{u_1'^2} = \gamma\overline{u_T'^2} + (1-\gamma)\overline{u_P'^2} + \gamma(1-\gamma)(\bar{U}_T - \bar{U}_P)^2$$

Zero-pressure-gradient boundary layer on a flat plate

Transition for $\mathrm{Re}_{x_1} \simeq 3.2 \times 10^5$ or equivalently for $\mathrm{Re}_\delta = U_{e1}\delta/\nu \simeq 2800$

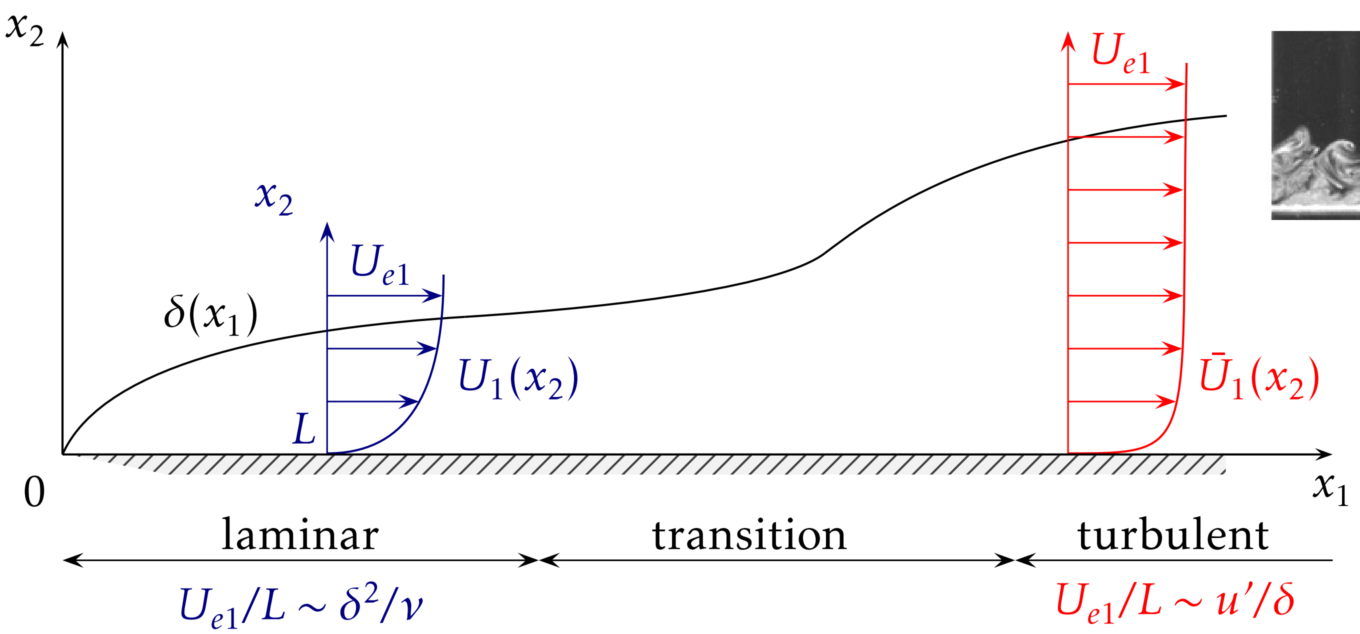

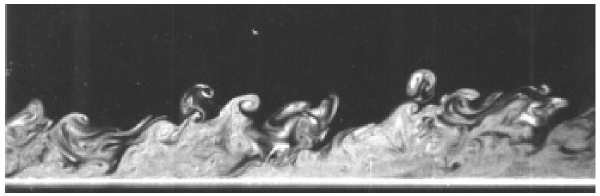

(F. Laadhari, LMFA, $\mathrm{Re}_{\delta_\theta} \simeq 1000$ $U_{e1} = 2.1$ m.s^{-1} $\delta \simeq 7$ cm)

In laminar regime, molecular diffusion $\tau \sim \delta^2/\nu$ in the transverse direction, compared with the turbulent regime, turbulent diffusion δ/u' with $u' \simeq 0.1\,U_{e1}$

Lee, Kwon, Hutchins & Monty (Melbourne University)

Intermittence in a boundary layer

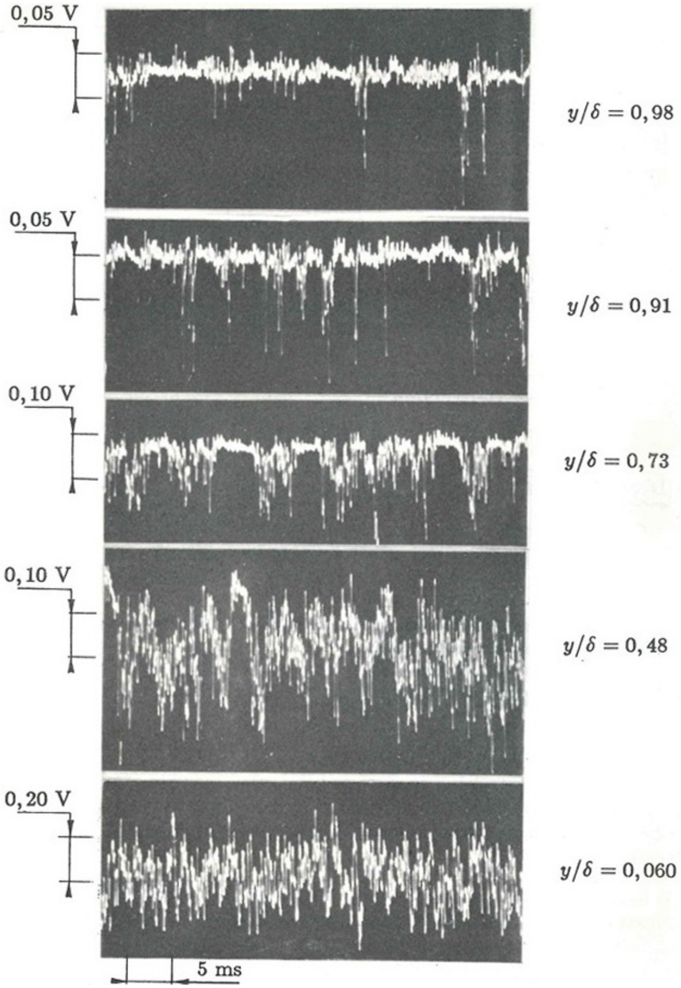

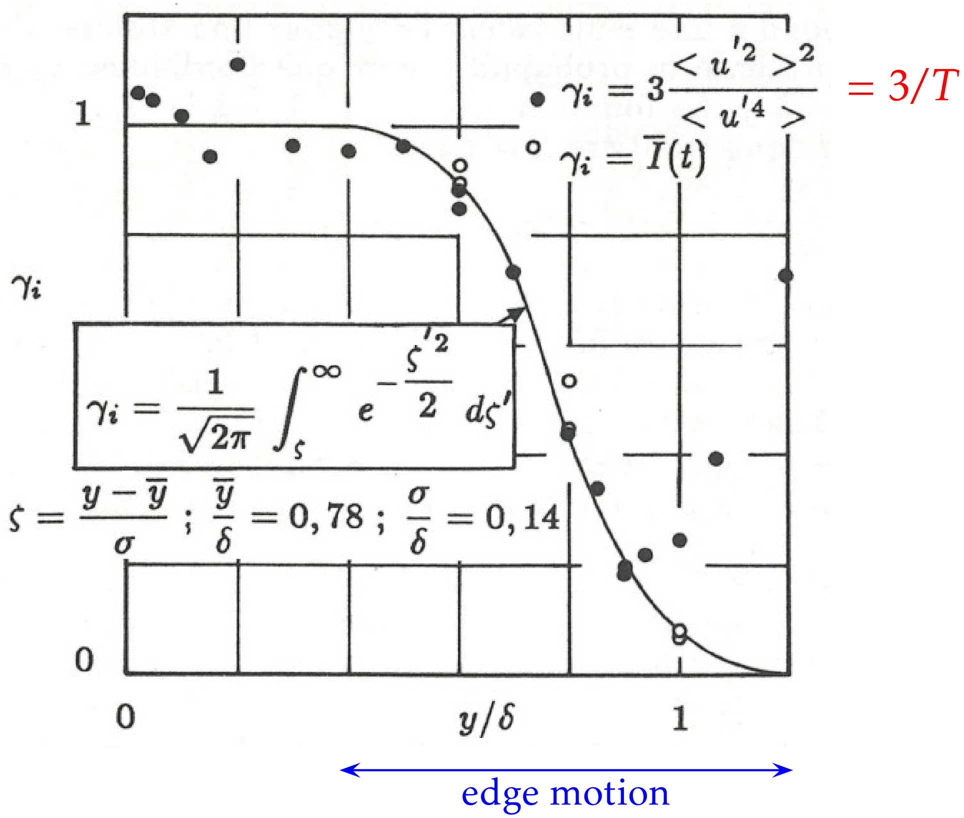

$U_\infty = 38$ m.s^{-1} (Cousteix, 1989)

The intermittency factor • γ_i (see slide 33) is here defined as the probability to be inside a turbulent burst of the boundary layer (internal flow)

Klebanoff, 1954, NACA TN 3178 ; See also Cousteix (1989)

Intermittence in a boundary layer (cont.)

Longitudinal velocity

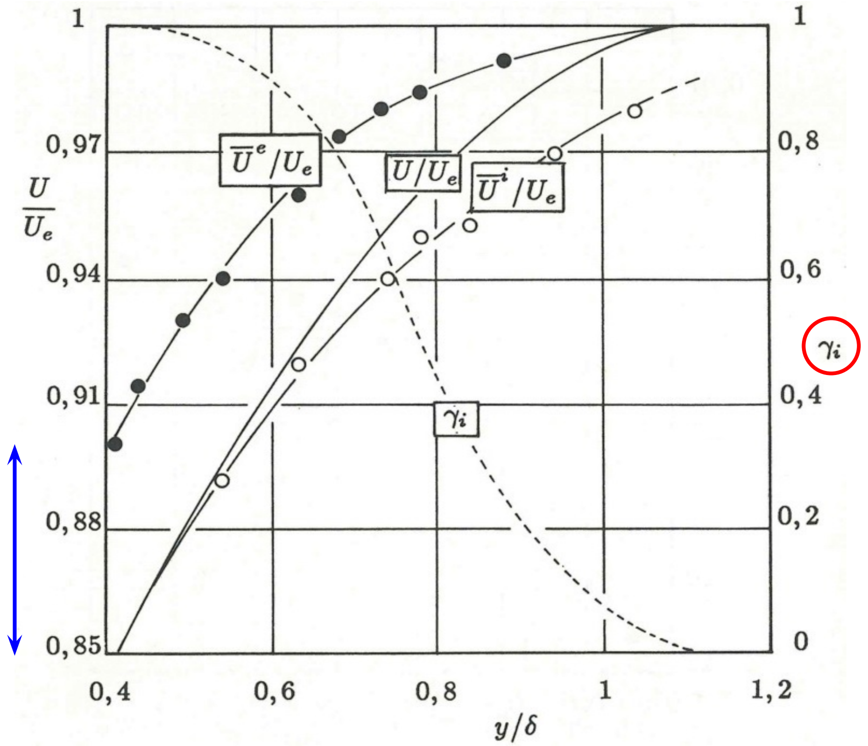

Transverse velocity

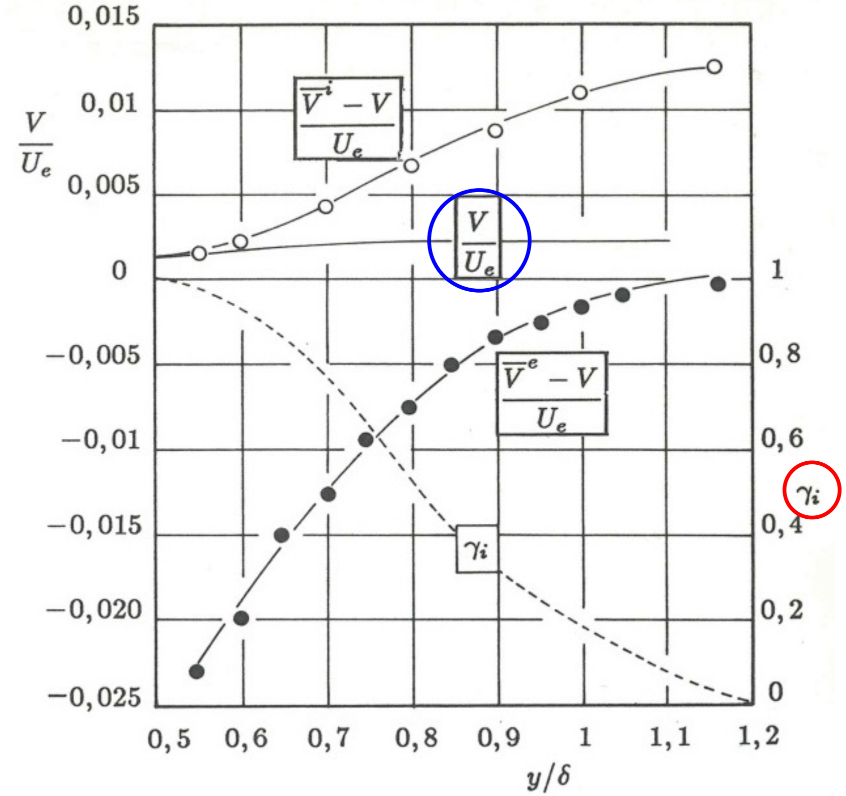

conditional means : $\overline{-}^i$ inside a turbulent burst, $\overline{-}^e$ outside a turbulent burst, entrainment of the external flow

U_e external velocity

Kovasznay, Kibens & Blackwelder, 1970, *J. Fluid Mech.*,**41**(2), 283-325 ; See also Cousteix (1989)

Reynolds decomposition

(see slides of first year, revision of Chapter 5)

Navier-Stokes equations

As a reminder, Navier-Stokes Eqs. for an incompressible flow,

$$\begin{cases} \nabla \cdot \boldsymbol{u} = 0 \\ \dfrac{\partial \boldsymbol{u}}{\partial t} + \boldsymbol{u} \cdot \nabla \boldsymbol{u} = -\dfrac{1}{\rho} \nabla p + \nu \nabla^2 \boldsymbol{u} \end{cases}$$

The acceleration of the fluid particle $D\boldsymbol{u}/Dt$ is balanced by two terms on the right hand-side :

- acceleration of the fluid particle towards the low pressure regions of the flow
- viscous diffusion of the momentum

Mean and fluctuating quantities

The statistical mean $\bar{F}(\boldsymbol{x},t)$ of a variable $f(\boldsymbol{x},t)$ is defined as

$$\bar{F}(\boldsymbol{x},t) = \lim_{N\to\infty} \frac{1}{N} \sum_{i=1}^{N} f^{(i)}(\boldsymbol{x},t)$$

where $f^{(i)}$ is the i-th realization : convenient when manipulating equations but difficult to implement in practice, or even impossible for geophysical flows !

We approximate the ensemble mean $\bar{F}$ of $f = \bar{F} + f'$ by a sufficiently long time average of one realization only :

$$\bar{F}(\boldsymbol{x}) = \lim_{T\to\infty} \frac{1}{T} \int_{t_0}^{t_0+T} f(\boldsymbol{x},t')dt'$$

Time average makes sense only if turbulence is stationary, that is statistics are independent of time (refer to signal processing, associated with the hypothesis of ergodicity).

Reynolds decomposition

For a given variable f, Reynolds decomposition $f = \bar{F} + f'$ into mean and fluctuating (deviation) components is introduced.

- Centered fluctuating field

  $f \equiv \bar{F} + f'$ with $\overline{f'} = 0$ $\quad (f' = f - \bar{F}$ and $\overline{f'} = \bar{F} - \bar{F} = 0)$

- Rule for the product of two any variables (f and g here),

  $fg \equiv (\bar{F} + f')(\bar{G} + g') = \bar{F}\bar{G} + \bar{F}g' + f'\bar{G} + f'g'$

  and thus, $\overline{fg} = \bar{F}\,\bar{G} + \bar{F}\,\overline{g'} + \overline{f'}\,\bar{G} + \overline{f'g'} = \bar{F}\,\bar{G} + \overline{f'g'}$

$$\boxed{\overline{fg} = \bar{F}\,\bar{G} + \overline{f'g'}} \qquad (1)$$

Reynolds decomposition for velocity : $U_i \equiv \bar{U}_i + u_i'$ with $\overline{u_i'} = 0$

$\bar{U}_i$ part which can be reasonably calculated

u_i' part which must be modelled (turbulent fluctuations)

Reynolds Averaged Navier-Stokes (RANS) equations

Assumptions (to simplify) : incompressible flow $\nabla \cdot \boldsymbol{U} = 0$
and homogeneous fluid, constant density ρ

How to determine the transport equation of the mean quantities ?

First, substitute the Reynolds decomposition and then,
average the equation,

$$\frac{\partial(\bar{U}_i + u'_i)}{\partial x_i} = 0 \qquad \overline{\frac{\partial(\bar{U}_i + u'_i)}{\partial x_i}} = 0 \qquad \Longrightarrow \qquad \frac{\partial \bar{U}_i}{\partial x_i} = 0 \tag{2}$$

Second, substract the averaged equation from the instantaneous one,
which provides

$$\frac{\partial U_i}{\partial x_i} = 0 \quad \text{and} \quad \frac{\partial \bar{U}_i}{\partial x_i} = 0 \qquad \Longrightarrow \qquad \frac{\partial u'_i}{\partial x_i} = 0$$

The mean flow field $\bar{\boldsymbol{U}}$ is incompressible, and so is the fluctuating field $\boldsymbol{u}'$

- **Reynolds Averaged Navier-Stokes (RANS) equations**

$$\frac{\partial(\rho U_i)}{\partial t} + \frac{\partial}{\partial x_j}\left(\rho U_i U_j\right) = -\frac{\partial p}{\partial x_i} + \frac{\partial \tau_{ij}}{\partial x_j} \qquad \tau_{ij} = 2\mu D_{ij}$$

By introducing the Reynolds decomposition, and taking the average

$U_i \equiv \bar{U}_i + u'_i \qquad p \equiv \bar{P} + p' \qquad \tau_{ij} \equiv \bar{\tau}_{ij} + \tau'_{ij}$

$$\frac{\partial(\rho \bar{U}_i)}{\partial t} + \frac{\partial(\rho \bar{U}_i \, \bar{U}_j)}{\partial x_j} = -\frac{\partial \bar{P}}{\partial x_i} + \frac{\partial}{\partial x_j}\left(\bar{\tau}_{ij} - \rho \overline{u'_i u'_j}\right) \tag{3}$$

The term $-\rho \overline{u'_i u'_j}$ is Reynolds stress tensor, unknown, thus leading to a closure problem for Eqs. (2) and (3). Generally this term is larger than the mean viscous stress tensor $\bar{\boldsymbol{\tau}}$ except for wall bounded flows, where the viscosity effects become preponderant close to the wall (no-slip condition, $\overline{u'_i u'_j} = 0$ at the wall)

Turbulent kinetic energy and dissipation

The turbulent kinetic energy k_t and the turbulent dissipation ϵ are two key quantities to examine turbulence dynamics. By introducing the Reynolds decomposition, using the rule (1), we obtain

for the kinetic energy

$$\frac{\overline{U_i U_i}}{2} = \frac{\bar{U}_i \bar{U}_i}{2} + \frac{\overline{u_i' u_i'}}{2} \qquad k_t \equiv \frac{\overline{u_i' u_i'}}{2}$$

k_t is the turbulent kinetic energy

for the dissipation

$$2\nu \overline{D_{ij} D_{ij}} = 2\nu \bar{D}_{ij} \bar{D}_{ij} + 2\nu \overline{d_{ij}' d_{ij}'} \qquad \epsilon \equiv 2\nu \overline{d_{ij}' d_{ij}'}$$

ϵ ($m^2.s^{-3}$) is the dissipation rate of k_t ($m^2.s^{-2}$) induced by the molecular viscosity

- **Concept of turbulent viscosity for turbulence models**
  introduced by Boussinesq (1877)

  To model Reynolds stress tensor $-\rho\overline{u_i'u_j'}$, one defines by analogy with the viscous stress tensor $\overline{\overline{\boldsymbol{\tau}}}$,

$$-\rho\overline{u_i'u_j'} = 2\mu_t\bar{D}_{ij} - \frac{2}{3}\rho k_t\delta_{ij} = \mu_t\left(\frac{\partial\bar{U}_i}{\partial x_j} + \frac{\partial\bar{U}_j}{\partial x_i}\right) - \frac{2}{3}\rho k_t\delta_{ij} \tag{4}$$

  where $\mu_t = \mu_t(\boldsymbol{x}, t)$ is the turbulent viscosity, a property of the flow field, and not of the fluid as for the molecular viscosity. It is thus expected that $\mu_t = \mu_t(\mathrm{Re})$.

  The introduction of a turbulent viscosity for closing Reynolds stress tensor is an assumption, so not always verified by turbulent flows. In addition, it is also assumed in Eq. (4) that the turbulent viscosity remains positive (thus inducing specific behaviours in terms of energy transfer)

- **Illustration for a free subsonic round jet**
  M = 0.16 and $\mathrm{Re}_D = 9.5 \times 10^4$ (from Hussein, Capp & George, 1994)

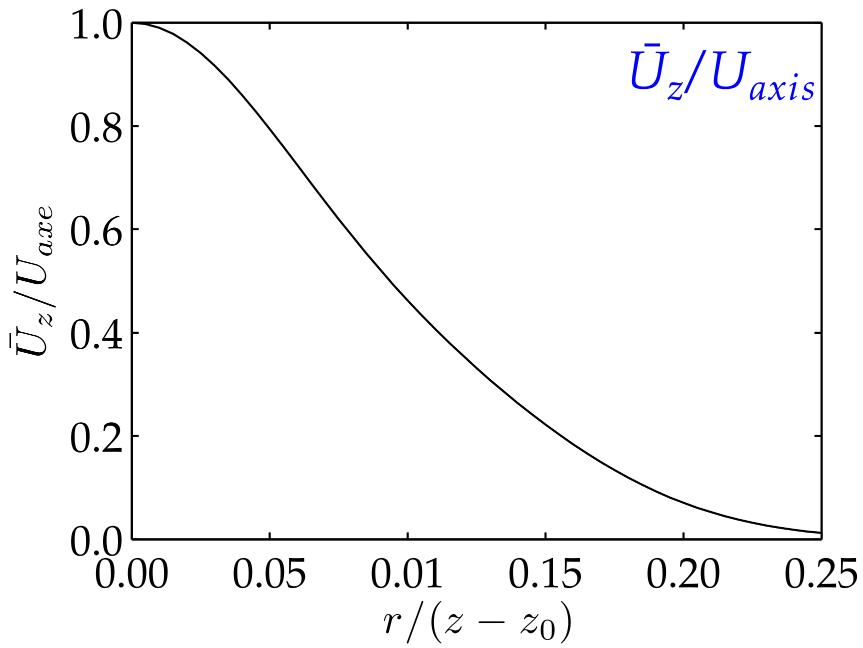

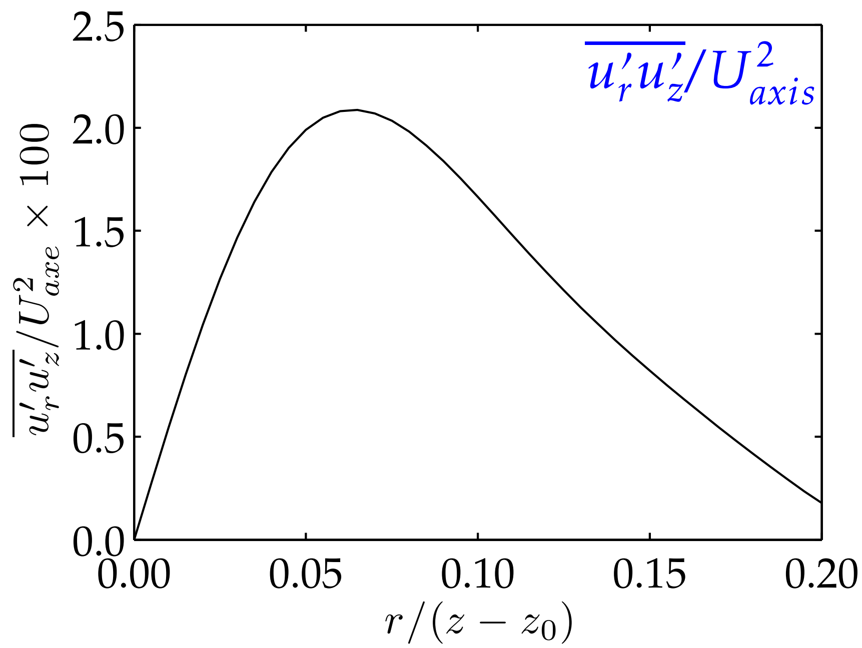

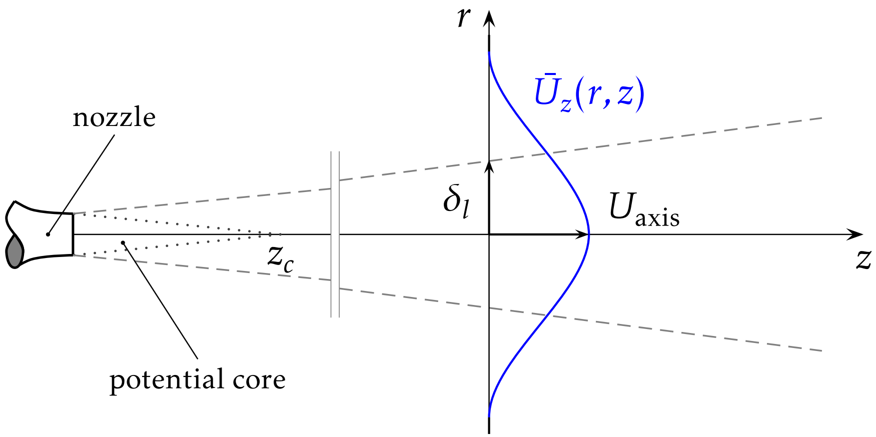

$$\rho \overline{u'_r u'_z} \simeq -\mu_t \frac{\partial \bar{U}_z}{\partial r}$$

self-similar solution $\dfrac{r}{\delta_l} \sim \dfrac{r}{z - z_0}$

Concept of turbulent viscosity for turbulence models (cont.)

Reynolds Averaged Navier-Stokes (RANS) equations

$$\frac{\partial \bar{U}_i}{\partial x_i} = 0$$

$$\frac{\partial(\rho \bar{U}_i)}{\partial t} + \frac{\partial(\rho \bar{U}_i \bar{U}_j)}{\partial x_j} = -\frac{\partial(\bar{P} + \frac{2}{3}\rho k_t)}{\partial x_i} + \frac{\partial}{\partial x_j}\Big(2(\mu + \mu_t)\bar{D}_{ij}\Big)$$

How to compute the turbulent viscosity $\nu_t(\boldsymbol{x}, t)$?

From dimensional arguments, the product of a velocity scale by a length scale, for example $\nu_t \sim k_t^{1/2} \times k_t^{3/2}/\epsilon \sim k_t^2/\epsilon$, and then write a transport equation for k_t and ϵ to obtain the famous $k_t - \epsilon$ model.

There are about 200 turbulent viscosity models published in the literature !
(see Wilcox and Durbin books among others)

- **Turbulent kinetic energy budget**
  (the demonstration can be found in textbooks)

$$\underbrace{\frac{\partial(\rho k_t)}{\partial t} + \frac{\partial(\rho k_t \bar{U}_j)}{\partial x_j}}_{\text{advection by the mean flow}} = \underbrace{-\rho\overline{u_i' u_j'}\frac{\partial \bar{U}_i}{\partial x_j}}_{\text{production } \mathcal{P}} \underbrace{-\rho\epsilon}_{\text{dissipation}}$$

$$+ \underbrace{\frac{\partial}{\partial x_k}\left(-\frac{1}{2}\rho\overline{u_i' u_i' u_k'} - \overline{p' u_k'} + \overline{u_i' \tau_{ik}'}\right)}_{\text{transport terms}}$$

Case of homogeneous turbulence ?
(when turbulence statistics are independent of space)

Heuristic interpretation of the production term $\mathcal{P}$

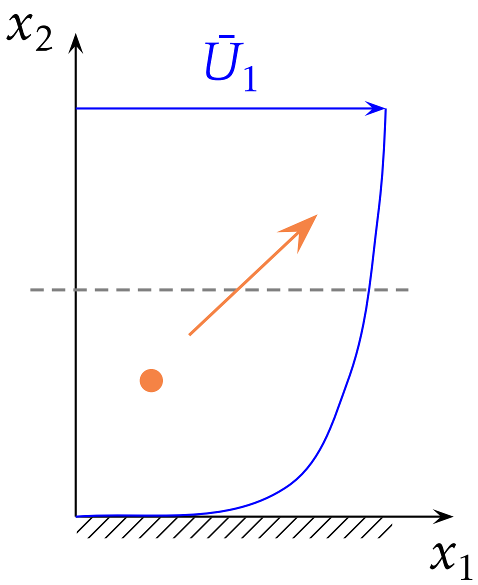

$$\begin{cases} u_2' > 0 \\ u_1' < 0 \end{cases} \qquad \overline{u_1' u_2'} < 0$$

$$\begin{cases} u_2' < 0 \\ u_1' > 0 \end{cases} \qquad \overline{u_1' u_2'} < 0$$

$\mathcal{P} \simeq -\rho \overline{u_1' u_2'} \dfrac{d\bar{U}_1}{dx_2} > 0$ is thus expected !

The production term $\mathcal{P}$ is – in general – a transfer from the shear mean flow $\bar{\boldsymbol{U}}$ to the turbulent field $\boldsymbol{u}'$; but becomes always a positive transfer term using a turbulent viscosity model (4), a drawback of turbulence models

Scales and energy cascade

Scales

Large scale in $\mathcal{O}(L, u')$ – associated with the geometry (cavity, cylinder, jet, wake, car, airfoil, pipe, ...) and thus with the size of the flow itself

$\rightsquigarrow$ energy transfer (basically) from large scale structures to small scale structures, but this transfer is stopped by the molecular viscosity when

$$\frac{\partial \boldsymbol{u}'}{\partial t} \sim \nu \nabla^2 \boldsymbol{u}'$$

Small scale in $\mathcal{O}(l_\eta, u_\eta)$ – known as Kolmogorov (viscous) scales with $\mathrm{Re} = u_\eta l_\eta / \nu = 1$. Kolmogorov's length scale l_η plays a fundamental role in experiments (sampling frequency) as well as in numerical simulations (grid size)

- **Turbulent mixing layer (Brown & Roshko, 1974)**

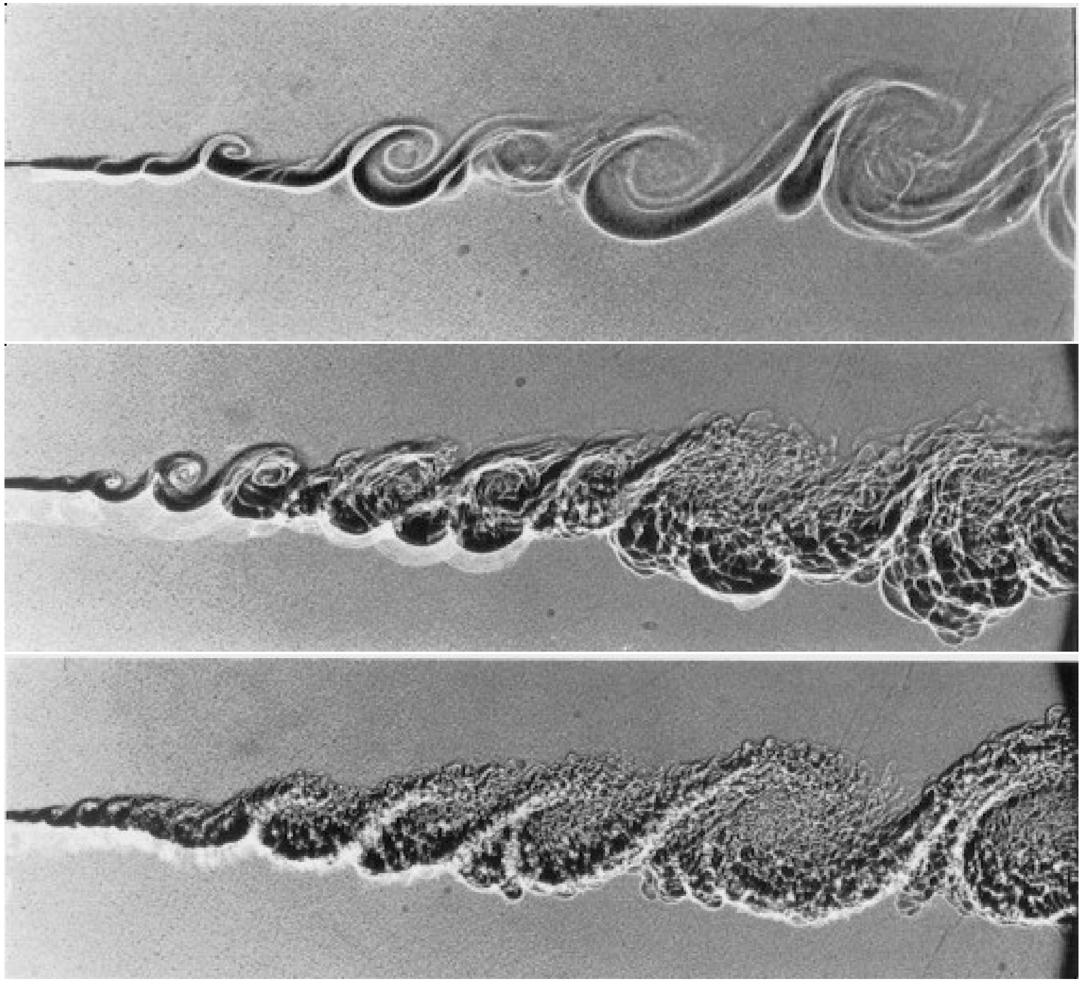

(Shadowgraphs with a spark source)

Energy cascade in a mixing layer by increasing the Reynolds number (through pressure and velocity, ×2 for each view)

More small-scale structures are produced without basically altering the large-scale ones (linked to the transition process, as shown by Winant & Browand, 1974)

Anatol Roshko (1923-2017)

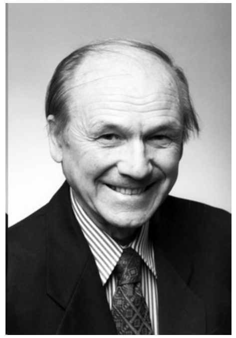

- **Local nature of the energy cascade in space**

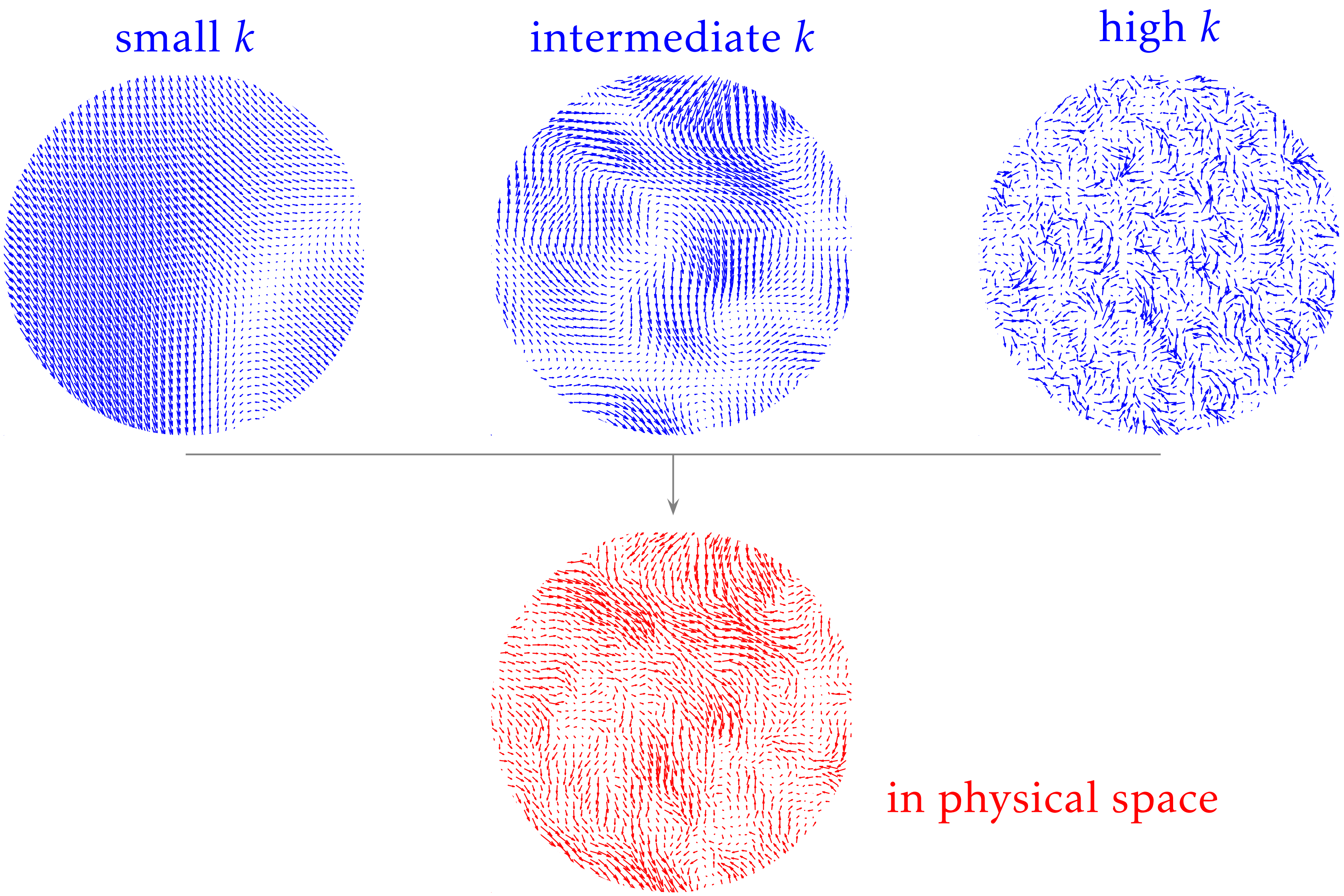

- **Taylor-Green vortex flow**
  Re = 3000 on a 384^3 grid at times $t = 0$, $t = 9$ and $t = 18$ (dimensionless variables)
  From Fauconnier *et al.* (2013)

Vortex structures colored by z-vorticity

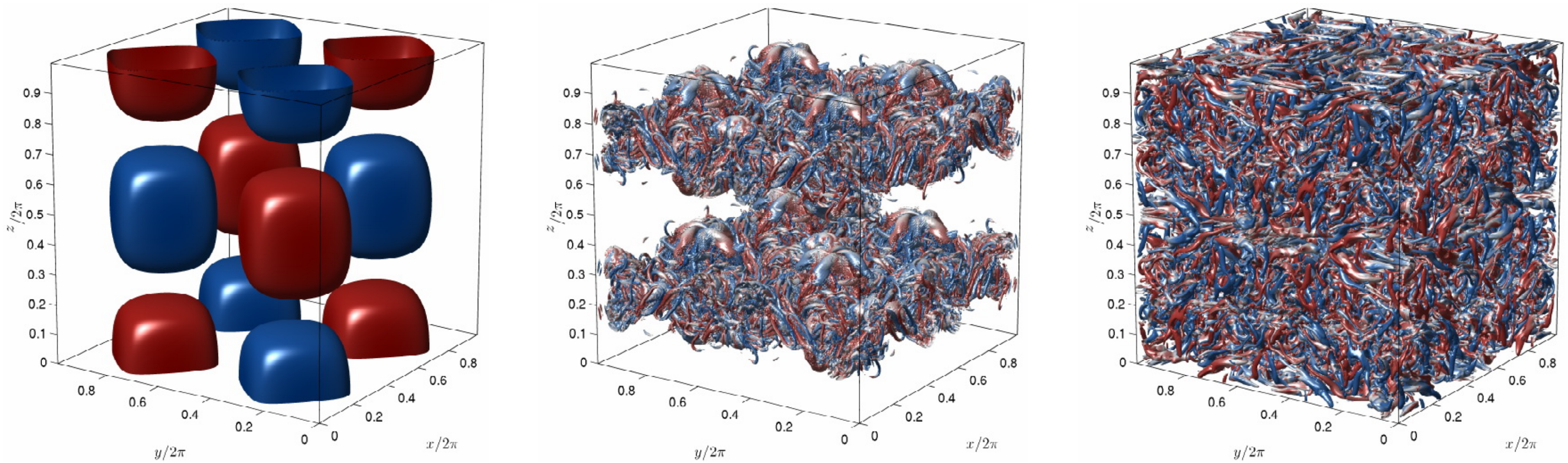

Introduction to the energy cascade

From Navier-Stokes Eqs, we can calculate the power developed by the viscous friction,

$$P = \boldsymbol{u}' \cdot \nu \nabla^2 \boldsymbol{u}' = u_i' \nu \frac{\partial^2 u_i'}{\partial x_j \partial x_j} = \nu \frac{\partial}{\partial x_j}\left(u_i' \frac{\partial u_i'}{\partial x_j} \right) - \nu \frac{\partial u_i'}{\partial x_j} \frac{\partial u_i'}{\partial x_j}$$

$$= \underbrace{\nu \nabla^2 \left(\frac{\boldsymbol{u}'^2}{2} \right)}_{\text{(a)}} - \underbrace{\nu \nabla \boldsymbol{u}' : \nabla \boldsymbol{u}'}_{\text{(b)}}$$

(a) = diffusion of the kinetic energy

(b) = rate ϵ of dissipation (per unit mass) of the kinetic energy on average, see slide 44

High velocity gradients (and thus small scale activity) are required to ensure dissipation

Introduction to the energy cascade

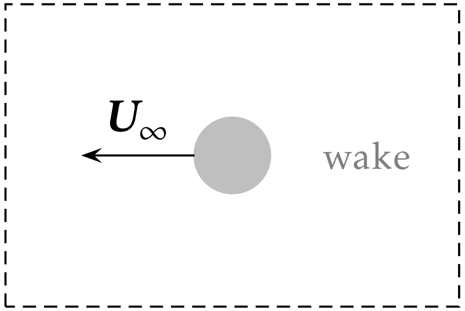

e.g. energy dissipated by the motion at U_∞ of a sphere of diameter D

$$\boldsymbol{F}_D \cdot \boldsymbol{U}_\infty \propto C_D(\mathrm{Re}_D)\rho U_\infty^3 D^2$$

The power developed by the drag force F_D, that is $F_D U_\infty$, is balanced by the energy dissipated with the flow $\rho\mathcal{V} \times \epsilon$ where $\mathcal{V} \propto D^3$

$$\epsilon \propto C_D\left(\mathrm{Re}_D\right)\frac{U_\infty^3}{D}$$

- As $\mathrm{Re}_D \to 0$, $\nu \nearrow$ as well as energy which must be dissipated to move inside the fluid
- As $\mathrm{Re}_D \to \infty$, $C_D = C_D(\mathrm{Re}_D) \simeq \mathrm{cst}$

  $\epsilon \propto \dfrac{U_\infty^3}{D}$ is independent of the viscosity

- **Drag coefficient for a smooth sphere** (adapted from Clift, Grace, & Weber, 1978)

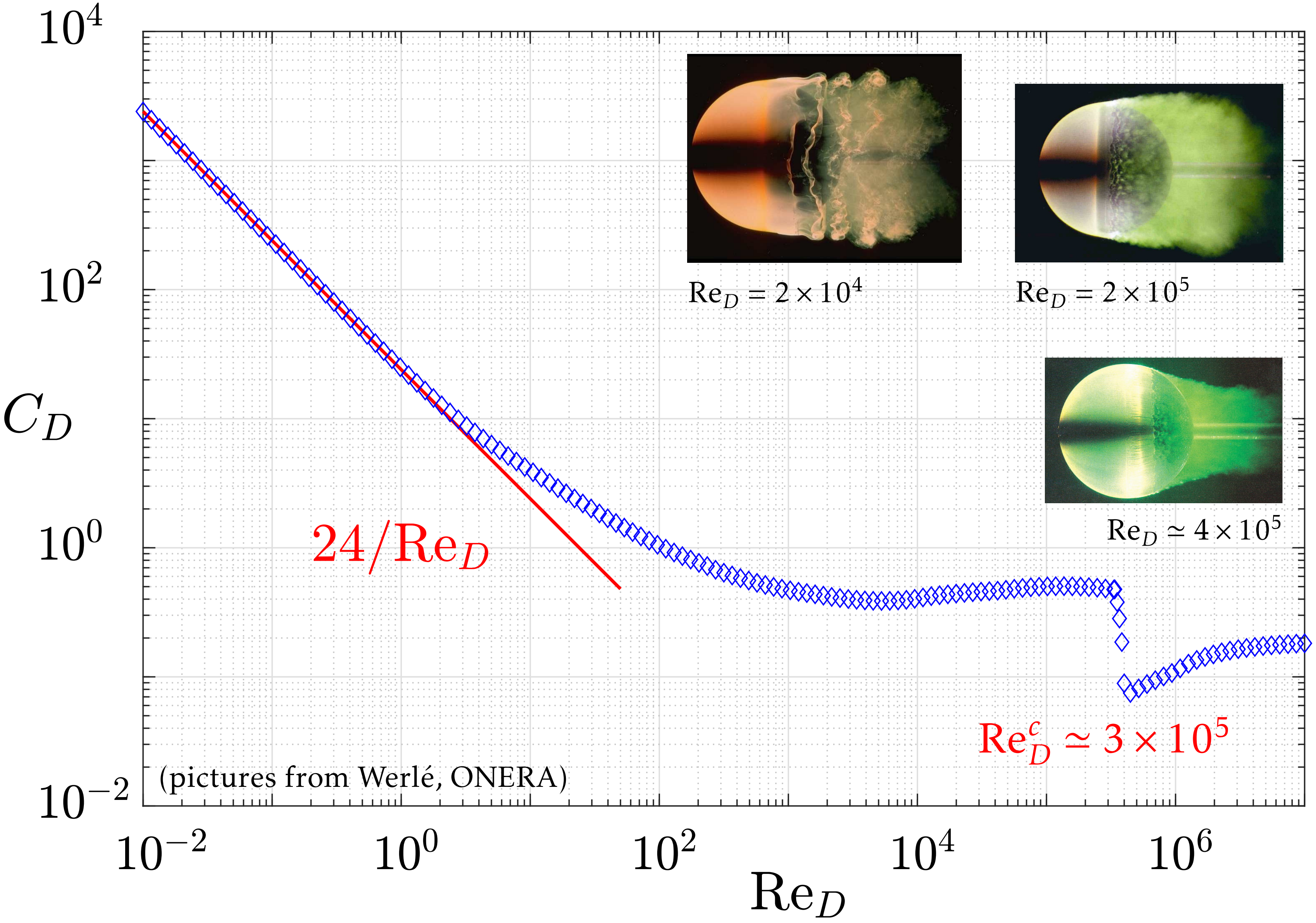

and paradox of the energy cascade ...

For high Reynolds number flows when ν goes to zero, the rate of dissipation per unit mass ϵ becomes independent of the viscosity ν

$\epsilon = \nu \overline{|\nabla \boldsymbol{u}'|^2} \simeq \text{cst}$, leading to possible singularities for the velocity gradients $\nabla \boldsymbol{u}' \nearrow$ (fragmentation of fine scales, still a research topic in turbulence)

Energy cascade - Kolmogorov (1941)

Kinetic energy is not conserved from scales to scales, but the rate of transfer of this energy ϵ is conserved

$$\begin{cases} \dfrac{l_\eta u_\eta}{\nu} = 1 \qquad \epsilon = \dfrac{u_\eta^3}{l_\eta} \qquad l_\eta = \nu^{3/4} \epsilon^{-1/4} \\ \epsilon = \dfrac{u'^3}{L} \qquad \mathrm{Re}_L = \dfrac{u' L}{\nu} \qquad \dfrac{L}{l_\eta} \sim \mathrm{Re}_L^{3/4} \end{cases}$$

As an illustration

Soccer ball

$D = 22$ cm

$U_\infty = 100$ km.h$^{-1} \simeq 27.8$ m.s^{-1}

$\mathrm{Re}_D \simeq 4.1 \times 10^5$

$u' \simeq 0.15 U_\infty$

$L \simeq D/2$

$\mathrm{Re}_L \simeq 3.1 \times 10^4$

$l_\eta \simeq L/\mathrm{Re}_L^{3/4} \simeq 4.7 \times 10^{-5}$ m !

$$k = \frac{\omega}{U_\infty} \quad f = \frac{U_\infty}{l_\eta} \simeq 5.8 \times 10^5 \text{ Hz}$$

Free shear flows
(flows in the absence of walls!)

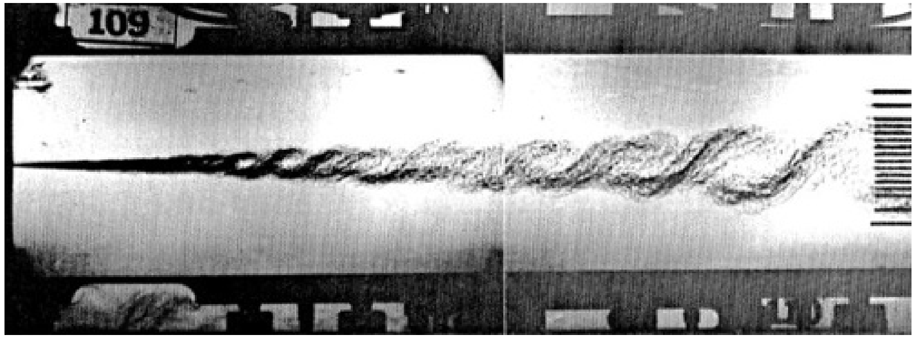

Composite schlieren of the free shear layer, with the two streams injected parallel to each other. The upper stream is 100% N2 while the lower is a mixture of 1/3 He and 2/3 Ar, with $M_1 = 0.59$ and $M_2 = 0.29$ Hall, Dimotakis & Rosemann, 1993, *AIAA J.*, **31**(12), 2247-2254.

- **Almost parallel and two-dimensional flow :** slow evolution in the x_1 direction, and statistics independent of the spanwise coordinate x_3

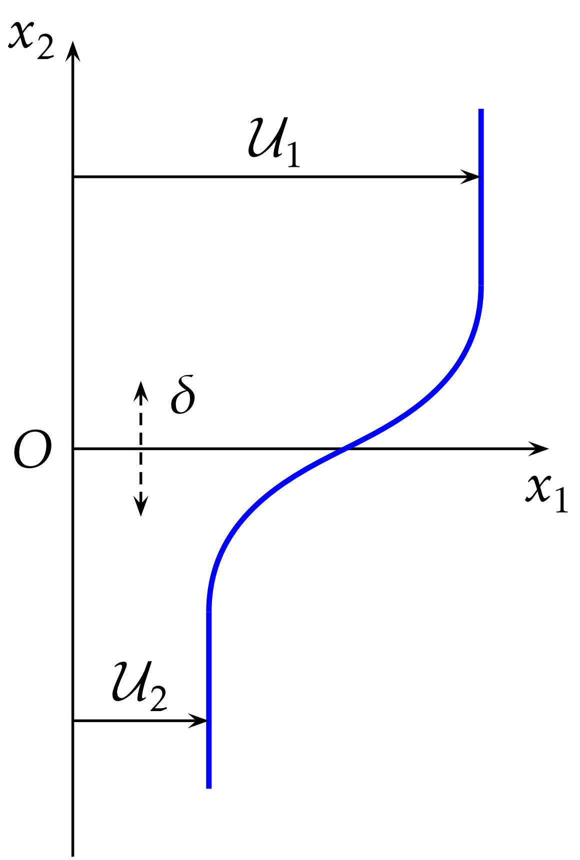

$\mathcal{U}_1$ and $\mathcal{U}_2$ high- and low-speed

$u_m \equiv \dfrac{\mathcal{U}_1 + \mathcal{U}_2}{2}$ convection velocity scale

$\Delta U \equiv \mathcal{U}_1 - \mathcal{U}_2$ velocity difference, which characterizes the turbulent diffusion

$\delta(x_1)$ mixing layer width

L scale of change in the x_1 direction
l scale of change in the x_2 direction

$l/L \ll 1$ is a small parameter (parallel flow), and $\mathrm{Re} = \Delta U \delta/\nu \gg 1$ (inviscid flow)

- **Digression : solution for the laminar viscous diffusion**
  in the frame moving at u_m

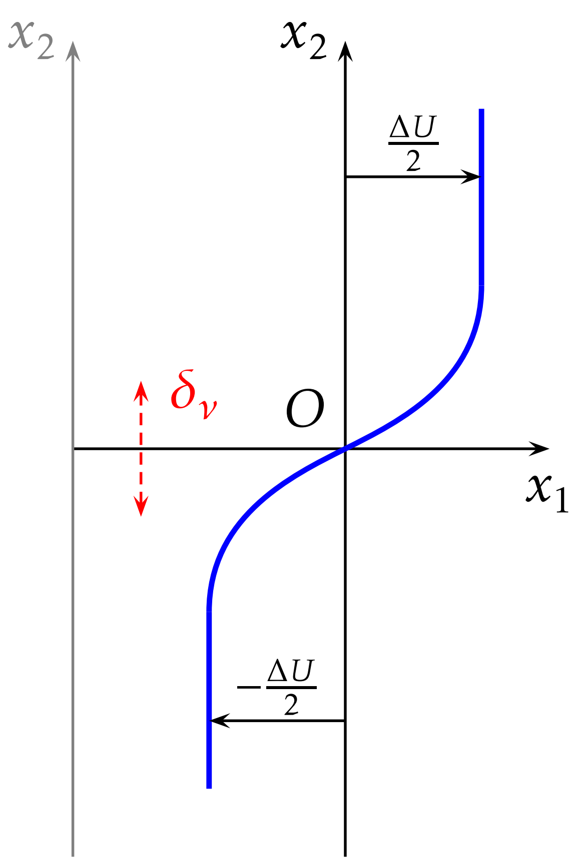

In the local convected frame,

$$\frac{\partial U}{\partial t} = \nu \frac{\partial^2 U}{\partial x_2^2}$$

Self-similar solution

$$\eta = \frac{x_2}{2\sqrt{\nu t}} \qquad U = \frac{\Delta U}{2} f(\eta) \qquad \begin{cases} f = 0 & \eta = 0 \\ f = 1 & \eta \to \infty \end{cases}$$

$$f'' + 2\eta f' = 0$$

$$U(x_2, t) = \frac{\Delta U}{2\sqrt{\pi \nu t}} \int_0^{x_2} e^{-\tilde{x}_2^2/(4\nu t)} d\tilde{x}_2 \qquad \delta_\nu \sim \sqrt{\nu t}$$

Solution never observed alone in practice : unstable flow, leading to the development of Kelvin-Helmholtz instability waves (a fundamentally inviscid process)

Mean velocity field

Conservation of mass, which provides the transverse velocity scale V
(where $\sim$ stands for order of magnitude)

$$\frac{\partial \bar{U}_1}{\partial x_1} + \frac{\partial \bar{U}_2}{\partial x_2} = 0 \qquad \frac{\partial \bar{U}_1}{\partial x_1} \sim \frac{\Delta U}{L} \quad \Longrightarrow \quad V \sim \frac{l}{L}\Delta U$$

Reynolds-averaged Navier-Stokes equation in the x_1 direction

$$\bar{U}_1 \frac{\partial \bar{U}_1}{\partial x_1} + \bar{U}_2 \frac{\partial \bar{U}_1}{\partial x_2} = -\frac{1}{\rho}\frac{\partial \bar{P}}{\partial x_1} - \frac{\partial \overline{u_1' u_1'}}{\partial x_1} - \frac{\partial \overline{u_1' u_2'}}{\partial x_2} + \nu \nabla^2 \bar{U}_1$$

– for the convection terms,

$$\bar{U}_1 \frac{\partial \bar{U}_1}{\partial x_1} + \bar{U}_2 \frac{\partial \bar{U}_1}{\partial x_2} = u_m \frac{\partial \bar{U}_1}{\partial x_1} + \underbrace{(\bar{U}_1 - u_m)\frac{\partial \bar{U}_1}{\partial x_1} + \bar{U}_2 \frac{\partial \bar{U}_1}{\partial x_2}}_{\sim \Delta U \frac{\Delta U}{L}}$$

Mean velocity field (cont.)

– for the Reynolds stress,
with $u \sim \Delta U$ for the scale of velocity fluctuations,

$$-\frac{\partial \overline{u_1' u_2'}}{\partial x_2} \sim \frac{u^2}{l} \sim \frac{(\Delta U)^2}{l}$$

Then, by considering the balance between the two dominant (red) terms

$$u_m \frac{\Delta U}{L} \sim \frac{(\Delta U)^2}{l} \quad \Longrightarrow \quad \Delta U \sim \frac{l}{L} u_m$$

– for the pressure term, using the RANS Eq. in the x_2 direction

$$\underbrace{\bar{U}_1 \frac{\partial \bar{U}_2}{\partial x_1}}_{\sim \frac{l}{L}\frac{u_m \Delta U}{L}} + \bar{U}_2 \frac{\partial \bar{U}_2}{\partial x_2} = -\frac{1}{\rho}\frac{\partial \bar{P}}{\partial x_2} - \frac{\partial \overline{u_1' u_2'}}{\partial x_1} \underbrace{- \frac{\partial \overline{u_2' u_2'}}{\partial x_2}}_{\sim \frac{u_m \Delta U}{L}} + \nu \nabla^2 \bar{U}_2$$

- **Mean velocity field (cont.)**

  – for the pressure term (cont.)

  and by integration in the transverse direction,

  $$\bar{P} + \rho\overline{u_2'^2} \simeq \text{cst} = p_\infty \quad \Longrightarrow \quad \frac{1}{\rho}\frac{\partial \bar{P}}{\partial x_1} \simeq 0 \quad \text{in the RANS Eq. in the } x_1 \text{ direction}$$

Finally, the equation governing the mean velocity is

$$u_m \frac{\partial \bar{U}_1}{\partial x_1} \simeq -\frac{\partial \overline{u_1' u_2'}}{\partial x_2} \qquad (5)$$

Self-similar solution

We now look for self-similar solutions of Eq. (5)

Definition of the mixing layer width $\delta(x_1) = x_2^{0.9} - x_2^{0.1}$
where x_2^{α} is the transverse location such that $\bar{U}_1 = \mathcal{U}_2 + \alpha\Delta U$

Hence, from this definition, we have $\bar{U}_1(\pm\delta/2) = u_m \pm 0.4\Delta U$

Self-similar variable $\eta = \dfrac{x_2 - \bar{x}_2}{\delta}$
where $\bar{x}_2(x_1)$ is usually the line along which $\bar{U}_2 = 0$ (the flow is indeed not symmetric about $x_2 = 0$ for various reasons)

$$\begin{cases} \bar{U}_1 = u_m + \Delta U\, f(\eta) \\ \overline{u_1' u_2'} = (\Delta U)^2 g(\eta) \end{cases}$$

We expect that the nondimensionalized quantities f and g are indeed functions of η only (see tutorials)

Champagne, Pao & Wygnanski (*J. Fluid Mech.*, 1976)

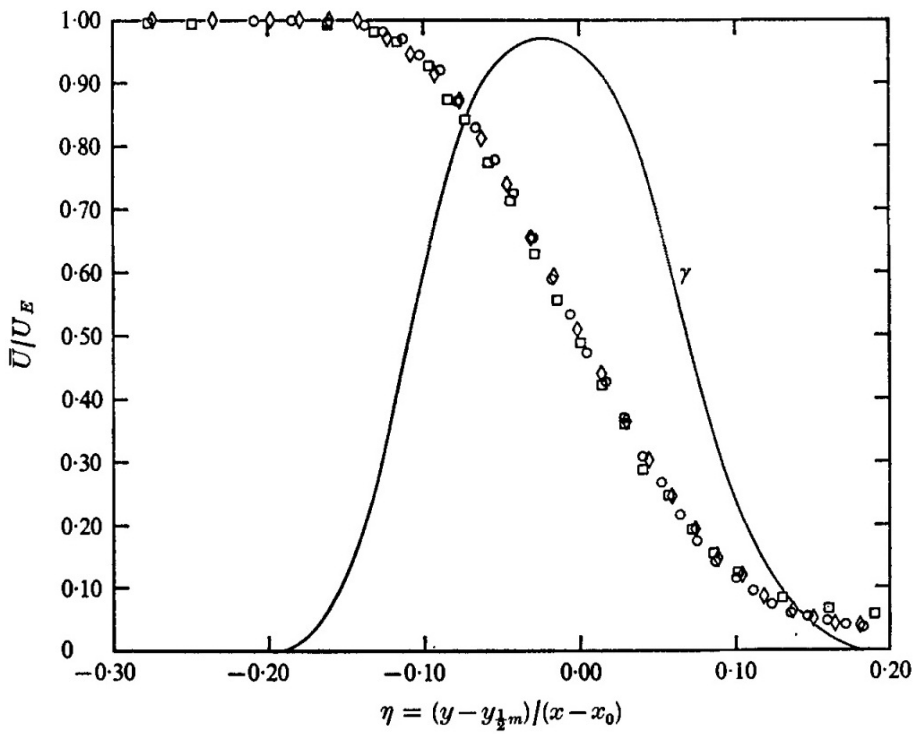

FIGURE 2. Development of mean velocity field. x: ◇, 39·5 cm; □, 49·5 cm; ○, 59·5 cm. γ = intermittency.

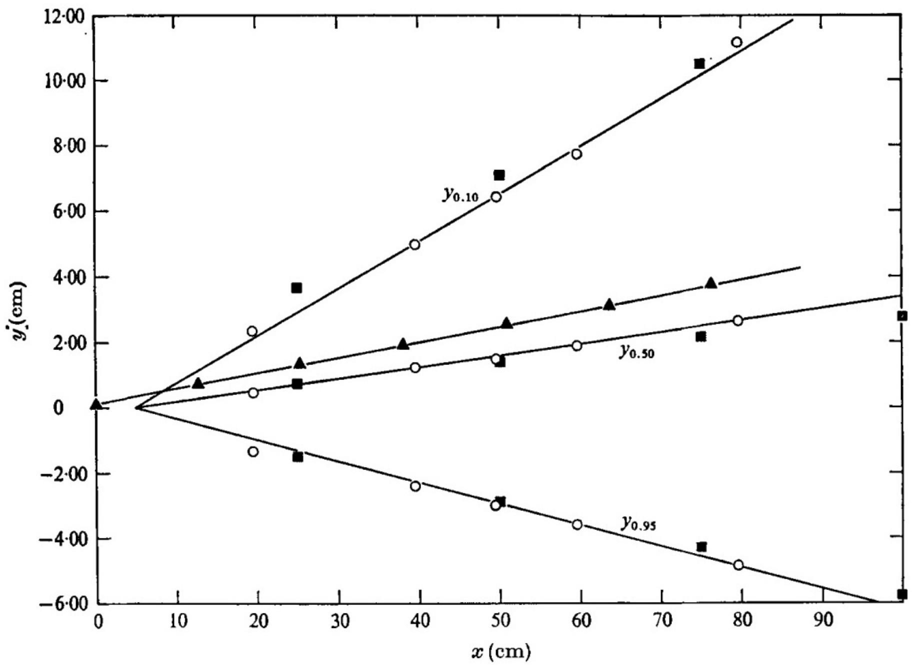

FIGURE 3. The growth of the mixing region with downstream distance. ▲, W & F; ■, Patel; ○, present results.

$$\mathcal{U}_1 = U_E = 8 \text{ m.s}^{-1}, \mathcal{U}_2 = 0$$

(the flow, running from the right to the left, spreads preferentially into the low-speed stream)

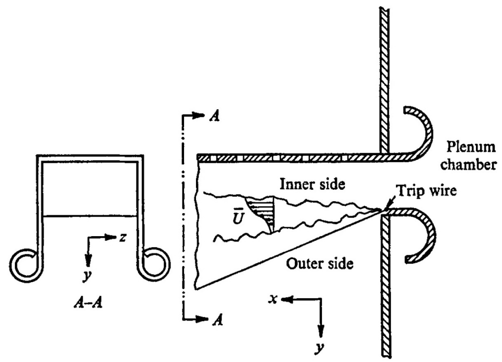

Flow visualization by laser-induced fluorescence in a cross-section plane

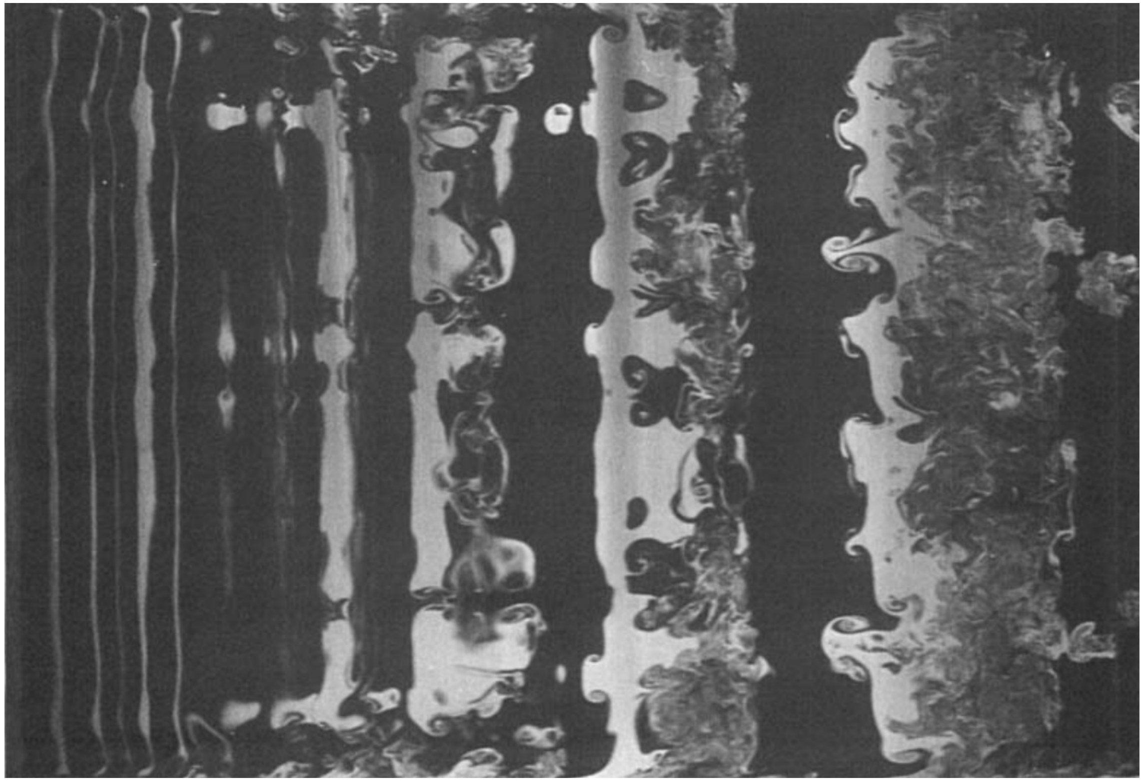

Experiments performed in water, $U_1 = 57$ cm.s^{-1}, $U_2 = 23$ cm.s^{-1}, the lower low-speed fluid is marked with fluorescein dye

Bernal & Roshko, 1986, *J. Fluid Mech.*, **170**

Shear layer at a stream confluence

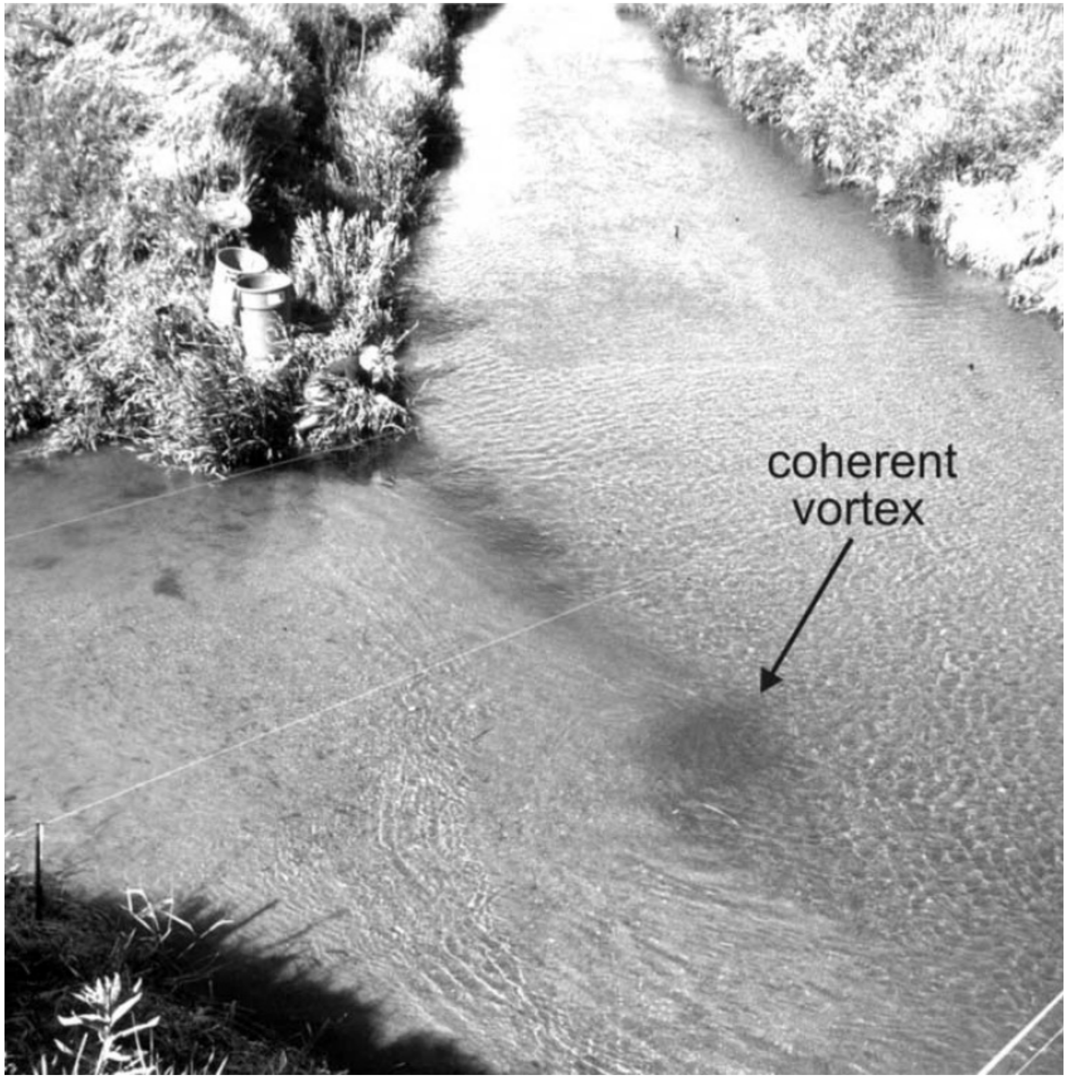

Kaskaskia River - Copper Slough confluence in East Central Illinois

(Rhoads & Sukhodolov, 2004, *Water Resources Research*)

- **Rhône and Saône rivers meeting point, Lyon**

Lyon 2021-05-08

Incursion into the field of forced plumes !

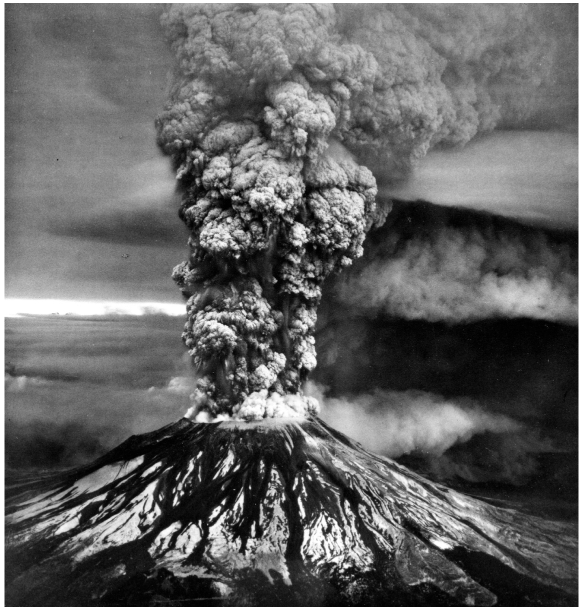

Mount St. Helens Eruption on 16 May 1980 (Washington, USA). *Courtesy of Longview Daily News, Washington* (Rodi, 1982)

Eruption of the subglacial Grimsvötn volcano, Iceland, on 21 May 2011
An initial large plume of smoke and ash rose up to about 17 km height.
Courtesy of Thördïs Högnadóttir, Institute of Earth Sciences, University of Iceland
(Bailly & Comte-Bellot, 2015)

Incursion into the field of forced plumes (cont.)

Smoke plume in the presence of a near surface temperature inversion, which hinders vertical turbulent motion and drives the plume horizontally. *The Quays Shopping Centre*, near to Tiur and Cloghoge, taken by Eric Jones (Bailly & Comte-Bellot, 2015)

Two examples of application

1. Forced plume in atmosphere. At what altitude does the difference between the temperature of the plume and the temperature of the quiescent surroundings become less than 1 deg. ?

Data to solve the problem later

$D = 1$ m

$U_P = 3$ m.s^{-1}

$\Theta_P = 273$ K

$T_0 = 273$ K

2. Thermal pollution. At a river mouth, fresh water is pumped out to sea in a large round pipe and released at the bottom. At what depth must the fresh water be released to avoid raising the temperature in the first 30 m below the surface by more than 1 deg. ?

Data to solve the problem later

$Q_v = 10$ m^3.s^{-1}

$\rho_P = 1.0 \times 10^3$ kg.m^{-3}

$T_P = 35°$C

$\rho_0 = 1.03 \times 10^3$ kg.m^{-3}

$T_0 = 5°$C

- **Boussinesq approximation (1903)**
  - Density fluctuations which appear in gouverning equations result principally from thermal (as opposed to pressure $\sim \mathrm{M}^2$) effects, $\rho \simeq \rho(T)$. Its Taylor series leads to

$$\rho \simeq \rho_0(1 - \beta(T - T_0)) \qquad \beta = -\frac{1}{\rho}\frac{\partial \rho}{\partial T}\bigg|_p = \frac{1}{T_0}$$

(thermal expansion coefficient for ideal gas)

  - In the equations for the momentum and mass conservation, density variations may be neglected except in the buoyancy force $\rho \boldsymbol{g}$

These approximations are valid if the velocity perturbations are small ($\mathrm{M} \ll 1$), and when the variations in $\rho_0(z)$ and $T_0(z)$ of the quiescent surroundings are small over the vertical size of the flow. As an exercise, you can check from hydrostatic balance that the temperature varies by 1 degree every 100 meters for an adiabatic atmosphere (6.5 degree /km with a more realistic model)

Gouverning equations

Viscosity and conductivity are neglected (free jet flow, no wall, Re and Pe $\gg 1$). The hydrostatic balance $-\nabla p_0 + \rho_0 \boldsymbol{g} = 0$ is also substracted from the momentum conservation, which leads to

$$\frac{\partial \boldsymbol{U}}{\partial t} + \boldsymbol{U} \cdot \nabla \boldsymbol{U} = -\frac{1}{\rho_0} \nabla (p - p_0) - \frac{1}{T_0}(T - T_0)\boldsymbol{g}$$

$$\nabla \cdot \boldsymbol{U} = 0$$

$$\frac{\partial (T - T_0)}{\partial t} + \boldsymbol{U} \cdot \nabla (T - T_0) = 0$$

Reynolds decomposition

$$\begin{cases} T - T_0 = \bar{T} + \theta' \\ p - p_0 = \bar{P} + p' \\ \boldsymbol{u} = \bar{\boldsymbol{U}} + \boldsymbol{u}' \quad \text{(no wind, } \boldsymbol{U}_0 = 0\text{)} \end{cases}$$

Boundary-layer approximation applied to free turbulent flow : the divergence of the thin shear layer is slow.

- **Gouverning equations (cont.)**
  Reynolds-averaged Euler Eqs. including the buoyancy force

$$\frac{1}{r}\frac{\partial(r\bar{U}_r)}{\partial r} + \frac{\partial \bar{U}_z}{\partial z} = 0 \tag{6}$$

$$\frac{1}{r}\frac{\partial(r\bar{U}_r\bar{U}_z)}{\partial r} + \frac{\partial(\bar{U}_z\bar{U}_z)}{\partial z} = -\frac{1}{r}\frac{\partial(r\overline{u'_r u'_z})}{\partial r} + \frac{\bar{T}}{T_0}g \tag{7}$$

$$\frac{1}{r}\frac{\partial(r\bar{U}_r\bar{T})}{\partial r} + \frac{\partial(\bar{U}_z\bar{T})}{\partial z} = -\frac{1}{r}\frac{\partial(r\overline{u'_r\theta'})}{\partial r} \tag{8}$$

Densimetric Froude number Fr

ambient fluid : ρ_0, T_0
forced plume : D, U_P, ρ_P, $T_P = T_0 + \Theta_P$ $\quad (\rho_P T_P = \rho_0 T_0)$

$$\mathrm{Fr} = \left(\frac{\text{inertial forces}}{\text{buoyancy forces}}\right)^{1/2} = \left(\frac{U_P^2/D}{g\Theta_P/T_0}\right)^{1/2} = \frac{U_P}{\sqrt{D\,g(\rho_0/\rho_P - 1)}} \tag{9}$$

Froude number for forced plumes

Sketch of the mean velocity and temperature fields in the region where the flow has reached a self-similar state ($z/D \geq 10$)

Pure plume : Fr = 0

Buoyant jet / forced plume :
$0 < \mathrm{Fr} < \infty$

Pure jet : $\mathrm{Fr} = \infty$

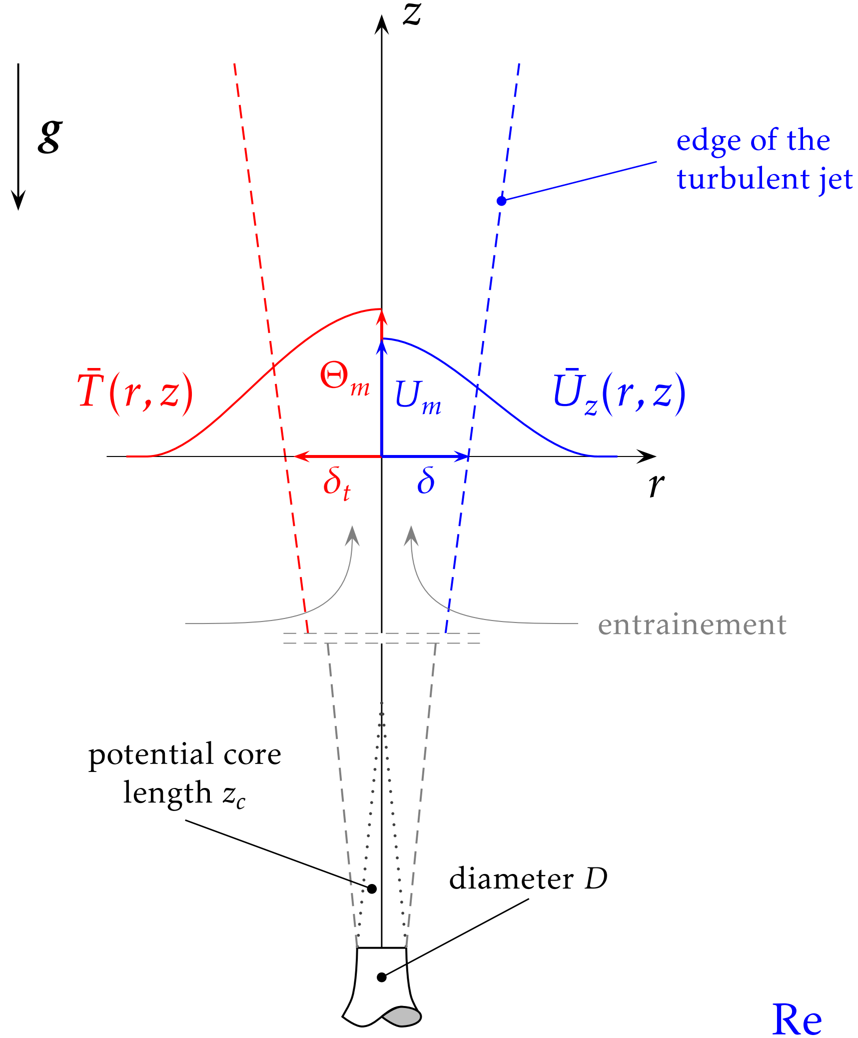

Fr

Re

Froude number for forced plumes (cont.)

Visualization of starting plumes

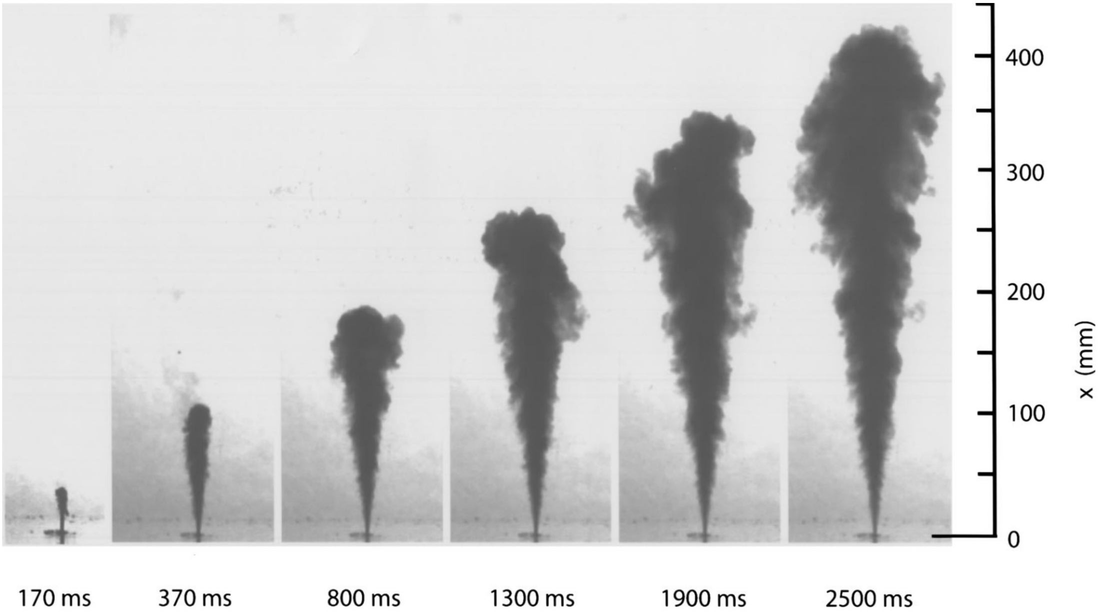

Re = 9000, Fr = 58.5

$D = 3.2$ mm
$U_P = 3700$ mm.s^{-1}
$\rho_P/\rho_0 = 1.150$

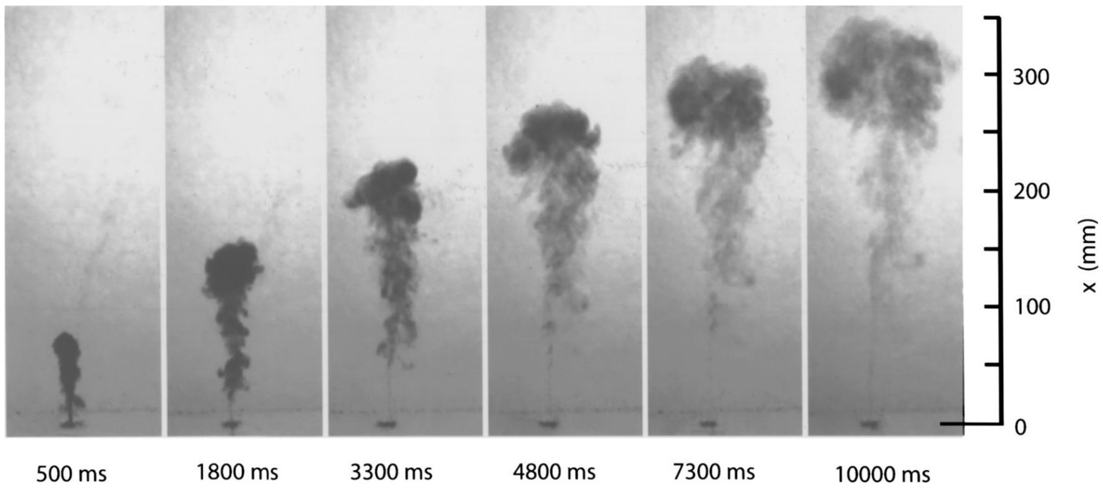

Re = 4000, Fr = 29.3

$D = 3.2$ mm
$U_P = 1850$ mm.s^{-1}
$\rho_P/\rho_0 = 1.150$

Diez, Sangras & Faeth, 2003, *J. Heat Transfer*, **125**

Derivation of the self-similar solution

Only one length scale ($\delta_t \simeq \delta$) is considered to find the self-similar solution

$$\eta = \frac{r}{\delta_l(z)} \qquad \begin{cases} \bar{U}_z = U_m(z)\, f(\eta) \\ \bar{U}_r = U_m(z)\, g(\eta) \\ -\eta\overline{u_r' u_z'} = U_m^2(z)\, h(\eta) \\ \bar{T} = \Theta_m(z)\, F(\eta) \\ -\overline{u_r'\theta'} = U_m(z)\Theta_m(z)\, H(\eta) \end{cases} \tag{10}$$

At first, we are interested in the asymptotic behavior of the functions $U_m(z)$ (velocity on the plume axis), $\Theta_m(z)$ (temperature on the plume axis) and $\delta_l(z)$ (the half-width of the plume), and not in the expression of the profiles f, g, h, F and H.

Self-similar solution (cont.)

Eq. (7) $\Longrightarrow$

$$-r\overline{u_r' u_z'} = \int_0^r \frac{\partial \bar{U}_z \bar{U}_z}{\partial z} r' dr' - \bar{U}_z \int_0^r \frac{\partial \bar{U}_z}{\partial z} r' dr' - \int_0^r \frac{\bar{T}}{T_0} g r' dr'$$

$$= \frac{\partial}{\partial z}\left\{ U_m^2 \delta^2 \int_0^\eta f^2 \eta' d\eta' \right\} - U_m f \frac{\partial}{\partial z}\left\{ U_m \delta^2 \int_0^\eta f \eta' d\eta' \right\} - \theta_m \delta^2 \frac{g}{T_0} \int_0^\eta F \eta' d\eta'$$

with the change of variable $\eta' = r'/\delta(z)$

$$= \frac{d}{dz}(U_m^2 \delta^2) \int_0^\eta f^2 \eta' d\eta' + U_m^2 \delta^2 f^2(\eta) \eta \frac{d\eta}{dz}$$

$$-U_m f \frac{d}{dz}(U_m \delta^2) \int_0^\eta f \eta' d\eta' - U_m^2 \delta^2 f^2(\eta) \eta \frac{d\eta}{dz} - \theta_m \delta^2 \frac{g}{T_0} \int_0^\eta F \eta' d\eta'$$

by using $\displaystyle \frac{d}{dx}\int_{a(x)}^{b(x)} I(x,y)dy = \int_{a(x)}^{b(x)} \frac{\partial I}{\partial x} dy + I(x,b(x))\frac{db}{dx} - I(x,a(x))\frac{da}{dx}$

Self-similar solution (cont.)

The Reynolds shear stress is finally recast as,

$$\underbrace{-\eta\frac{\overline{u_r'u_z'}}{U_m^2}}_{\text{given by Eq. (10)}} = h(\eta) = \frac{(U_m^2\delta^2)'}{U_m^2\delta}\int_0^\eta f^2\eta' d\eta' - \frac{(U_m\delta^2)'}{U_m\delta} f\int_0^\eta f\eta' d\eta' - \frac{\theta_m\delta}{U_m^2}\frac{g}{T_0}\int_0^\eta F\eta' d\eta'$$

A self-similar solution can be obtained only if the red terms are constant terms, and not terms functions of z, which leads to the following behaviours for a plume,

$$\delta \sim z \qquad U_m \sim z^m \qquad \Theta_m \sim z^{2m-1}$$

Self-similar solution (cont.)

Conservation of the heat flux in a cross-section to determine m

By integration of Eq. (8) in the radial direction,

$$\underbrace{\left[r\bar{U}_r\bar{T}\right]_0^\infty}_{=0} + \int_0^\infty \frac{(\partial \bar{U}_z\bar{T})}{\partial z} r' dr' = \underbrace{\left[-r\overline{u'_r\theta'}\right]_0^\infty}_{=0}$$

Therefore,

$$\int_0^\infty \bar{U}_z\bar{T} r' dr' = \text{cst} \qquad \Longrightarrow \qquad U_m\Theta_m\delta^2 \int_0^\infty f F \eta' d\eta' = \text{cst}$$

A self-similar solution is then only possible if

$$\delta \sim z \qquad U_m \sim z^{-1/3} \qquad \Theta_m \sim z^{-5/3}$$

- Faster decrease in temperature than in velocity (for a single free round jet, we have $\delta \sim z$ and $U_m \sim z^{-1}$)
- The Froude number value is a constant, $\text{Fr}^2 = (U_m^2/\delta)/(g\Theta_m/T_0) = \text{cst}$

Self-similar solution (cont.)

Experimental data collected by Rodi (1986)

In the plume region,
for $z/z^\star > 5.0$ with $z^\star/D = \mathrm{Fr}^{1/2}\,(\rho_P/\rho_0)^{1/4}$

$$\frac{U_m}{U_P} \simeq 3.5\,\mathrm{Fr}^{-1/3}\left(\frac{\rho_P}{\rho_0}\right)^{1/3}\left(\frac{z}{D}\right)^{-1/3} \qquad \frac{\Theta_m}{\Theta_P} \simeq 9.35\,\mathrm{Fr}^{1/3}\left(\frac{\rho_P}{\rho_0}\right)^{1/3}\left(\frac{z}{D}\right)^{-5/3}$$

Two examples of application

1. Forced plume in atmosphere. At what altitude does the difference between the temperature of the plume and the temperature of the quiescent surroundings become less than 1 deg. ?

Data to solve the problem

$D = 1$ m

$U_P = 3$ m.s^{-1}

$\Theta_P = 273$ K

$T_0 = 273$ K

Solution.

$T_P = T_0 + \Theta_P = 2T_0 \quad \Longrightarrow \quad \rho_P = \frac{1}{2}\rho_0$ (constant pressure in the plume, then using $p = \rho r T$)

From its definition (9),

$$\mathrm{Fr}^2 = \frac{3^2/1}{9.81 \times 1} \simeq 0.92 \text{ (plume)}$$

Numerically,

$$\frac{z}{D} \simeq \left(\frac{1}{9.35\,\mathrm{Fr}^{1/3}} \frac{\Theta_m}{\Theta_P} \right)^{-3/5} \left(\frac{\rho_0}{\rho_P} \right)^{-1/5}$$

$$\simeq \left(\frac{1}{9.35 \times 0.92^{1/3}} \frac{1}{273} \right)^{-3/5} 2^{-1/5}$$

$$\simeq 95 \text{ m}$$

(we verify that the ambient temperature T_0 is almost constant along this distance)

Two examples of application

2. Thermal pollution. At a river mouth, fresh water is pumped out to sea in a large round pipe and released at the bottom. At what depth must the fresh water be released to avoid raising the temperature in the first 30 m below the surface by more than 1 deg. ?

Data to solve the problem

$Q_v = 10\ \mathrm{m}^3.\mathrm{s}^{-1}$

$\rho_P = 1.0 \times 10^3\ \mathrm{kg.m}^{-3}$

$T_P = 35°\mathrm{C}$

$\rho_0 = 1.03 \times 10^3\ \mathrm{kg.m}^{-3}$

$T_0 = 5°\mathrm{C}$

Solution.

Two contribution for the buoyancy force : temperature T_P versus T_0, and also density of fresh water (fw) versus salt water (sw)

Mixing of salt and fresh water by entrainment inside the plume to reach $T = 6°\mathrm{C}$; from the conservation of energy,

$$M_{\mathrm{fw}} C_p T_P + M_{\mathrm{sw}} C_p T_0 = (M_{\mathrm{fw}} + M_{\mathrm{sw}}) C_p T$$

$$\frac{M_{\mathrm{sw}}}{M_{\mathrm{fw}}} = \frac{T_P - T}{T - T_0} = \frac{35 - 6}{6 - 5} = 29$$

In other words, 1 kg of fresh water has entrained 29 kg of salt water in order to reach $T = 6°\mathrm{C}$. For this temperature (and this altitude), the plume density is then estimated at

$$\rho = \frac{\rho_{\mathrm{fw}} + 29\rho_{\mathrm{sw}}}{30} \simeq 1.029 \times 10^3\ \mathrm{kg.m}^{-3}$$

Two examples of application

Solution (cont.)

For an ideal gas, $p = \rho r T$, and for $p = \text{cst}$, it yields by logarithmic differentiation

$$-\frac{\Delta\rho}{\rho} = \frac{\Delta T}{T}$$

and for a liquid, the boyancy force is $-g\Delta\rho/\rho_0$, where $\Delta\rho$ takes into account temperature and density effects here. Hence, by analogy with the gas plume, we still use for the liquid plume

$$\frac{\rho - \rho_0}{\rho_P - \rho_0} \simeq 9.35\,\mathrm{Fr}^{1/3}\left(\frac{\rho_P}{\rho_0}\right)^{1/3}\left(\frac{z}{D}\right)^{-5/3}$$

Numerically, $z \simeq 70$ m, and the required distance from the nozzle to the surface is thus 100 m.

Identification of vortical structures
(When is a region of vorticity a vortex?)

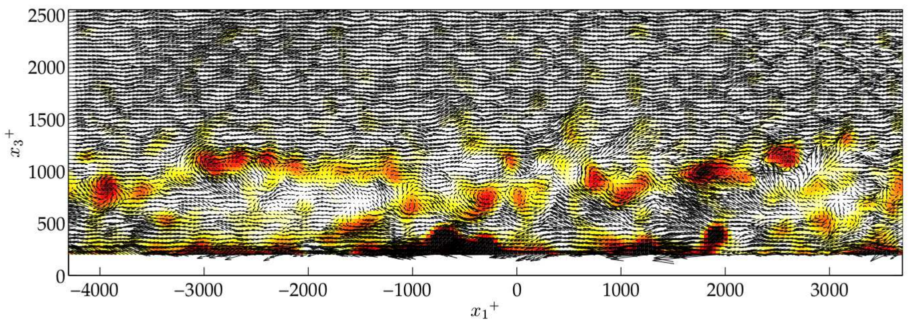

2-D 2-C PIV snapshot, $\boldsymbol{u} - 0.85\boldsymbol{U}_\infty$, colored by vorticity magnitude ω_2, from Salze *et al.* (2015)

Introduction : deformation of a fluid particle

Taylor series for the velocity in the vicinity of a fluid particle at $\boldsymbol{x}_P$ (at a given time t)

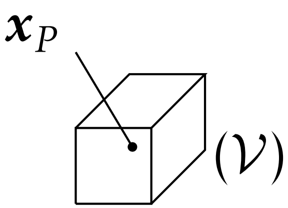

$$\boldsymbol{u}(\boldsymbol{x}) = \boldsymbol{u}(\boldsymbol{x}_P) + \nabla\boldsymbol{u}(\boldsymbol{x}_P)\cdot(\boldsymbol{x}-\boldsymbol{x}_P) + \cdots$$

$$u_i(\boldsymbol{x}) = u_i(\boldsymbol{x}_P) + \left.\frac{\partial u_i}{\partial x_j}\right|_{x_P}(x_j - x_{Pj}) + \cdots$$

$$\frac{\partial u_i}{\partial x_j} = \underbrace{\frac{1}{2}\left(\frac{\partial u_i}{\partial x_j}+\frac{\partial u_j}{\partial x_i}\right)}_{D_{ij}} + \underbrace{\frac{1}{2}\left(\frac{\partial u_i}{\partial x_j}-\frac{\partial u_j}{\partial x_i}\right)}_{\Omega_{ij}}$$

- $\overline{\overline{\boldsymbol{D}}}$ symmetric part of $\nabla\boldsymbol{u}$
- $\overline{\overline{\boldsymbol{\Omega}}}$ antisymmetric part of $\nabla\boldsymbol{u}$

Ω_{ij} is associated with the rotation of the fluid particle

$$\overline{\overline{\boldsymbol{\Omega}}} = \begin{pmatrix} 0 & -\Omega_3 & \Omega_2 \\ \Omega_3 & 0 & -\Omega_1 \\ -\Omega_2 & \Omega_1 & 0 \end{pmatrix} \qquad \boldsymbol{\Omega} \equiv \frac{1}{2}\nabla\times\boldsymbol{u} \quad (\neq \overline{\overline{\boldsymbol{\Omega}}})$$

Deformation of vorticity

$$\boldsymbol{u}(\boldsymbol{x}) = \boldsymbol{u}(\boldsymbol{x}_P) + \underbrace{\overline{\overline{\boldsymbol{D}}}(\boldsymbol{x}_P)\cdot(\boldsymbol{x}-\boldsymbol{x}_P)}_{\text{deformation}} + \underbrace{\boldsymbol{\Omega}(\boldsymbol{x}_P)\times(\boldsymbol{x}-\boldsymbol{x}_P)}_{\text{rotation}} + \dots$$

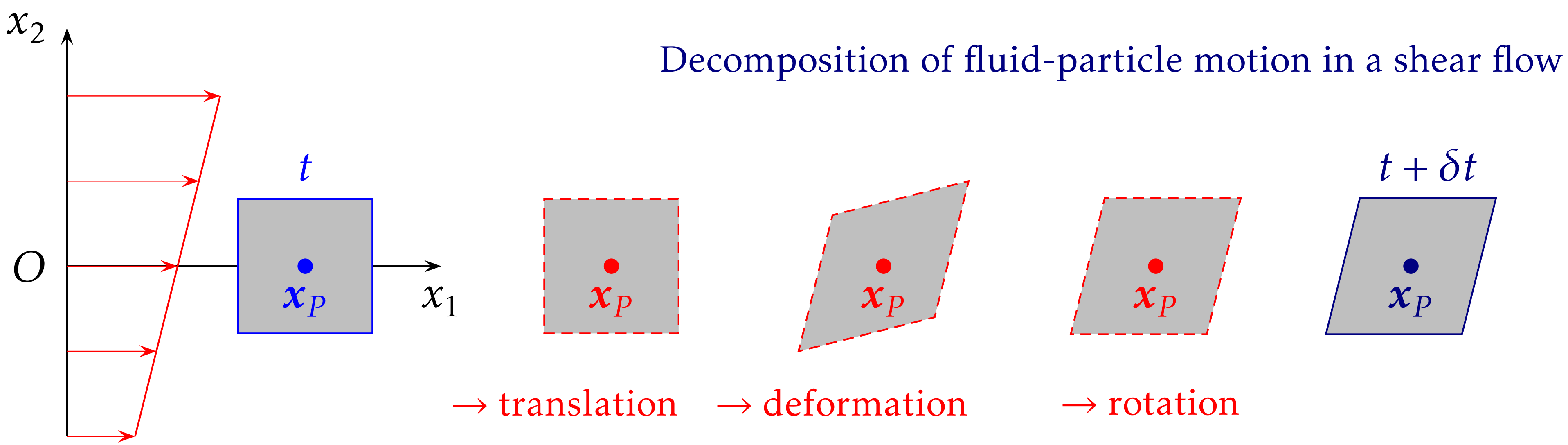

The vorticity vector is defined as $\boldsymbol{\omega} = \nabla \times \boldsymbol{u}$

When $\boldsymbol{\omega} = 0$, absence of vorticity, the flow is irrotational

The vorticity vector $\boldsymbol{\omega}$ is twice the angular velocity of the solid-body rotation motion of the fluid particle, $\boldsymbol{\omega} = 2\boldsymbol{\Omega}$.

Example of the Rankine vortex (1858)

Rankine (1820-1872)

$$\begin{cases} u(r) = v_0 \dfrac{r}{r_0} = \Omega_0 r & r \leq r_0 \\ u(r) = v_0 \dfrac{r_0}{r} = \Omega_0 r_0 \dfrac{r_0}{r} & r > r_0 \end{cases}$$

$(v_0 = \Omega_0 r_0 = \omega_0 r_0 / 2)$

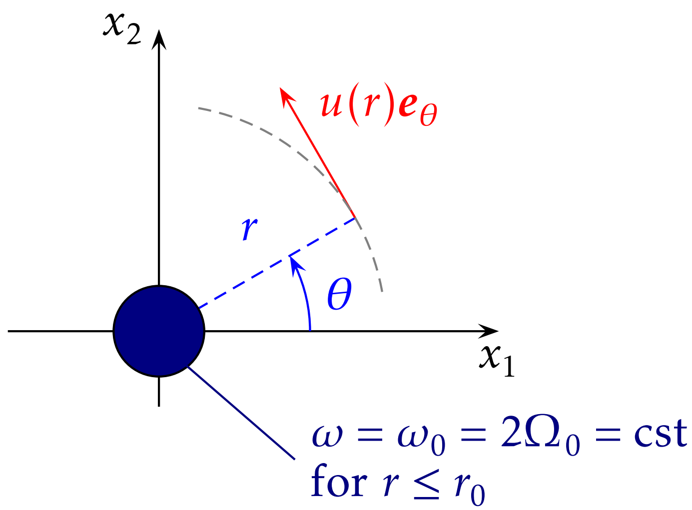

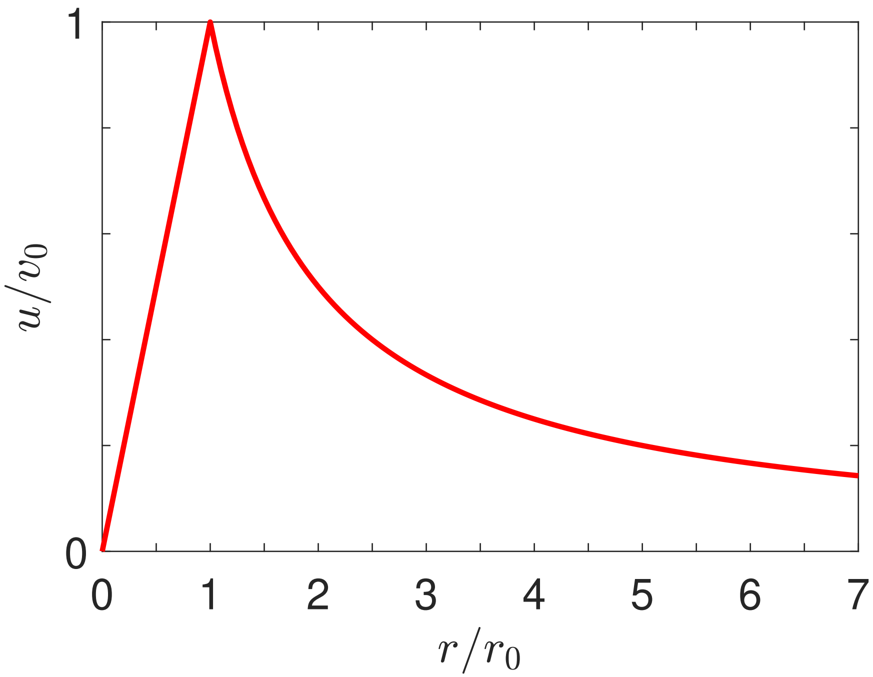

Solid body motion inside the vortex itself, *i.e.* for $r \leq r_0$ in the vortical region

Irrotational flow outside, for $r > r_0$: the localized circular patch of vorticity produces a velocity field away from the vortical region

Example of the Rankine vortex (cont.)

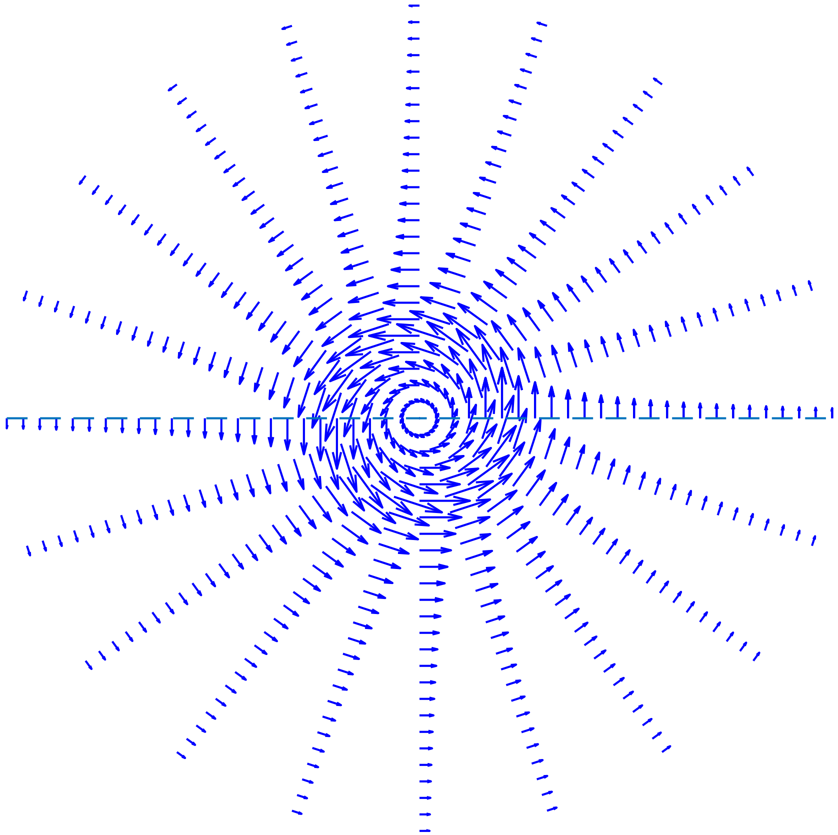

Pressure field ?

Inviscid steady flow, Euler's equation

$$-\frac{1}{\rho}\frac{\partial p}{\partial r} = -\frac{u_\theta^2}{r}$$

$$\begin{cases} p = p_\infty - \dfrac{\rho v_0^2}{2}\left(2 - \dfrac{r^2}{r_0^2}\right) & r \leq r_0 \\ p = p_\infty - \dfrac{\rho v_0^2}{2}\dfrac{r_0^2}{r^2} & r > r_0 \end{cases}$$

More generally, can vortex structures be identified with local pressure minimum ?

Identification of vortices in turbulent flow

Equation for the pressure (incompressible flow, $\rho = \text{cst}$), by taking the divergence of Navier-Stokes equation

$$-\frac{1}{\rho}\nabla^2 p = \frac{\partial u_i}{\partial x_j}\frac{\partial u_j}{\partial x_i}$$

Using the previous decomposition of the velocity gradient tensor (the product of a symmetric and an antisymmetric tensor is zero)

$$\frac{\partial u_i}{\partial x_j}\frac{\partial u_j}{\partial x_i} = (D_{ij} + \Omega_{ij})(D_{ij} - \Omega_{ij}) = D_{ij}D_{ij} - \Omega_{ij}\Omega_{ij} = \overline{\overline{\boldsymbol{D}}} : \overline{\overline{\boldsymbol{D}}} - \overline{\overline{\boldsymbol{\Omega}}} : \overline{\overline{\boldsymbol{\Omega}}}$$

$$\frac{1}{\rho}\nabla^2 p = \overline{\overline{\boldsymbol{\Omega}}} : \overline{\overline{\boldsymbol{\Omega}}} - \overline{\overline{\boldsymbol{D}}} : \overline{\overline{\boldsymbol{D}}}$$

A vortex may then be defined by a concentrated flow region dominated by $\overline{\overline{\boldsymbol{\Omega}}} : \overline{\overline{\boldsymbol{\Omega}}}$, and consequently we expect $\nabla^2 p > 0$ (positive curvature, local minimum)

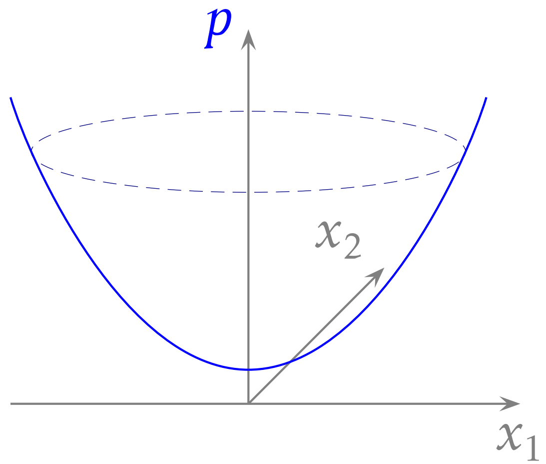

Identification of vortices (cont.)

The source term of Poisson's equation for the pressure is one of the three invariants (invariant, that is independent of the orientation of the coordinate system) of the velocity gradient tensor $A_{ij} \equiv \partial u_i / \partial x_j = (\nabla \boldsymbol{u})_{ij}$

The three invariants of a second-order tensor ($\overline{\overline{\boldsymbol{A}}}$ here) are given by

$$\begin{cases} P = \mathrm{tr}(\overline{\overline{\boldsymbol{A}}}) = A_{ii} \\ Q = \dfrac{1}{2}\left[\mathrm{tr}^2(\overline{\overline{\boldsymbol{A}}}) - \mathrm{tr}(\overline{\overline{\boldsymbol{A}}}^2)\right] = \dfrac{1}{2}\left[(A_{ii})^2 - A_{ij}A_{ji}\right] \\ R = \det(\overline{\overline{\boldsymbol{A}}}) = \dfrac{1}{6}\mathrm{tr}^3(\overline{\overline{\boldsymbol{A}}}) - \dfrac{1}{2}\mathrm{tr}(\overline{\overline{\boldsymbol{A}}})\mathrm{tr}^2(\overline{\overline{\boldsymbol{A}}}) + \dfrac{1}{3}\mathrm{tr}(\overline{\overline{\boldsymbol{A}}}^3) \end{cases}$$

The incompressibility condition $\nabla \cdot \boldsymbol{u} = 0$ leads to $P = 0$ and to $Q = -A_{ij}A_{ji}/2$. Hence, the previous pressure equation reads

$$\frac{1}{\rho}\nabla^2 p = \overline{\overline{\boldsymbol{\Omega}}} : \overline{\overline{\boldsymbol{\Omega}}} - \overline{\overline{\boldsymbol{D}}} : \overline{\overline{\boldsymbol{D}}} = 2Q$$

Vortical structures are thus expected to be identified for high positive values of the invariant Q, leading to the so-called Q-criterion

- **As an illustration : total drag breakdown of a car, and iso-surfaces of Q-criterion colored with velocity magnitude**

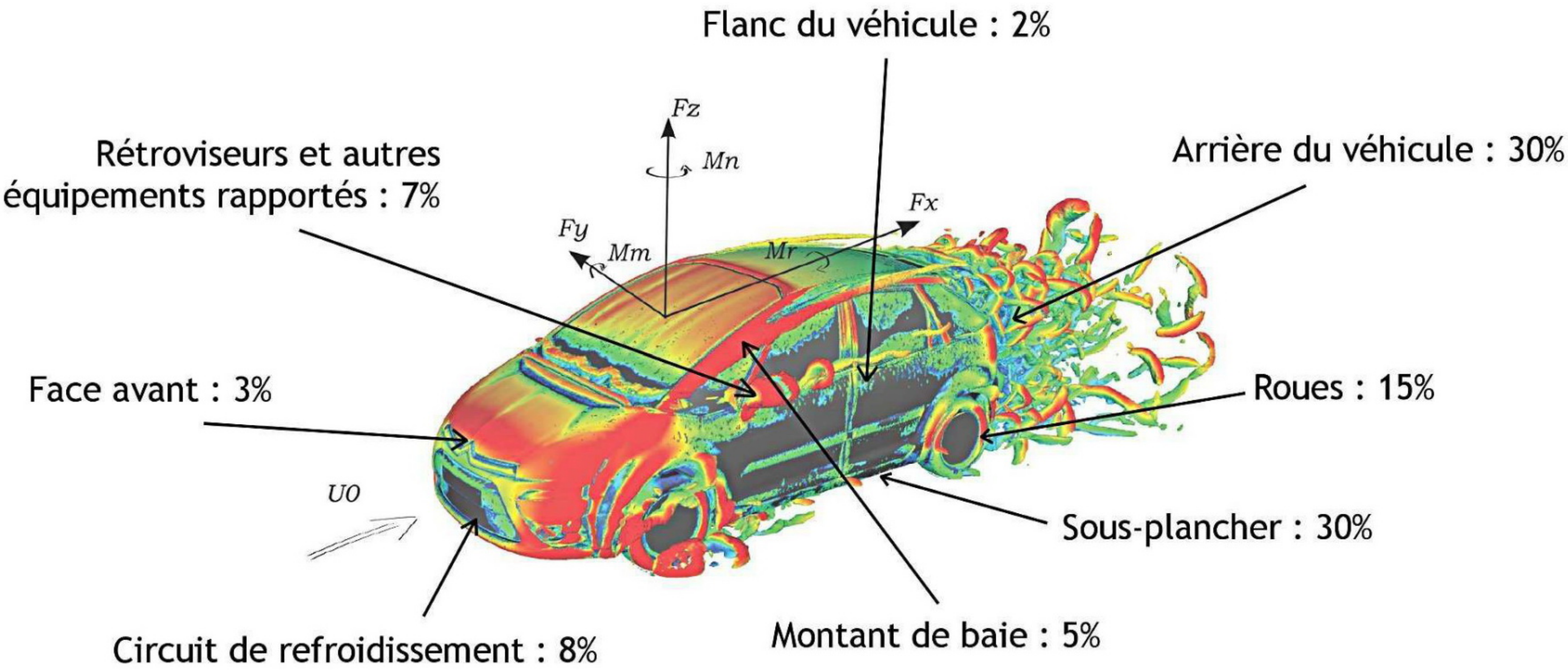

(Fiabane, PhD thesis, 2011, ENSTA-PSA)

Illustration : corner separation in a compressor cascade

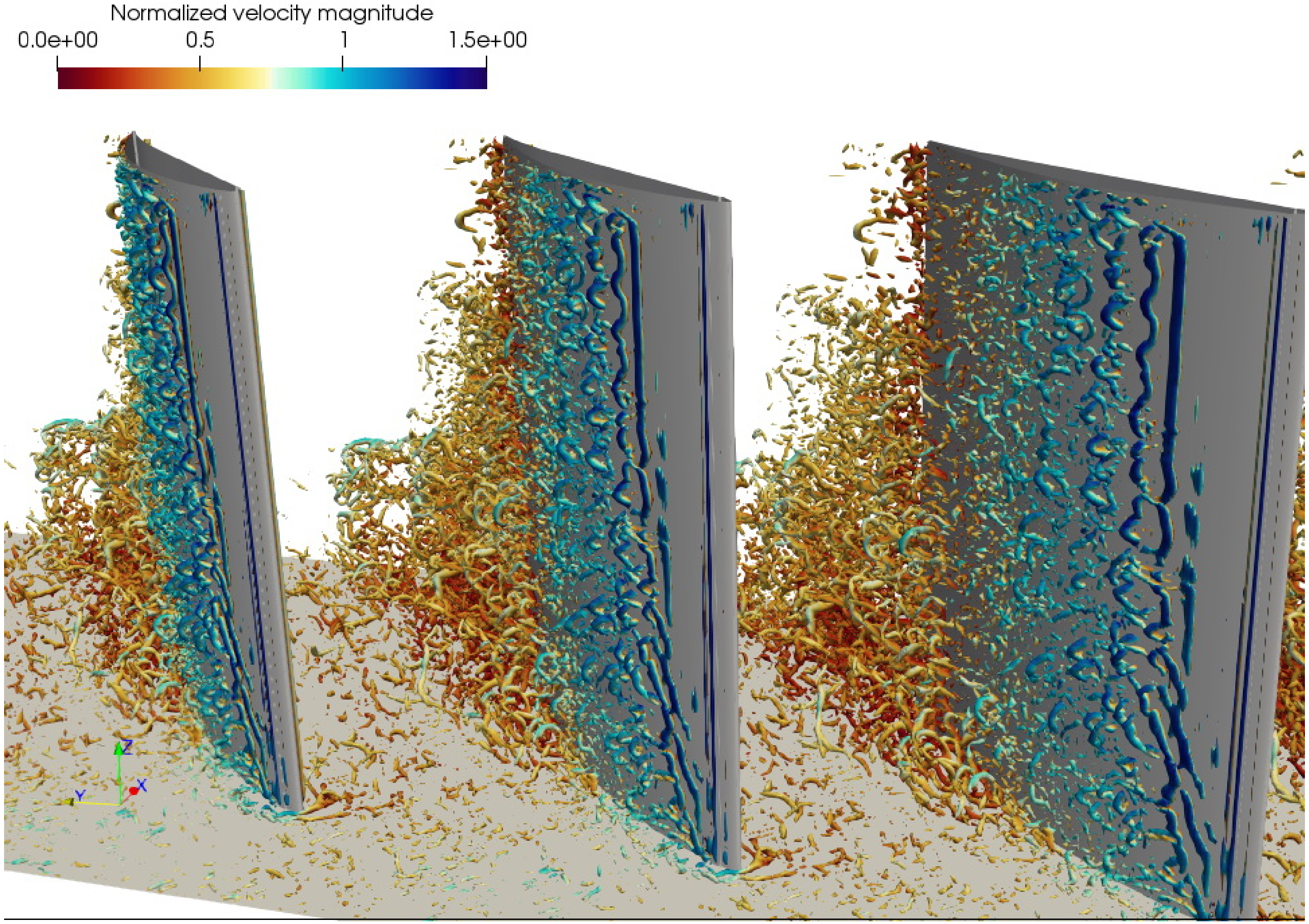

Lattice Boltzmann simulations of corner separation flow in a compressor cascade. Instantaneous isosurface of Q-criterion, colored by velocity magnitude. Turbulent structures develop around the blades and accumulate in the separation zone.

Boudet, Lévêque & Touil, 2022, *J. Turbomachinary*, **144**

Identification of vortices (cont.)

The eigenvalues λ_i of $\overline{\overline{A}}$ are the roots of the characteristic equation
$\lambda^3 - P\lambda^2 + Q\lambda - R = 0$,
with $P = \lambda_1 + \lambda_2 + \lambda_3$ ($P = \nabla \cdot \boldsymbol{u} = 0$ for incompressible flow),
$Q = \lambda_1\lambda_2 + \lambda_2\lambda_3 + \lambda_1\lambda_3$ and $R = \lambda_1\lambda_2\lambda_3$

Hence, the characteristic equation reads $\lambda^3 + Q\lambda - R = 0$. In introducing the discriminant $\Delta = Q^3/27 + R^2/4$, one finds three real values λ_i for $\Delta < 0$, or two complex conjugate values $\lambda_{1,2} = \sigma \pm i\omega$ and one real value λ_3 for $\Delta > 0$.

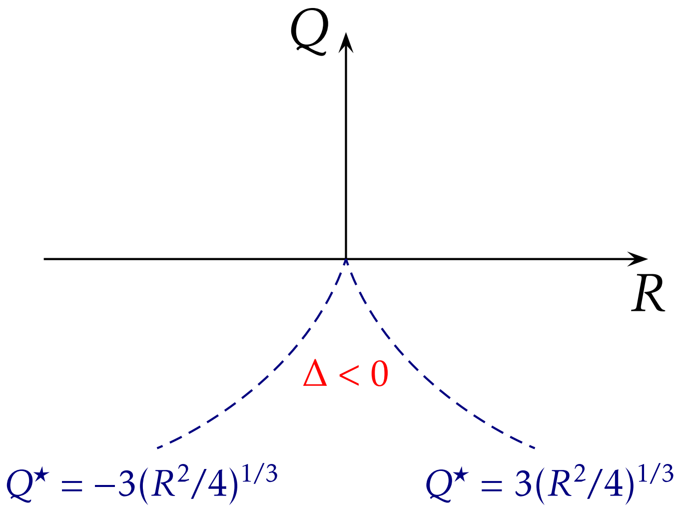

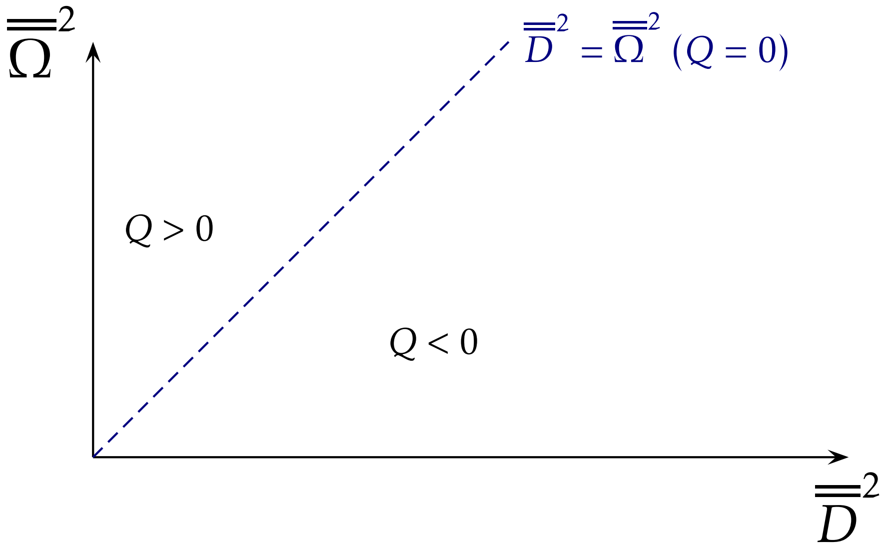

Illustration with an incompressible 2-D flow

Stream function $\psi = ax_1^2 + bx_2^2$ and velocity field

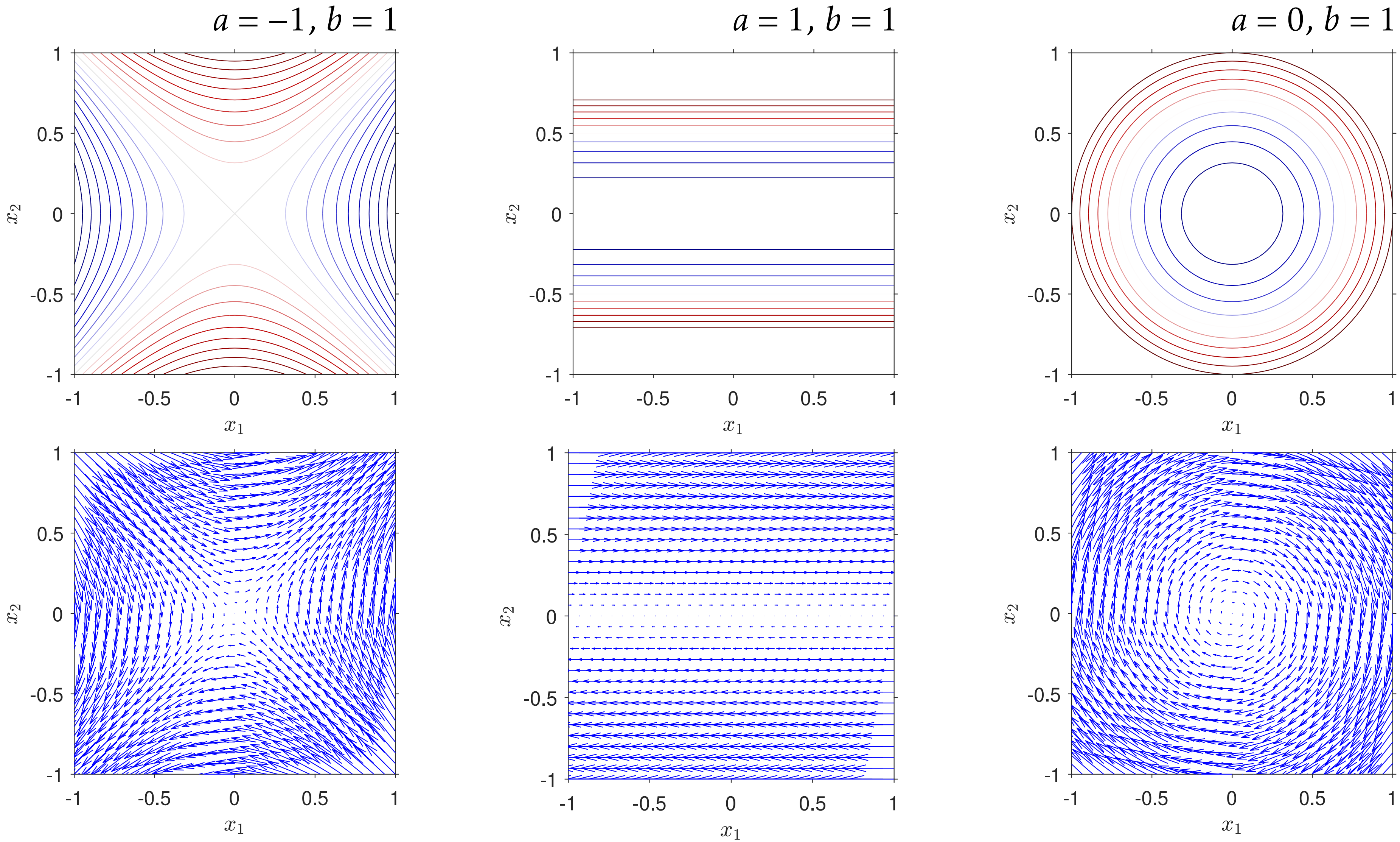

Illustration with an incompressible 2-D flow

$$\psi = \frac{\omega - s}{4} x_1^2 + \frac{\omega + s}{4} x_2^2 \qquad \begin{cases} u_1 = \dfrac{\partial \psi}{\partial x_2} = \dfrac{\omega + s}{2} x_2 \\ u_2 = -\dfrac{\partial \psi}{\partial x_1} = -\dfrac{\omega - s}{2} x_1 \\ \omega_3 = \dfrac{\partial u_2}{\partial x_1} - \dfrac{\partial u_1}{\partial x_2} = -\nabla^2 \psi = -\dfrac{\omega - s}{2} - \dfrac{\omega + s}{2} = -\omega \end{cases}$$

$$\overline{\overline{\boldsymbol{D}}} = \begin{pmatrix} 0 & s/2 \\ s/2 & 0 \end{pmatrix} \qquad \overline{\overline{\boldsymbol{\Omega}}} = \begin{pmatrix} 0 & \omega/2 \\ -\omega/2 & 0 \end{pmatrix}$$

$$\frac{1}{\rho} \nabla^2 p = \Omega_{ij}\Omega_{ij} - D_{ij}D_{ij} = \frac{1}{2}(\omega^2 - s^2) = 2Q$$

Topologie des lignes de courant $\psi = \mathrm{cst}$
elliptiques $(\omega - s)(\omega + s) > 0 \Longrightarrow Q > 0 \Longrightarrow \nabla^2 p > 0$
hyperboliques $(\omega - s)(\omega + s) < 0 \Longrightarrow Q < 0 \Longrightarrow \nabla^2 p < 0$

Illustration with an incompressible 2-D flow (cont.)

rotation pure, $s = 0$ et par conséquent $Q < 0$
cisaillement pur, $\omega = 0$ et par conséquent $Q > 0$
cisaillement simple $\omega = s$, et $Q = 0$

Champ de pression

$$\begin{cases} u_2 \dfrac{\partial u_1}{\partial x_2} = -\dfrac{1}{\rho}\dfrac{\partial p}{\partial x_1} \\ u_1 \dfrac{\partial u_2}{\partial x_1} = -\dfrac{1}{\rho}\dfrac{\partial p}{\partial x_2} \end{cases} \qquad \begin{cases} -\dfrac{\omega^2 - s^2}{4} x_1 = -\dfrac{1}{\rho}\dfrac{\partial p}{\partial x_1} \\ -\dfrac{\omega^2 - s^2}{4} x_2 = -\dfrac{1}{\rho}\dfrac{\partial p}{\partial x_2} \end{cases}$$

$$p = p_0 + \frac{\omega^2 - s^2}{8}(x_1^2 + x_2^2)$$

Local topologies for incompressible flow

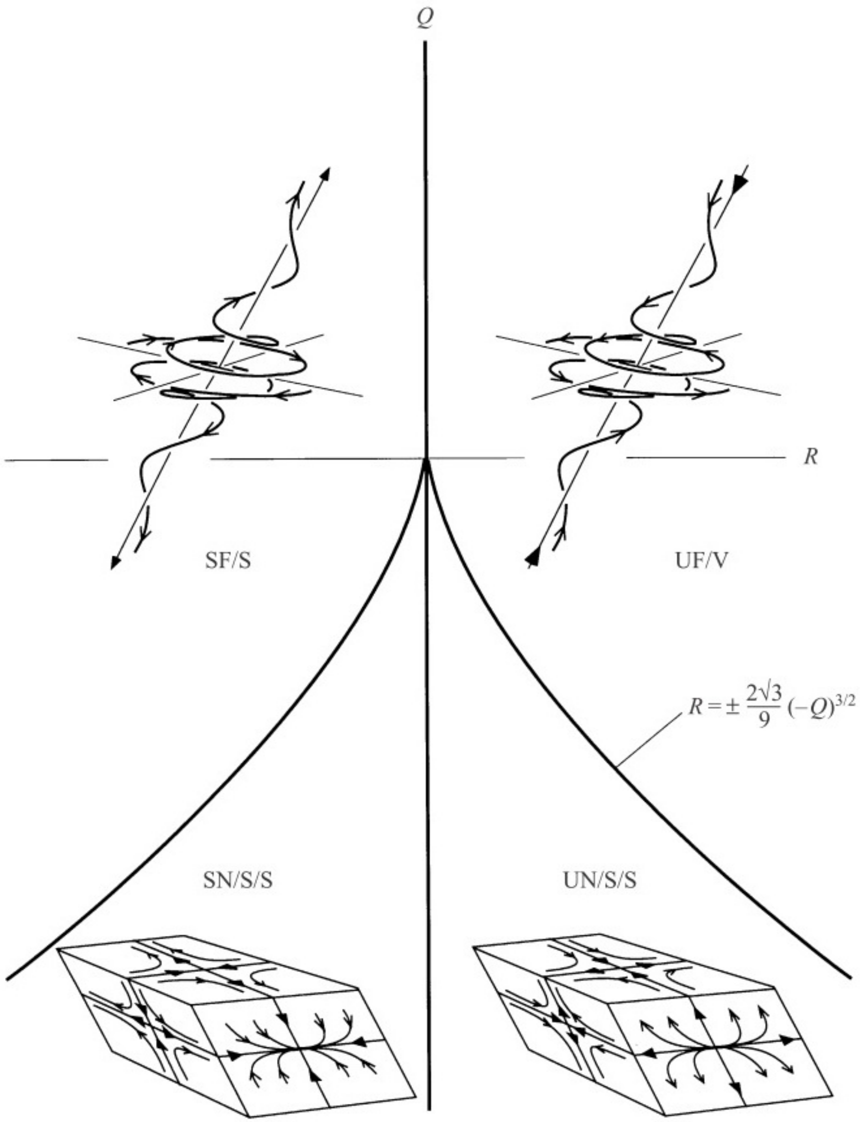

From Ooi *et al.*, 1999, *J. Fluid Mech.*

Presence of instability waves in turbulent flows
(concluding remarks)

Control of a mixing layer

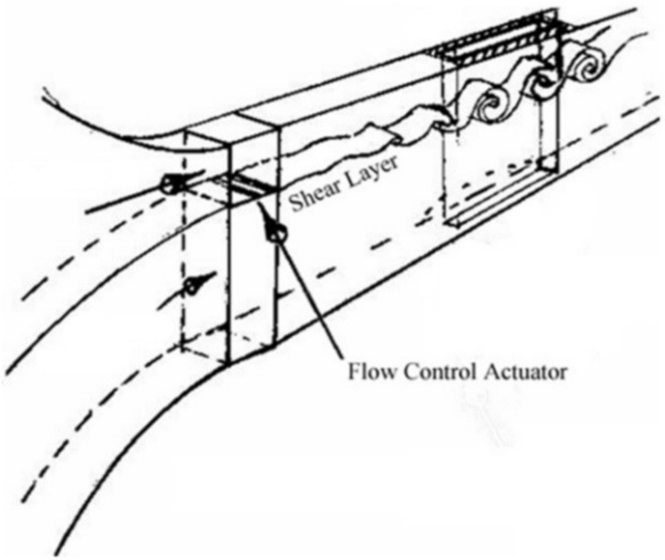

On cherche à forcer le développement d'une couche de mélange, en imposant une perturbation spatiale de longueur d'onde α_e au bord de fuite de la plaque séparant les deux flux rapide et lent.

1. Rappeler en deux ou trois phrases les caractéristiques des ondes qui se développent en aval du bord de fuite de la plaque séparatrice.
2. Comment déterminer le taux d'amplification de ces ondes ?
3. On sait que cet écoulement admet une solution autosimilaire. Quel mécanisme physique – à décrire en une phrase – permet d'obtenir un taux de turbulence borné ?

- **Flow-induced cavity oscillations**

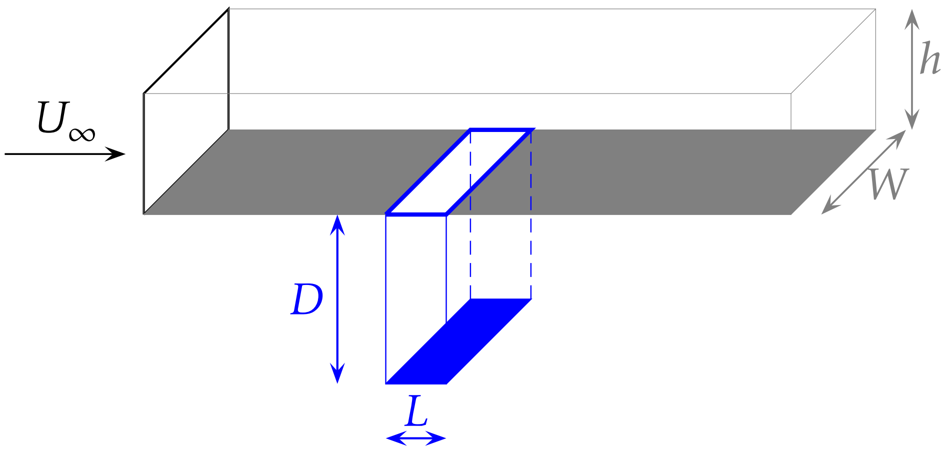

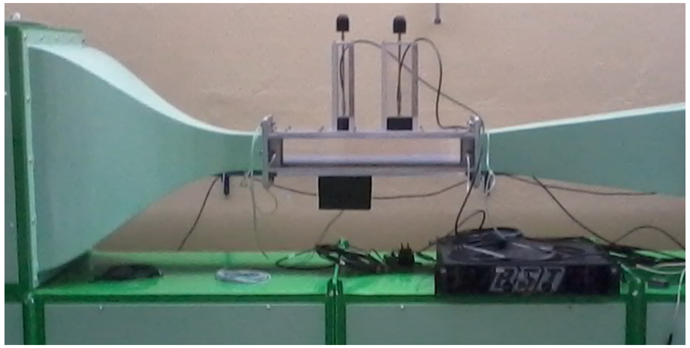

SPL measured inside the cavity

$$\begin{cases} L = 0.04 \text{ m} \\ h = 0.1 \text{ m} \\ U_\infty = 52.2 \text{ m.s}^{-1} \\ 0 \leq D \leq 4L \end{cases}$$

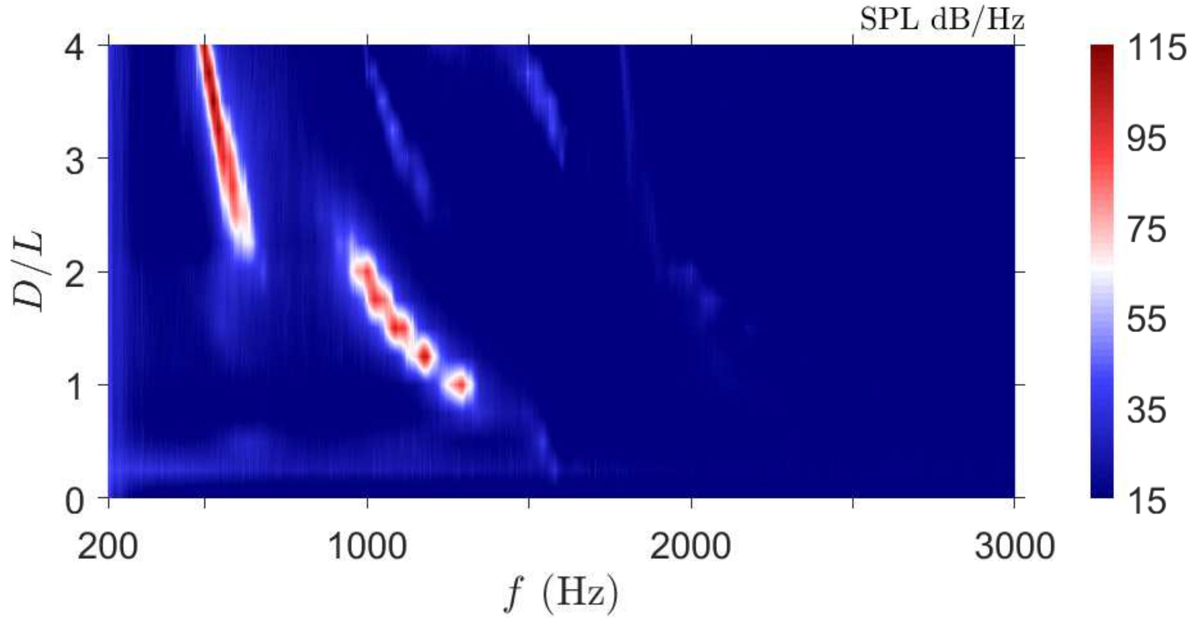

Flow-induced cavity oscillations (cont.)

Cavity depth modes $---$ $n = 0$
(cavity+end-correction)

$$f = (2n+1)\frac{c_\infty}{4(D+0.41L)}$$

Acoustic modes $-\cdot-\cdot-$ $n = 1$
(cavity+channel height)

$$f = n\frac{c_\infty}{2(h+D)}$$

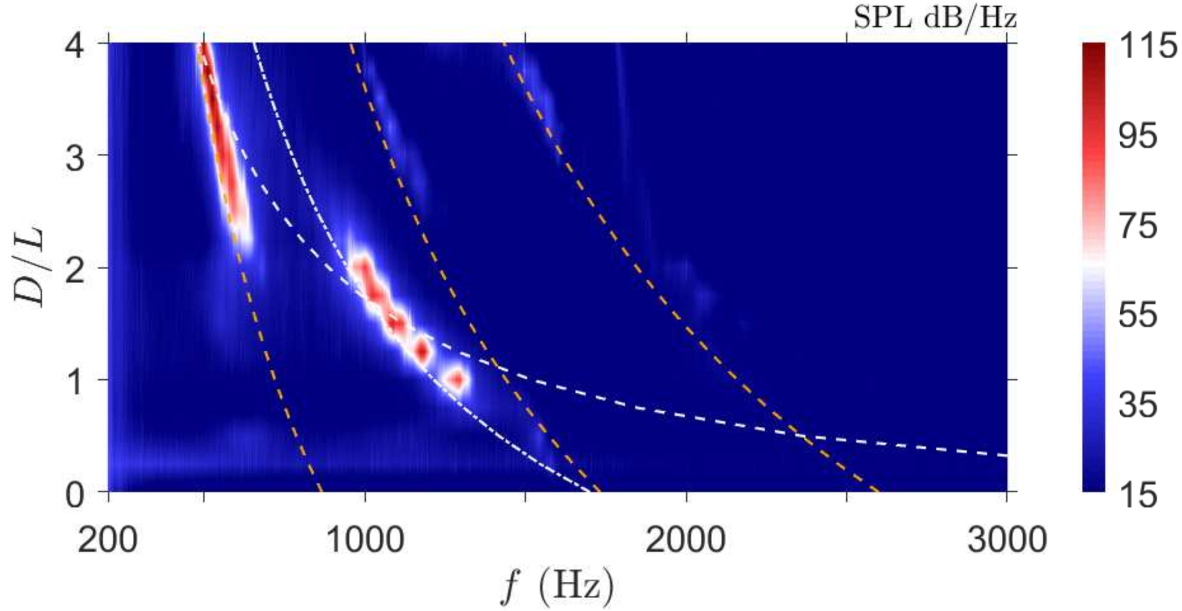

Aeroacoustic feedback loop
$---$ $n = 1, 2, 3$

$$f = \frac{n}{L/U_c + 2D/c_\infty}$$

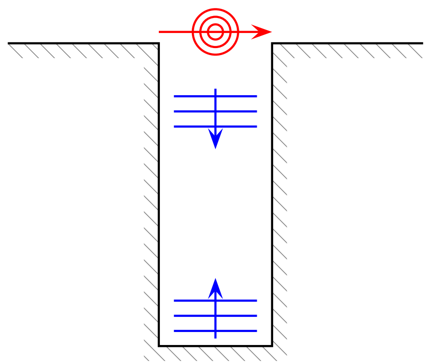

Convection of turbulent structures within the shear layer, which impact at the downstream corner, generation of acoustic waves (depth modes) and excitation of the shear layer upstream.

Modelling : frequency selection + gain $\rightsquigarrow$ whistle

Cavity noise : a long-lasting problem in transport

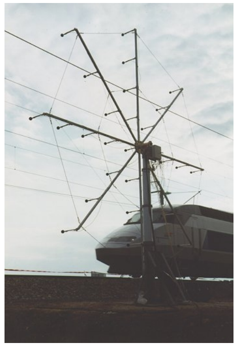

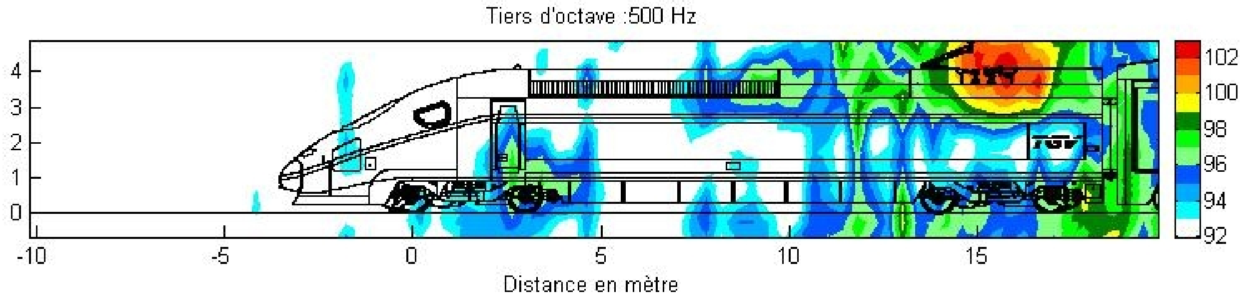

TGV - high speed train (rear engine) - courtesy of SNCF

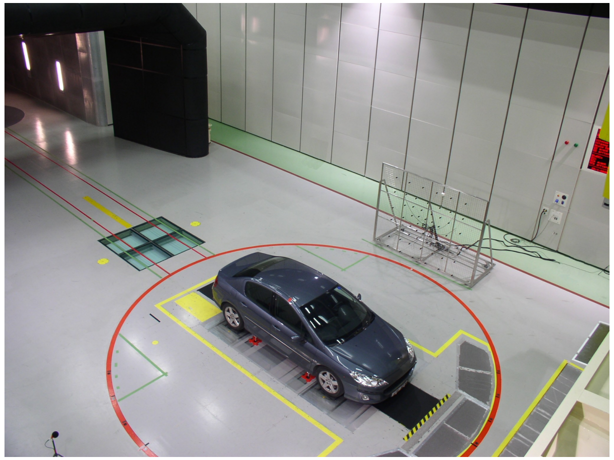

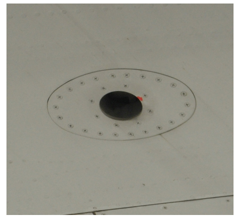

fuel pressure relief vent on a A319

Courtesy of Jan Delf (DLR), refer to *AIAA Paper 2002-2470*

Measured acoustic spectra at 1 m above a cylindrical cavity

Diameter $D = 10$ cm, depth $H = D$, flow speed $50 \le U_\infty \le 110$ m/s TR-PIV 

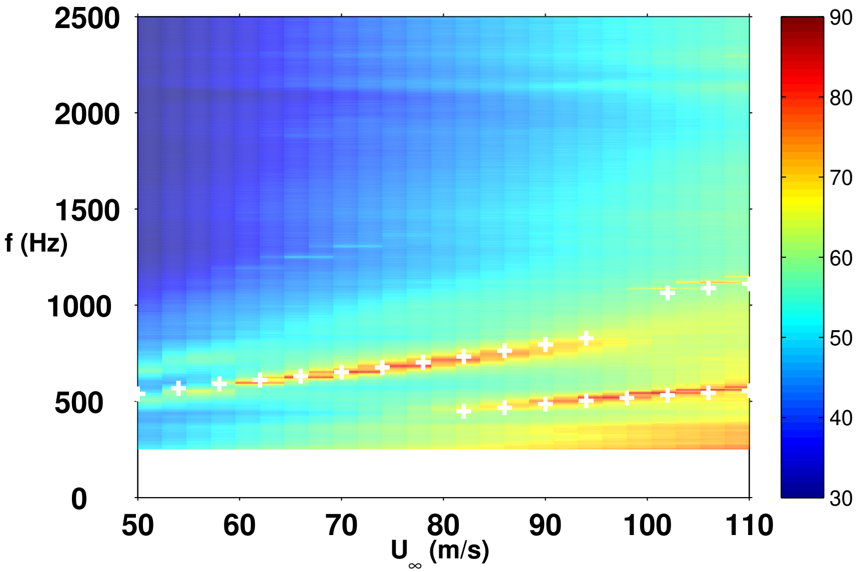

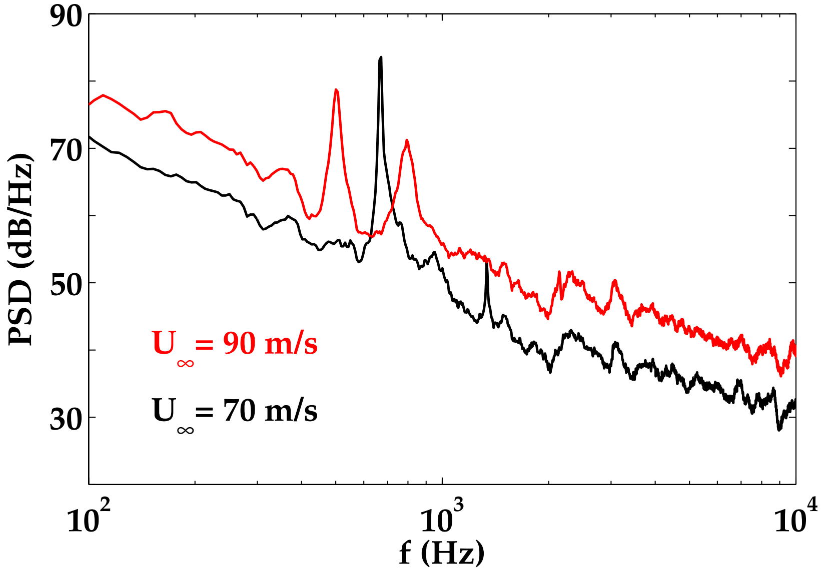

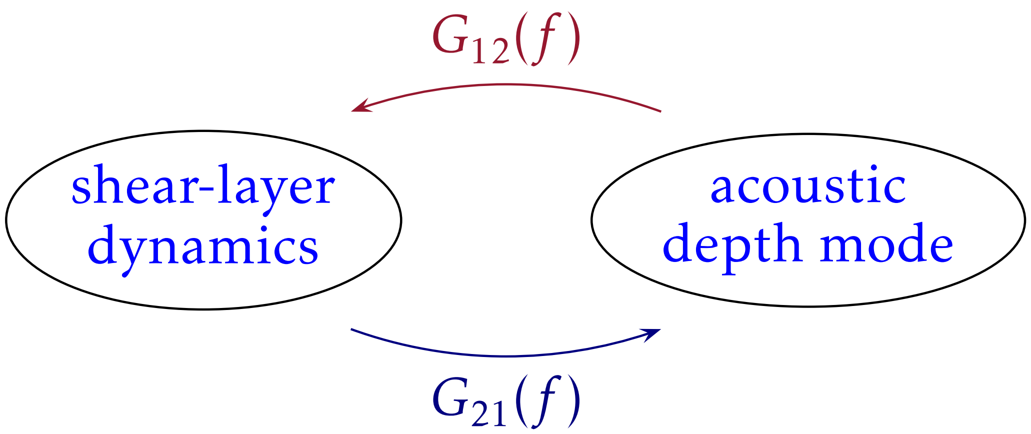

$\mathfrak{Im}\,(G_{12} \times G_{21}) = 0$

$\Longrightarrow$ resonance frequencies +

Marsden *et al.*, 2012, *J. Sound Vib.*, **331**

Elder, 1978, *J. Acoust. Soc. Am.*, **63**(3)

Shinkansen (Tokyo – Sendai, july '08)

E2 series – 275 km/h
E4 series – 240 km/h

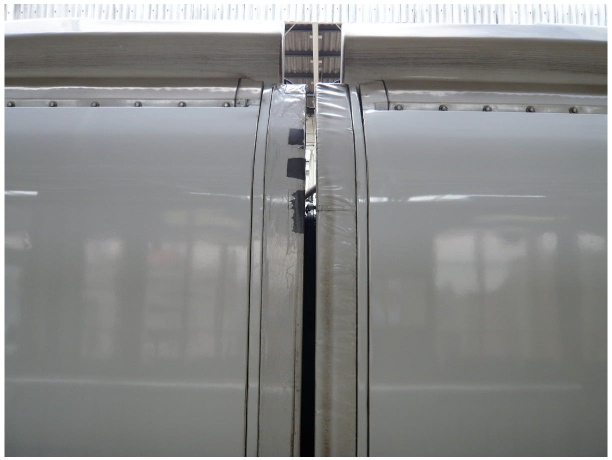

aerodynamic noise generated by intercoach spacing

- **New Hayabusa Shinkensan train ('the bullet train')**

THE DAILY YOMIURI

SUNDAY, MARCH 6, 2011

THE DAILY YOMIURI (2011)

PRICE ¥120 (¥2,650 per calendar month)—tax included

The Yomiuri Shimbun

Fast trainspotting

Train fans snap pictures as the new Hayabusa bullet train on the Tohoku Shinkansen line leaves Tokyo Station on its maiden trip to Shin-Aomori Station on Saturday morning. The train, the first entirely new model introduced by East Japan Railway Co. since 1997, achieved speeds of up to 300 kph, 25 kph faster and quieter than the conventional Hayate superexpress. It connects Tokyo and Shin-Aomori in three hours and 10 minutes. (Related story on Page 2)

7% annual growth eyed in new 5-yr plan

BEIJING (Reuters)—China is on course for another five years of robust growth although inflation threatens social stability and must be tamed, Premier Wen Jiabao said Saturday.

In China's version of a "State of the Union" address to the annual parliament session, Wen said the top priority this year was to curb price rises that were making life difficult for ordinary people.

- **Flow-induced cavity oscillations : aeroacoustic feedback loop for shallow cavities (at rather high Mach numbers)**

$L/U_c + L/c = n/f$

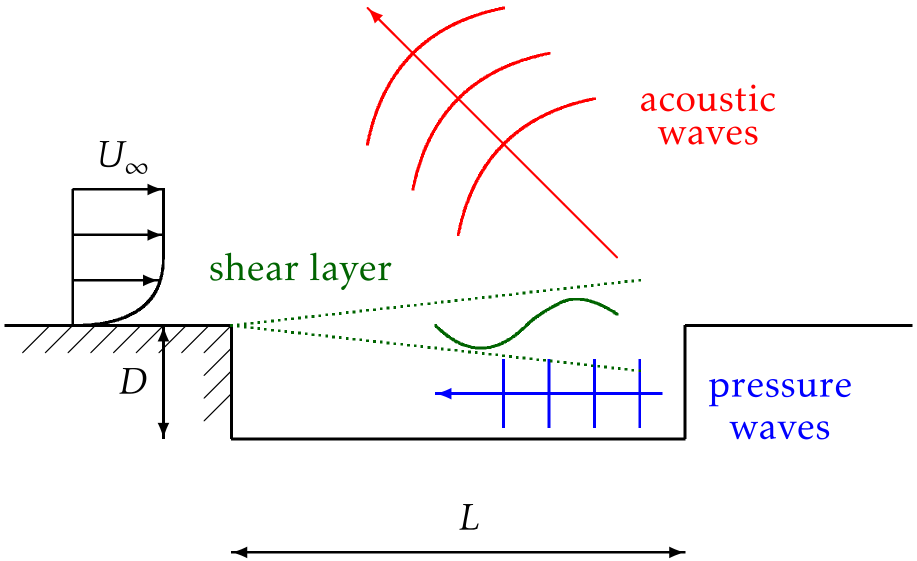

Rossiter formula (1964)

$$\mathrm{St} = \frac{fL}{U_\infty} = \frac{n-\alpha}{M + \dfrac{1}{\kappa}}$$

f frequency
L length
U_∞ free stream velocity
n number of vortices
α phase lag
$\kappa = U_c/U_\infty$, U_c convection velocity
$M = U_\infty/c$

– No information about amplitude or mode selection (L/δ_θ)
– Acoustic resonance can superimpose (longitudinal or depth mode)